THE UNIVERSITY OF MANITOBA

FACULTY OF GRADUATE STUDIES

STRUCTURAL HEALTH MONITORING OF THE GOLDEN BOY

BY

BOGDAN ANDRES BOGDANOVIC

A Thesis/ Practicum submitted to the Faculty of Graduate Studies of The University of Manitoba in partial fulfilment of the requirements of the degree of

MASTER OF SCIENCE

DEPARTMENT OF CIVIL ENGINEERING
WINNIPEG, MANITOBA
JULY 2004

THE UNIVERSITY OF MANITOBA

FACULTY OF GRADUATE STUDIES

*****

COPYRIGHT PERMISSION

STRUCTURAL HEALTH MONITORING OF THE GOLDEN BOY

BY

BOGDAN ANDRES BOGDANOVIC

A Thesis/Practicum submitted to the Faculty of Graduate Studies of The University of Manitoba in partial fulfillment of the requirement of the degree

Of

MASTER OF SCIENCE

ABSTRACT

The elaborate inspections performed on civil structures tend to be very time and cost consuming. It is somewhat difficult to asses the damage or deterioration by visual inspection and may perhaps lead to the sudden demise of the structure. The Golden Boy statue was faced with this problem. Through an extensive inspection of the statue's shaft, it was determined that the diameter of the shaft had reduced by approximately 10% due to corrosion. A wind tunnel test and theoretical analysis of the statue demonstrated that for a hundred year wind the steel shaft would reach approximately 91% of its ultimate strength. To avoid this sudden collapse, the Golden Boy was removed from the top of the legislature's dome and the shaft was replaced. In addition, sensors were installed on the shaft of the Golden Boy as a mean to asses the behaviour and condition of the structure in the future. It provides an effective and cost effective method for condition assessment and Structural health monitoring (SHM). This thesis presents the installation of sensors, the key elements of a successful SHM system and an in-depth processing and interpretation of the SHM data. A mathematical model and theoretical analysis of two diagnostics tests are also presented.

The accuracy of the diagnostic tests and model is demonstrated by comparing the behaviour of the analysis of the strain gauge data collected. The strain gauge data records only the dynamic and thermal strains of the statue due to the wind and temperature, respectively. The analysis consist of removing the

thermal strains and obtaining the dynamic strains due to the wind action experienced at that instant. The diagnostic tests are determined by two different types of theoretical approaches which are able to set some kind of confidence in the data. The results are compared to one another as a result of the maximum gust of wind intensity during some time frame. The diagnostic test of the accelerometer at high wind velocity ranging from 30Km/hr to the maximum of 59Km/hr, demonstrates an average increase of 9% in maximum strain when compared to the strain gauge analysis results. The diagnostic test of the wind meter shows a quite higher average increase of 35%. The diagnostic tests demonstrate an alternative way to establish the structural movement of the Golden Boy, should the strain gauges malfunction. The analysis provides some guidelines for what is expected for maximum strain during a typical windy day (max. gust velocity) and allows for a simplified formula to predict the maximum boundary strain limits for different winds. The natural frequency of 3 Hertz is verified by both theoretical analysis of the mathematical model and the Fast Fourier Transform (FFT) of the live data sensor (Accelerometer). It establishes the main criterion of the statue being in great health as well as set the limit for the future if the natural frequency changes. All findings are based on the early stage of the SHM process. This work will serve as the initial starting point and foundation for the long term and continuous monitoring of the Golden Boy. The data collected has shown the reliability of the instrumentation and SHM system. Furthermore, the study has produced observation and recommendation for future work in the SHM of the Golden Boy.

ACKNOWLEDGEMENTS

This research project was carried out under the direct supervision of Dr. Aftab. A. Mufti. The author wishes to express his gratitude to Dr. Aftab A. Mufti for his academic support, guidance and advise as well as experience and knowledge throughout the investigation.

Appreciation is extended to the technical assistant of Mr. Moray Mcvey, Mr. Grant Whiteside and Chad Klowak for their Laboratory assistance and the installation of all sensors devices for the SHM process of the Golden Boy.

The author wishes to thank Ms. Liting Han and Mr. Gregory Page for all their assistance in the civionic and computer aspect of the project, respectively. Their expertise and knowledge in the field of electrical and computer web designing is very essential part in the remote monitoring process. The evolution of "CIVIONICS" continues to expand in ways unimaginable for Engineers. Also recognise the helpful advise in writing and editing the report by Dr. Ashutosh Bagchi and as well as his guidance, advise and expertise Knowledge in the field of Structural Health monitoring.

Gratitude is extended to Dillon Consulting Engineer, Mr. Bob Wiebe, Government Service Engineer, Mr. Mike Hawrylak and Legislative Building Superintendent, Mr. Todd Mickalash for their constant guidance, patients, concerns and assessment on the SHM aspects at the Legislature Building.

Finally, the author wishes to express his sincere gratitude to his parents and son Colton for their support throughout my studies and also for their strength, support and encouragement throughout this project.

CONTRIBUTION TO SHM KNOWLEDGE

The following involvement was obtained through the SHM of the Golden Boy project:

- The implementation and contribution of Civionics which includes the combination of two different disciplines, electrical and civil engineering.
- The execution of instrumentations preparation and installation.
- The contribution to the SHM system.
- The contribution to designing the web site for continuous monitoring of different projects around the ISIS Canada Network.
- The implementation of the mathematical model.
- The implementation of the data collecting, data retrieval, data processing and data interpreting for the analytical part of the SHM project.
- The correlation and comparison of the theoretical model analyses to the actual live data recorded.

TABLE OF CONTENTS

LIST OF FIGURES

LIST OF TABLES

1. INTRODUCTION

1.1. PROBLEM

In present times we are encountering the growing problem of infrastructure failure and collapse as structures are aging with time due to natural causes or degradation and deterioration, particularly the corrosion of steel reinforcement in concrete. This is of great concern, and it affects a wide range of infrastructure in the world, particularly highway bridges. All over the world, a large number of bridges are getting older. Forty two percent of bridges in the United States, for example, are structurally deficient and in need of repair or retrofitting. Also many bridges are approaching the end of their 50 year design life. It is projected that infrastructure inspection, maintenance, repair and retrofitting will cause a huge deficit in the amount of billions of dollars. So, what better way to deal with the problem than by repairing the structures by innovative materials and introducing "smartness" into them by installing sensors. "Smart Structure" will help to avoid catastrophic structural failure and costly retrofit or repair in the long run. It will also help eliminate costly inspections and maintenance work throughout the life of the structures. Defects will no longer go unnoticed, resulting in timely repairs and reduced maintenance costs.

A smart structure consists of many different components working together. It includes a combination of sensors, data acquisition systems, storage equipment, communicating device, intelligent sensing devices etc... Sensors are

the key components in such structures, and since they are very small, they can easily be integrated into a structure. A structure is monitored through the measured data collected by the sensors installed in it resulting in long-term savings in labour, money and time. Problems are detected before they become too difficult to repair. Different software and diagnostic tests are developed for new and existing structures and boundary limits are implemented so that no catastrophic failure occurs. Each structure is unique in its own way and may require different techniques in evaluating and assessing the diagnostic tests. The diagnostic tests serve to produce benchmarks for the parameters defining the health of a structure. Therefore, proper diagnostic analysis and an efficient monitoring system allows for safer and more durable structures as well as the prevention of damage to structures. Long term monitoring also provides insight into the behavior of a structure in construction and in service.

The corrosion of steel is a major cause for concern to reinforced concrete structures. It affects many bridges around the world and is very damaging to structures exposed to humid conditions. The Golden Boy was going to be regilded with 24 karat gold leaf. Once the statue was accessible an inspection of the shaft which supports the Golden Boy at the top of the legislature's dome revealed severe corrosion to the base of the shaft. The corrosion around the shaft decreased the diameter by approximately ten percent (half an inch of the five inch diameter shaft). Both theoretical and experimental tests were performed which indicated that under expected wind velocities, the Golden Boy's shaft would reach approx. 93% of ultimate capacity. The shaft was then replaced with

a stronger and more superior shaft, and the expertise of ISIS Canada was used for installing sensors and a system for continuous Structural Health Monitoring.

1.2. OBJECTIVES

One of the major objectives of the current research is to examine the data from various sensors and correlate them. In order to achieve that, strains at the base of the shaft could be calculated form wind data, as well as accelerometer data and calculated strains could be compared to the strain gauge data. Another objective of the current research program is to study the trends in the structural behaviour of the Golden Boy statue on a daily basis and to establish some baseline for the Structural Health Monitoring based on the diagnosis of live data collected from the sensors. The diagnostic analysis would be based on linear static and dynamic theories. The diagnostic analyses will provide some kind of base line to future work and better input to the refinement of the mechanical model established in the study. It is also necessary to develop a reliable method and program to perform the task of diagnostic analysis. The program should allow the user to alter a number of variables pertaining to the structure and wind conditions, which includes the geometry, material properties, wind speed, and wind direction data. This thesis will investigate possible similarities between the results of different diagnostic schemes adopted here. Finally, this research would aim to establish a possible correlation between the actual live data from strain gauges to the strains obtained theoretically from the accelerometer of wind meter data.

1.3. SCOPE

The Manitoba Legislative Building with its monumental icon, the Golden Boy Statue, represents the bond between the modern civilized world and ancient mythology, which is illustrated through the artistic design work. It pays tribute to the past for the pleasure of future generations. An overview of the history of the Manitoba Legislature Building and the Golden Boy statue is presented in Chapter 2. The inspection and immediate concern related to the structural health of the Golden Boy, are also provided in Chapter 2. Furthermore, reviews of the concept of Structural Health Monitoring (SHM) along with a brief analogy of human health care are discussed.

A brief review on the restoration process is presented in Chapter 3, where a description of the dismantling process is discussed. Chapter 3 then discusses the instrumentation process; the preparatory work followed by the installation of the instrumentations on the Golden Boy's steel armature. Next, the Structural Health Monitoring (SHM) process is presented. The preparatory work needed to establish a SHM system and the installation of the SHM room inside the Legislature Building dome are also discussed. A detailed discussion on the SHM system and the Data Acquisition (DAQ) system is also presented. In addition, the preparation and installation of the Ultrasonic wind sensor are presented. Section 3 ends with a detailed schematic representation of the sensors locations and reveals the probable causes of damage in sensors.

A detailed discussion on the structural model of the Golden Boy statue is presented in Chapter 4 of the thesis. The model is analysed with the basic

theories of structures to produce the diagnostic tests described in chapter 5. The theories consist of basic static analysis, stress-strain theory, wind loading and dynamic theory. The static analysis concept is demonstrated by an elastic cantilever beam with resultant forces and moments due to applied external loading. A free body diagram along with the equation of static equilibrium is presented in the report. An in depth review of stress-strain theory is included. The wind loading design provisions of the National Building Code (NBCC), 1995 has been used to evaluate the forces in the shaft caused by wind, and a detailed calculation for a wind storm with a 100 year return period is demonstrated in this thesis. In addition, a dynamic analysis is performed in conjunction with the diagnostic tests.

Two diagnostic tests and the actual live data results are discussed in Chapter 5. The diagnostic tests consist of different theoretical approaches in the analysis of the accelerometer and the wind data. The accelerometer and wind analysis are discussed in more detail and the numerical results evaluated by this theory are compared to the results obtained from actual live data. The location of the stored data, the process used to retrieve the data and finally the data modification process that was used to achieve numerical results of the diagnostic tests are also discussed in this chapter.

In Section 6, a brief summary of the SHM of the Golden Boy will be reviewed, followed by the conclusion and the recommendation of the thesis.

2. BACKGROUND

2.1. MANITOBA LEGISLATURE BUILDING

At the beginning of the 20th century, Manitoba strived to receive recognition as the future looked very promising for immense growth and prosperity. In turn, Winnipeg would be looked upon differently by others. One architect in particular played a great role in turning this vision into reality. His name was Frank Worthington Simon, from Liverpool England. Simon's great vision and thoughts were incorporated into the then new and current Legislature building. Excavation started for the new legislature building in 1913, however the construction was delayed for quite some time due to World War I. In 1919 the construction of the new legislature was completed and Winnipeg came to be known as the Chicago of the north.

Frank Simon together with Georges Gardet attended the Paris School of Art. Both men were a major influence in the contribution of the vision of the Golden Boy statue, while also designing the monumental icons in the Manitoba Legislature Building.

Simon's way of thinking was to incorporate two of his very important and influential beliefs. With tremendous honour he did such that he would pay great respect to two ancient cultures and civilizations (Greek and Egyptian). The new building used the traditional Greek design principle, which is known as the 'preacher in stone'. Simon integrated the themes of social justice, law, courage

and discipline in the complex and artistic details of the building. Simon wanted to articulate to others that the new building would make a lasting impression to "make people around it more perceptive, more intelligent, better balanced and altogether more civilized human beings." (Gilles, 2001)

One of Simon's marks of respect to Egyptian civilization was to incorporate a huge sculpture of the sphinx on the front roof of the building as shown in Figure 2-1. The Sphinx originated in Egypt and the notion of the sphinx spread throughout the ancient world. It was depicted as a compound creature, having a human head, either male or female and the body of a lion. The heads of Egyptian sphinxes were royal portrayals and the lion's body symbolized the pharaoh's strength. He also captured Greek history with the prominent use of strong solid columns reminiscent of the magnificent Greek Parthenon as a tribute to the beauty of democracy, art and science (Mufti, 2003). The Manitoba Legislature shown in Figure 2-1 exhibits his passion for Greek culture.

The inside of the building, has its own beauty which portrays the hearts and spirits of famous lawmakers, philosophers and leaders from all passages of history (Mufti, 2003). The presence of stunning artistic artwork throughout the building is the creation of the sculptor, George Gardet and is shown in Figure 2-2. Gardet's vision will live in the hearts of Manitobans forever, as the great bison symbolizes the true north and free spirit of Canada. The statues represented in each corner shown in Figure 2-3, are symbolic of religious beliefs and laws. Solon, the statue to the right, denotes the code for humane laws and reforming the constitution. While Moses, represented to the left, denotes the criminal and

liturgical laws. These massive statues and their spirits saturate the air with the symbolic religious and secular thinking involved in making the laws of Manitoba and Canada. Stone tablets mounted on the walls record the names of five great world legislators. The names included on the wall are Confucius of China, Lycurgus of Greece, King Alfred of England, Justinian of Rome and Manu of India, creating a symbolic gathering of wisdom from five corners of the globe (Mufti, 2003).

Figure 2-1: Legislature Exhibits the Use of Greek's Culture, with Sphinxes and the Use of Strong Solid Columns.

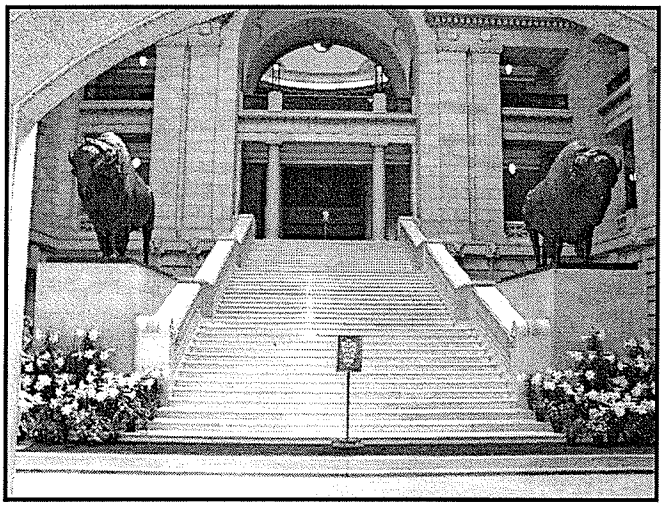

Figure 2-2: Gardet Created the Great Bison Statues

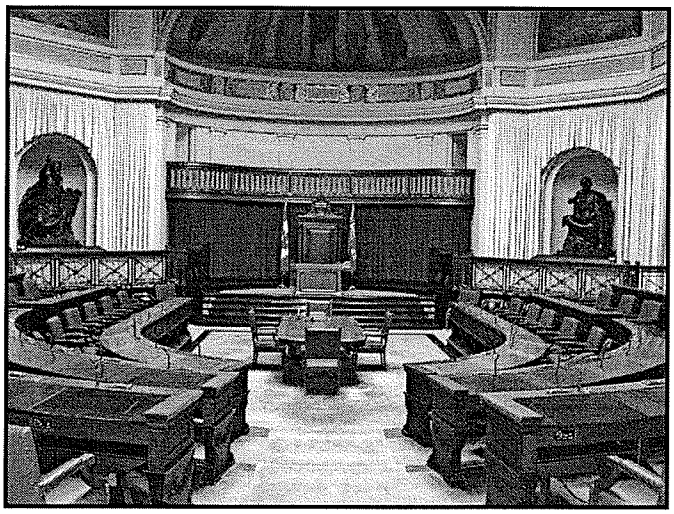

Figure 2-3: Gardet created the Statue of Moses (left) and Solon (right)

2.2. THE GOLDEN BOY STATUE

The collaboration between both sculptor's (Simon and Gardet) and their influence using Greek design, made way for the generation of the Golden Boy sculpture. Simon had great knowledge of the Greek god of science and eloquence, Hermes who was a messenger to the other gods. Hermes was also known as Mercury in Roman mythology and is reflected on the final appearance of the Golden Boy which Gardet legitimately named "Eternal Youth". Figure 2-4 through Figure 2-6 show the amount of resemblance starting with Mercury's statue, to Simon's sketch and finally the Golden Boy's statue. Simon's vision of the Golden boy is shown by a torch in its raised hand and a sheaf of wheat in its other hand which is shown in Figure 2-5.

The lines of the famous poem, In Flanders Fields, written by Colonel John McCrae during World War I, probably gave vision and inspiration to Simon to put a raised torch in the Golden Boy's hand (Mufti, 2003):

"To you from failing hands we throw the torch; be yours to hold it high"

The Golden Boy's torch symbolizes the spirit of enterprise and the youthful enthusiasm of the province. The sheaf of wheat in the left hand of the statue characterizes hardworking Manitobans. The running stance symbolizes moving forward and the evolution of industry in Manitoba, which will continue to grow and prosper as history unfolds. The statue faces north, looking toward the province's vast treasure of natural resources (Mufti, 2003).

The Golden Boy sculpture was cast in 1918 at the Barbidienne Foundry in France. The sculpture was hollow, made of bronze and stood about four meter in length, from his toes to the top of the torch. The statue had to withstand many obstacles before getting to Canada. The foundry was destroyed in World War I, however, the golden boy was unharmed. It was stored in the hull of a ship until the end of the war, due to the immediate need of the ship for troop transport. At the end of the war, after many trips across the Atlantic Ocean, the golden boy finally arrived at Halifax Harbour. It then went via rail to Winnipeg and was perched at the top of the Legislative Building on November 21, 1919 (Mufti, 2003). Before the installation of the Golden Boy, Simon expressed his repeated concerns regarding the sufficient dimensions of the shaft and its stability. Gardet intended to cast the statue monolithically with the shaft that was to fix the statue

to the building (Mufti, 2003). Due to World War I there was a shortage of steel. Therefore, monolithic casting was impossible. Instead, the steel shaft was purchased in Chicago, inserted in the left leg of the Golden Boy and plugged at the heel (Mufti, 2003).

By 1951, the statue's surface was treated and gilded with 24 karat gold leaf and most likely around this time, its name changed from "Eternal Youth" to the "Golden Boy". In 1967, the last major alteration to the Golden Boy included an electrical connection, light fixture mounted at top of its torch and holes drilled to accommodate the wiring which permitted the intrusion of precipitation and moisture into the statue (Mufti, 2003). This led to the deterioration of the statue's health.

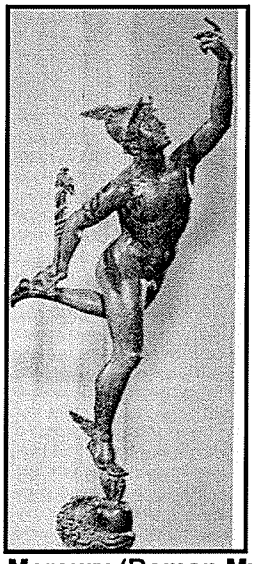

Figure 2-4: Mercury (Roman Mythology)

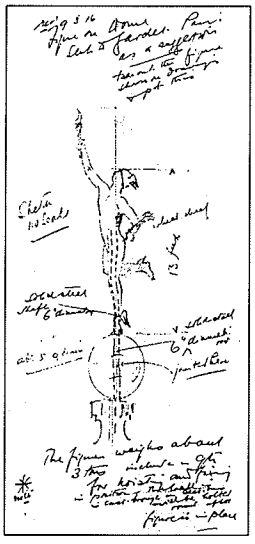

Figure 2-5: Simon's Sketch

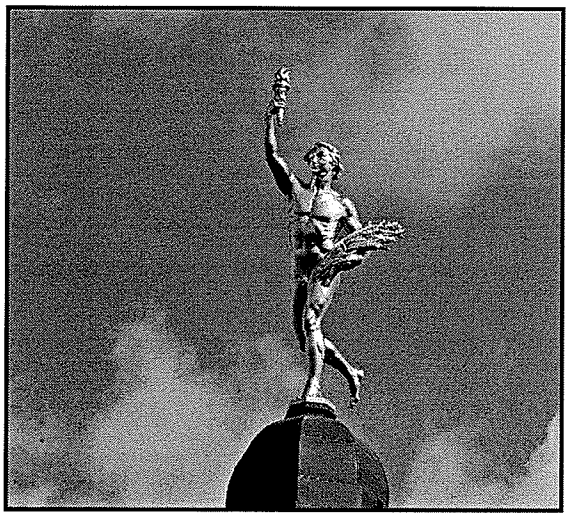

Figure 2-6: The Finished Statue, The Golden Boy

2.3. STRUCTURAL CONCERNS

A preliminary report on the Golden Boy in May 2001 by Susan Stock (Stock, 2001) stated that the sculpture had been wired brushed and re-painted in 1946. Again in 1951, its surface was treated and gilded with 24-karat gold leaf after a huge storm caused extensive damage (Stock, 2001). Baxter Signs was the company contracted to do the work in the mid-twentieth century. Erik Hunt, was one of the workers involved with the restoration process. Ken Hunt, son of Erik said "It was really rough. They had to climb up through primitive scaffolding, and there were no stairs" (Winnipeg Sun, 2002). Susan Stock was involved in the onsite inspection of the sculpture and concluded that the Golden Boy had some minor corrosion (given the size) due to its exposure over the last 50 years. The report gave valuable information on the present condition of the statue and recommendations for its conservation and future re-gilding.

Government Services Minister Steve Ashton and the architect of the Manitoba Legislature building were also concerned about the strength of the shaft, which connects the sculpture to the building. In June 2001, Dillon Consulting Limited provided a full detailed historical review and study of the Golden Boy's shaft. Bob Wiebe, P.Eng. of Dillon was the project manager. Endoscopic investigation and previous x-rays, confirmed that the steel shaft which runs from the fixity of the building up through the left foot of the golden boy and along the inside of left leg, finally terminating at torso height, had corrosion above the bronze plug as shown in Figure 2-7.

The corrosion of steel reduced the diameter of the shaft by approximately ten percent (10% reduction or 1/2 inch) shown in Figure 2-8. This corrosion is believed to be prompted December 31, 1966 by the addition of a light fixture of which holes were drilled to accommodate the wiring. The admission of precipitation and water condensation which accumulated above the plate and brass plug caused the two different metals (a mixture of iron with steel and, copper with bronze) to have a chemical electrode reaction acting as a catalyst to speed up this corrosion process (Wiebe, 2001). The corrosion continued, and led to detrimental effects on the statue's health. The reduction of the diameter of the steel shaft continued to propagate, and could have continued until it reached a sudden catastrophic collapse jeopardizing the public's safety.

Being aware of ISIS technologies, government officials informed Dillon Consulting that the Golden Boy was a candidate for Structural Health Monitoring (SHM). Dr. Aftab Mufti, president of ISIS Canada, confirmed that SHM would be

an affective way to help ensure the future health of the Golden Boy. An ISIS Canada research team joined in on the continuing debate with Dillon, to conclude that the Golden Boy perched on top of its dome was a cause for concern.

Photogrammetry was used to develop an accurate and complex CAD scale model of the statue shown in Figure 2-9. A 1:20 model of the Golden Boy was constructed of plastic and was used for wind tunnel testing at the University of Western Ontario (Kopp & Surry, 2001) which is also demonstrated in Figure 2-9. Figure 2-10 shows the wind tunnel tests that Kopp and Surry conducted on a detailed 1:100 foam model of the Manitoba Legislature Building.

Results obtained in the wind tunnel test were designed using the "point-structure" method and the wind was modeled using 100 year return period (Kopp & Surry,2001). Analytical calculations (Mufti and Tadros, 2001) indicated that the shaft supporting the statue was subjected to 91% of its ultimate capacity, while the predicted stress from the wind tunnel test was 93% of the ultimate capacity. Table 2-1 shows the comparison between both results.

The shaft of the Golden Boy is treated as a cantilever fixed at the base having a lumped mass at the free end. Total stresses should incorporate bending, axial and torsion. A detailed calculation is provided in Section 4.6 of the report.

The ongoing collaboration between all parties concluded that treating the sculpture on-site would be difficult because of safety considerations. The potential threat of fire from repair activity combined with the instability of the shaft

presented serious safety concerns. Therefore the best scenario was to remove the sculpture from the top of its dome for restoration and repair on the ground.

In February, 2002 the monumental icon was taken down from its perch where it had stood for about 84 years. With police escort, the Golden Boy was taken to the Manitoba museum for the publics viewing. It attracted over 140,000 Manitobans during its stay, before being moved to the Pritchard Machine Shop for the repair process.

Table 2-1: Comparison of theoretical and wind tunnel testing analysis - Diameter due to corrosion = 116mm (4.57in.) (Mufti, 2003).

Analysis	Maximum Stress, MPa	Yield Stress, MPa	%yield
Theoretical	249	275	91%
Wind Tunnel Test	255	275	93%

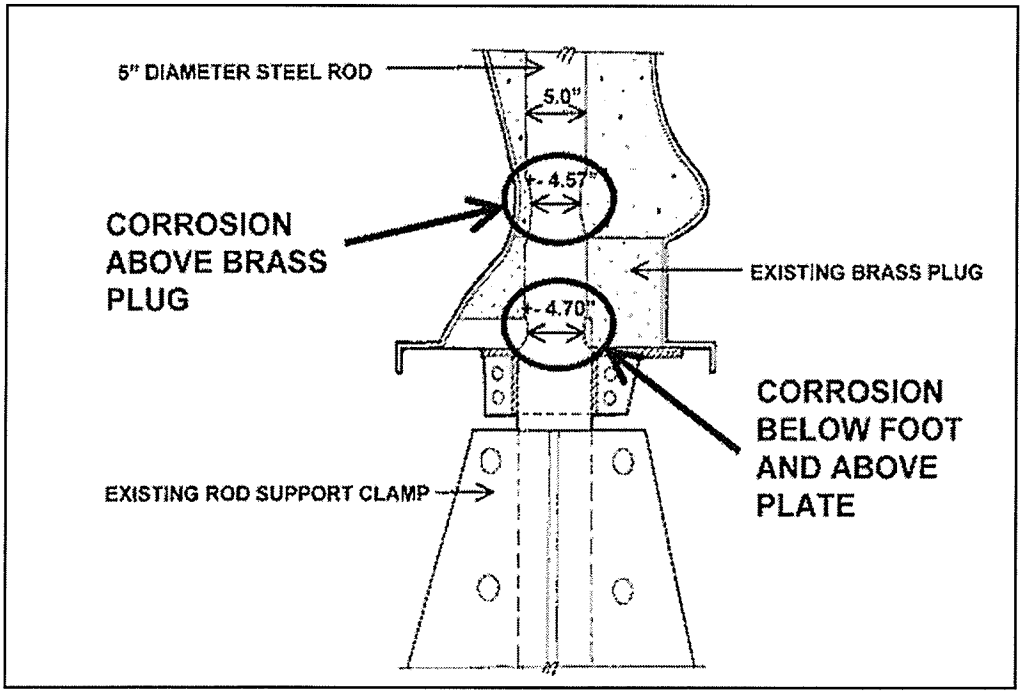

Figure 2-7: Corroding Support Shaft

Figure 2-8: The Actual Corroding Shaft

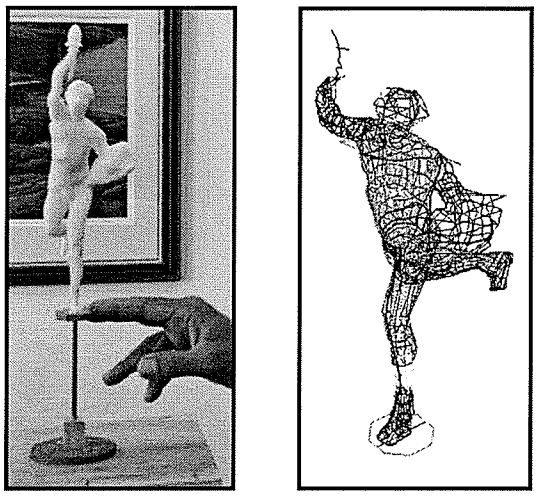

Figure 2-9: 1:20 Scaled Model and Complex AutoCAD Model

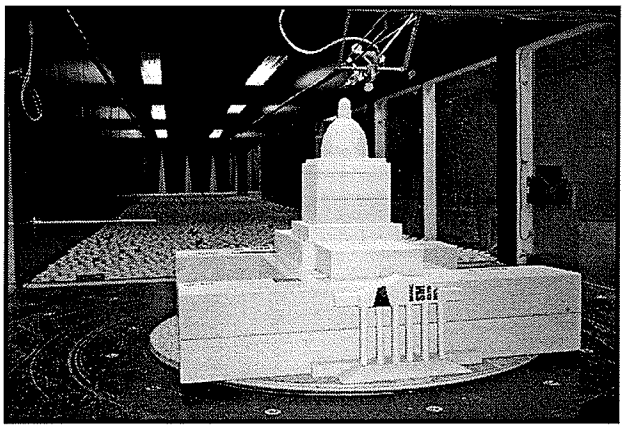

Figure 2-10: Scale Model of Legislature Building at the University of Western Ontario

2.4. STRUCTURAL HEALTH MONITORING (SHM)

As infrastructure in today's world is getting more advanced, demands on them are also growing very rapidly. The infrastructures are becoming more intricate and incredibly expensive. Therefore the question for us as engineers, is what approach should be used for meeting the growth in the demand in a reasonable way, while detecting damage to our structures early enough to maintain them in a cost-effective manner. We must strive to lower the cost of repair and increase the service life of the structures. The answer is Structural Health Monitoring (SHM). SHM is a relatively new term for civil engineering but is the wave of the future. Many structures have been integrated with the SHM systems as a means to detect damage and ensure proper behaviour.

The objective of SHM is to monitor the in-situ performance and behaviour of a structure accurately and efficiently. SHM allows for periodic or continuous monitoring under different loading conditions, such as, various service loads and dynamic loads including seismic or wind excitation. It also allows us to assess the deterioration in infrastructure and detect damage at critical positions to assess the health of structures. This tool is the back-bone for determining whether the structures are safe or at risk of failure. The information collected by SHM system will permit better management of infrastructure. It will improve maintenance methods, management strategies, and improve design guidelines, which will in turn reduce costs in the long run and also prevent of catastrophic failures to our infrastructures.

Structural Health Monitoring consists of many different types of sensing devices. These can be integrated to a secondary system which includes a data acquisition system, data processing system, communication system and damage detection system. Keep in mind that not all SHM systems are alike and may vary from project to project. For example, depending on different circumstances, regions, climates, boundaries and obstacles, the infrastructure may be monitored in different ways. Instrumentations are installed at critical locations where appropriate measurements are taken for evaluating the health condition of the structure. The engineers must design an effective monitoring system to obtain proper and useful data in a manner which will allow for periodic or continuous monitoring and quick decision making. The secondary (SHM) system will be discussed in a subsequent section.

The principles of SHM for the Golden Boy are analogous to the principles that guide our personal health monitoring. The physical health of humans is governed by medical doctors using stethoscopes and blood pressure gauges to obtain readings that measure heartbeat and blood pressure. Any reading outside the normal expected range indicates that there is some need for concern and the appropriate measures need to be administered for proper health. For SHM related to the Golden Boy, we use an accelerometer to record natural frequencies of the shaft and if the frequency remains unchanged from the expected value the Golden Boy is deemed healthy (Mufti, 2003). A good health criterion is shown in Figure 2-11 for the Golden Boy statue and a human being.

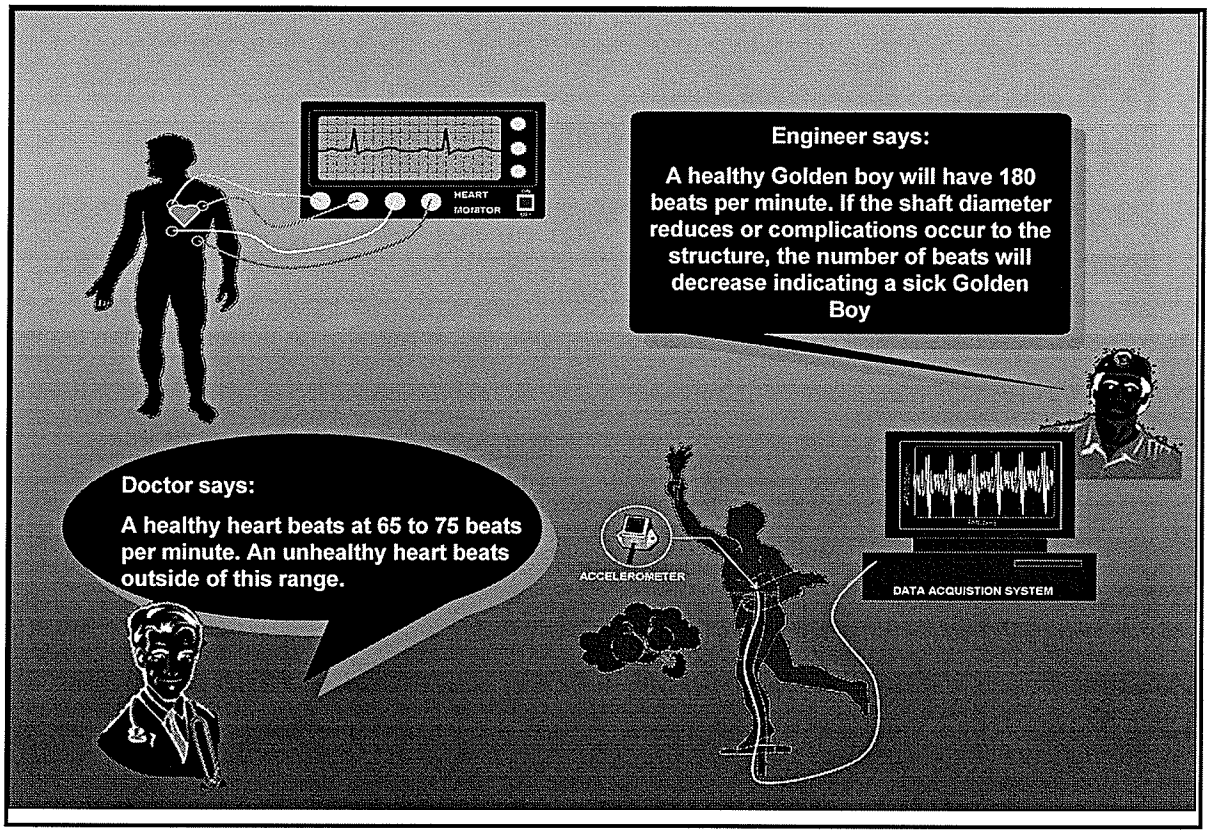

Figure 2-11: Good Health Criteria

2.5. CIVIONICS

CIVIONICS is a new term coined from Civil-Electronics, which is derived from the application of electronics to civil structures. It is similar to the term Avionics, which is used in the aerospace industry (Innovator, 2003). For SHM to become a part of civil structural engineering, it must become accustomed and include Civionics.

3. INSTALLATION OF THE SHM SYSTEM

3.1. RESTORATION PROCESS

In March, 2002 Pritchard Machine shop awaited the arrival of the Golden Boy for the commencement of the restoration process. The statue arrived in its aluminium, wood and steel support cage shown in Figure 3-1. The life-saving surgery on the Golden Boy (Peter Picker, 2002), took several months to complete the project, which consisted of:

- Identifying the locations of all joints.
- Locating the pins at the joints, and extraction of pins.
- The right arm (torch arm) had a major defect (loose). The removal of the torch arm was the first step in the dismantling of the statue.
- The left arm (wheat sheaf) was removed next, to allow for the dismantling of the body.
- The body was separated at belly height near the torso of the sculpture.
- Once the statue was dismantled into four parts, the corroded steel support shaft was extracted.
- The new stainless steel shaft was machined to size and slightly bent.
- The insertion of the new support shaft, internal collars and replacement of the drift pins.
- Brass plugs poured, which were located just below left arch of foot.

- Re-assembly of the statue.

Throughout the restoration process, there was one goal in mind: that was to maintain and preserve the sculpture as much as possible to its original appearance.

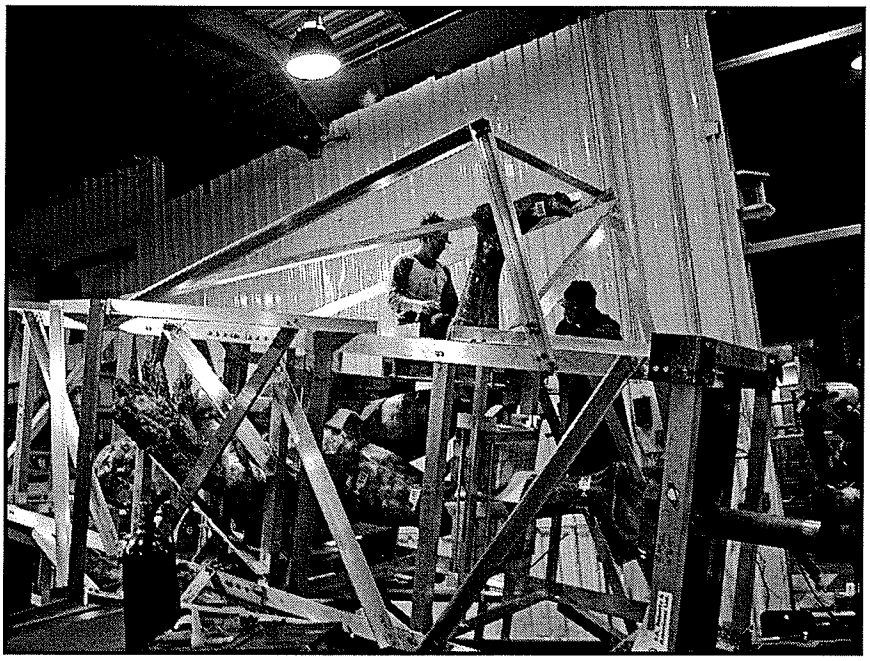

Figure 3-1: Golden Boy at Pritchard Machine Shop

3.2. THE CIVIONICS SYSTEM

As defined earlier, civionics (Innovator, 2003) is an essential part of the Structural Health Monitoring process ("Civionics Expanding the Limits of Civil Engineering", Innovator, 2003). Choosing the sensors types and locations, installation, protection and setting up the sensor data readout units, all come under purview of the civionics system. As the name indicates, Civil-Electronics, the term civionics in Civil Engineering has a meaning similar to what Avionics is

for the Aviation industry. In the selection and installation of sensors, data acquisition and management there is need for cooperation between Civil, Electrical and Computer Engineers. This section will provide the details on the civionics system of the Golden Boy SHM project.

The instrumentation process was coordinated collectively with the restoration process. Both processes took abundant preparation, and thus there was a great degree of collaboration among all parties involved. In the inauguration stage of the restoration process, a monitoring system was being designed to provide accurate and valuable data for the purpose of Structural Health Monitoring. The monitoring system was designed to record and monitor the following information:

- Strains in circumferential (horizontal) and vertical direction at points nearest to bottom of the steel shaft.
- Acceleration, movement and frequency in the transverse and longitudinal direction at the top of the steel shaft (near the torso of the statue).
- Temperature readings at any location on or near the steel shaft.
- Wind velocity and direction at close proximity to the statue.

The next objective was to assess the numbers, type and orientation of the sensors. It was determined that the following sensors be installed:

- Four bi-directional strain rosette sensors mounted on the circumference of the shaft. The gauges were to cover the north, south, east and west corners of the shaft, directly in line and nearest to the end of the shaft.
- Eight fibre brag grating sensors mounted in the same circumferential (horizontal) line of action as the strain gauges. Four pairs of two, one being at forty-five degrees and the other horizontal, located at the north-west, north-east, south-west and south-east corners of the support shaft.
- Two thermocouples located at the east and west circumference of the support shaft in close proximity of the other strain gauges.
- Two 3-D crossbow accelerometers placed at the top of the support shaft inside the statue's torso area.
- One ultrasonic wind sensor located on the roof of the north-west corner of the Legislature Building.

The orientation of the instruments on the stainless steel shaft is shown in Figure 3-2 and is only a preliminary sketch of its location. A detailed figure of its location will be shown in the Section 3.4.

All sensors signal wires were extended to approximately fifteen meters and identification tags were assigned to all sensors in the structural lab at the University of Manitoba, with the exception of the ultrasonic wind sensor. At the Pritchard machine shop, the installation of instrumentation was subdivided into three parts: 1) installation of gauges (FOS, Strain gauges, thermocouples). 2)

installation of accelerometers 3) all lead wires pulled through an electrical flextite conduit that clutches the instrumentation box.

3.2.1. Preparation of Instruments

The preparatory work was done to all selected instruments mentioned above, at the University of Manitoba, Structures Lab. The bi-directional strain tee rosettes were soldered to a fifteen meter length shielded cable as shown in Figure 3-3. The four rosettes were then covered by a plastic case to ensure the protection of the gauges. The identification of all instruments and cables was done meticulously to ensure that each device could properly be distinguished for monitoring purposes. Unique identification labels were assigned to each strain gauge rosette, and all the lead cables. Each strain gauge rosette located in the plastic case and there leads were labelled north, south, east or west respectively. The 24 gauge shielded cable had two sets of three wires which were identified by their color schemes. The color scheme consisted of one set of wires being solid green, orange and blue. The other set being white with strips of green, orange, or blue. The striped wires indicated the horizontal gauge and the solid indicated the vertical gauge.

The eight fibre brag grating (FBG) sensors, connectors and leads were ordered and delivered by the manufacturer. The fibre optic sensors (FBG) were labelled accordingly. An FBG sensor was assigned two letters followed by a digit from one to eight. The two letters indicated the orientation on the steel shaft, N denoting the north face, S denoting the south face, E denoting the east face and

W denoting the west face. The digit indicated the positioning of the FBG on the face of the steel shaft. Odd numbers indicated forty five degree angles from the horizontal and even number indicated the horizontal location. For example the identification NW1, is oriented on the north west face of the steel shaft and the FBG sensor positioned in a forty five degree angle with the horizontal. Figure 3-3 also shows the FBG sensors.

Two 3D LP series Crossbow Accelerometer CXL04LP3 high performance model were ordered and used. For technical literature on the accelerometer view the website www.xbow.com. The preparatory work consisted of splicing the accelerometer's lead wires with adjacent wires which extended the cable to approximately fifteen meters in length. The accelerometers and lead cables were labelled either A1 or A2.

Two temperature gauges were also extended to fifteen meters and labelled accordingly. The identification consisted of the letters TC followed by the number 1 or 2. The letters TC indicate the thermocouple. The number indicates the face of the steel shaft, 1 denoting the west face of the shaft directly underneath the strain gauge, and 2 indicating the east face of the shaft.

In order to apply pressure on the gauges during the bonding process to ensure proper adhesion, a clamping device was developed, as shown in Figure 3-4. The clamping device comprises a thin aluminium sheet of metal, orange rubber pressure pads along the circumference of the stainless steel shaft, bolts and nuts for tightening. The clamping system was extremely lightweight, easy to use and quick to install.

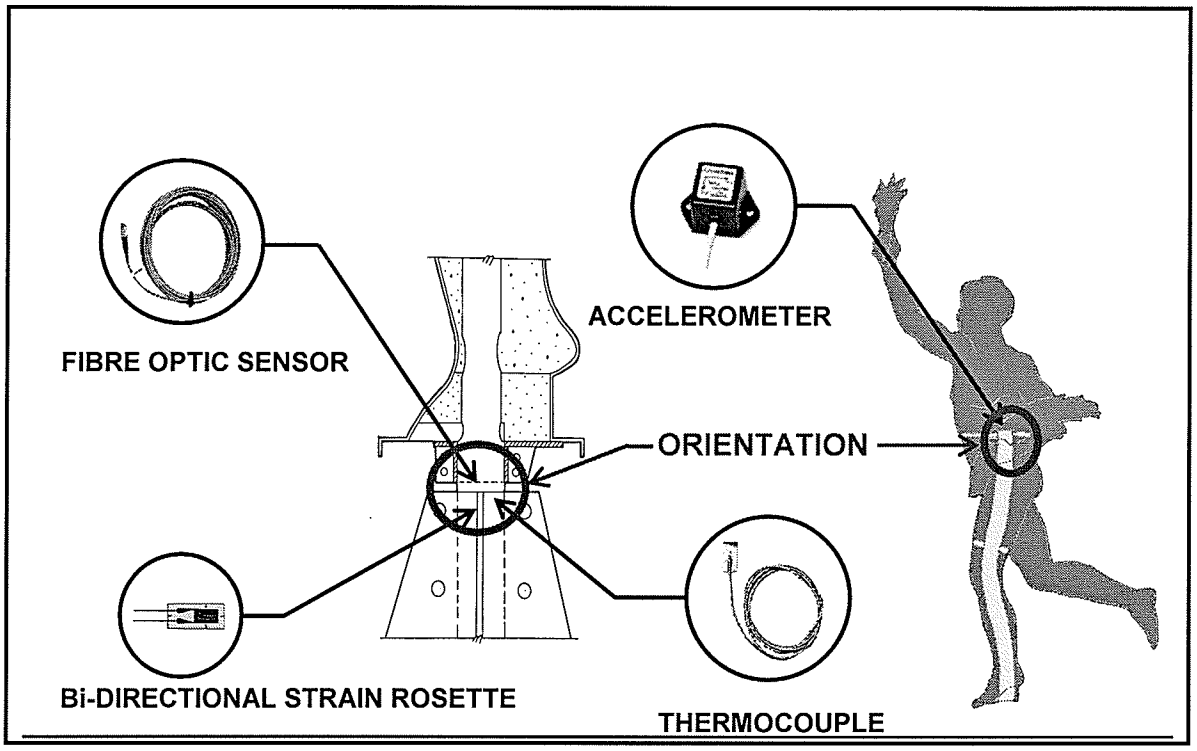

Figure 3-2: Preliminary Sketch of Instrumentation Location

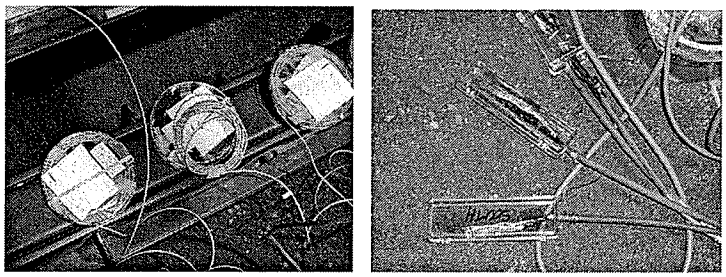

Figure 3-3: Strain Gauge Rosettes and Fibre Bragg Grating Sensors

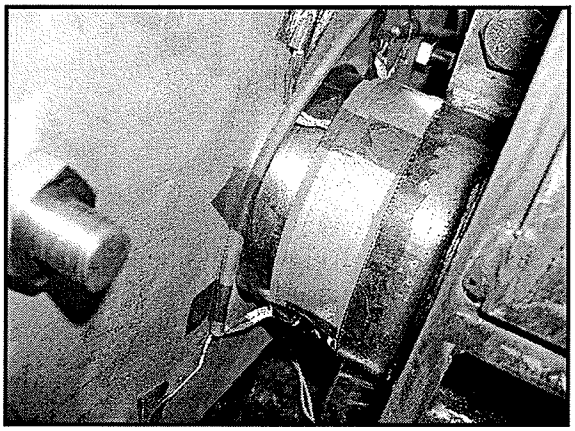

Figure 3-4: Clamping Device Around Shaft

3.2.2. Installation Process

Prior to the commencement of work, the Golden Boy's body was separated at the torso height, to allow for the removal of the corroded shaft. The new high strength stainless steel support shaft, internal collars and drift pins were positioned inside the Golden Boy which terminates at torso height as shown in Figure 3-6. The stainless steel support shaft is slightly bent and the total length is approximately 139 inches. The shaft runs along the inside of the Golden Boy's torso, down through the left leg, through the heel continuing through the plate and terminates at approximately 29 inches away. Most of the exposed shaft underneath the plate would be fixed to the support connection at the top of the Legislature's dome. The remaining six inches would be used for the placing of the instruments as shown in Figure 3-5 (above the hand).

The installation of sensors officially began in May, 2002 at the Pritchard Machine Shop. The first phase consisted of surface preparation and installation of gauges, followed by the installation of the accelerometers, and finally the installation of the instrumentation box. The surface preparation consisted of the following steps:

- Abrading of all surface area and removal of all loose materials.
- Thorough abrading of the gauge area with silicon-carbide paper of 320 grade grit.
- Rubbing of the surface to completely remove all oil, grease, organic and chemical residue, using a lint-free tissue.

- Cleaning and removal of all remaining residue using an alcohol base cleaner (ethanol) and lint-free tissue.

The location of each gauge was marked on the stainless steel shaft and the surface was cleaned and inspected once more.

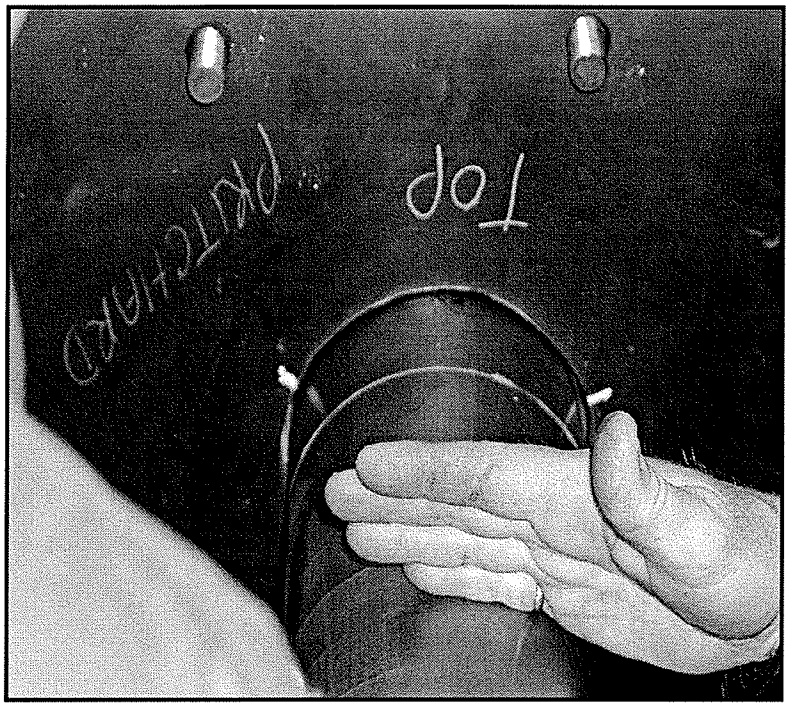

Figure 3-5: Allowable Area location for Sensors (Above Hand)

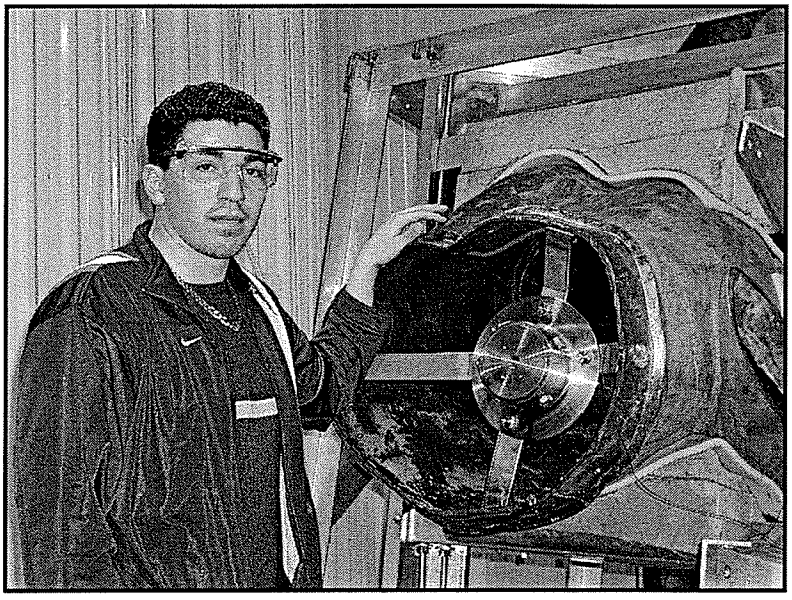

Figure 3-6: Golden Boy's Torso Area

3.2.2.1. Rosette Strain Gauges and Thermocouples

The rosette strain gauges were temporarily held in position at the spot already marked on the steel shaft, using the blue transparent flash breaker tape as shown in Figure 3-7. When all four rosettes were properly positioned and aligned corresponding to their locations as mentioned in the preceding section, the verticality and horizontality of the gauges were checked. The positioning of the gauges around the circumference of the shaft must follow the same horizontal line of action, which was checked visually. Once all gauges were installed accordingly a small quantity of two part epoxy was mixed which was then applied to the steel shaft surface and the back of the gauges. Then the gauges were forced down against the steel surface, and the positioning and alignment of all gauges were rechecked. The clamping device, mentioned earlier, was reassembled. First, the orange rubber pressure pad was mounted around the whole circumference of the shaft, covering all gauges. The thin aluminium sheet was then positioned over the pad and the clamping device was tightened at one end by a bolt and nut, until sufficient pressure was applied, as shown in Figure 3-8. The clamping device was removed after curing of the epoxy.

The surface preparation was already administered around the whole surface, but as a result of limited space, the procedure was repeated at the area of the gauge only. The area was rubbed clean and all traces of dust were removed. The thermocouples were aligned and positioned on the east and the

west face directly above the rosette gauge. The same procedure as used in the strain gauge installation was followed. All gauges were tested at every stage of installation.

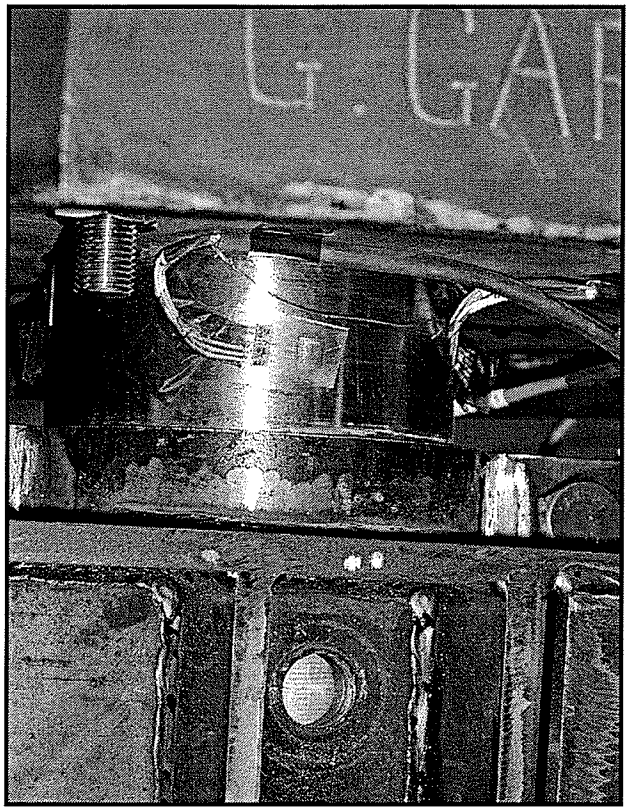

Figure 3-7: Installation of Strain Gauges

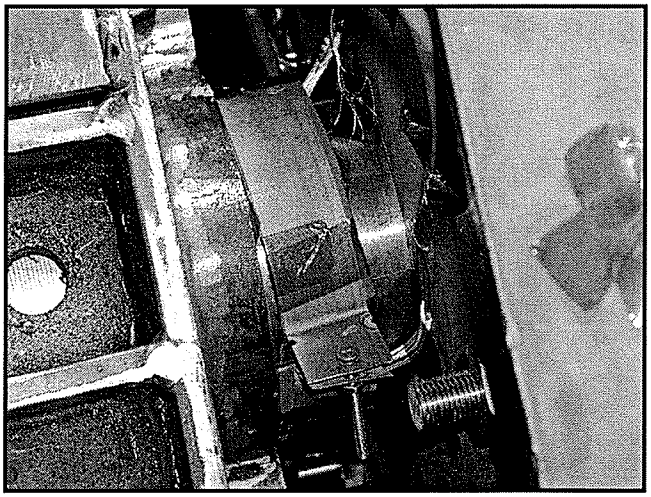

Figure 3-8: Clamping Device Around Gauges

3.2.2.2. Fibre Bragg Grating Sensors

The Fibre Bragg Grating (FBG) sensors were supplied in a coiled manner and had to be uncoiled during the installation process. The FBG were positioned on a work bench and secured with flash breaker tape at the ends. The excess optical fibre at the end was removed by applying pressure with a sharp object such as a screw driver. As mentioned in the preceding section, the surface preparation was done at the locations of the gauges. The final locations of the gauges around the circumference of the steel shaft, directly in line with the rosettes, were marked. The corresponding pairs of FBG gauges, one placed horizontally and the other placed at forty five degrees, were positioned appropriately depending on their identification tags, as mentioned earlier in the section. The pair of gauges was held in position at the locations already marked using the blue flash breaker tape. Small quantities of loctite adhesive gel were applied to both ends of the optical fibre which lie on the extreme ends of the bragg grating. The positioning and alignment were rechecked and the loctite accelerator was sprayed directly on the adhesive gel promoting an instant hardening of the gel. The procedure was repeated until all four faces on the steel shaft were completed as shown in Figure 3.9.

Once the pieces of tape were removed, a protective rubber coating (M-Coat B) was applied to the top of all strain gauge rosettes and thermocouples. The circumference of the whole shaft was covered with black rubber tape and all the leads were secured to the top of the plate in a clockwise direction as shown in Figure 3.10.

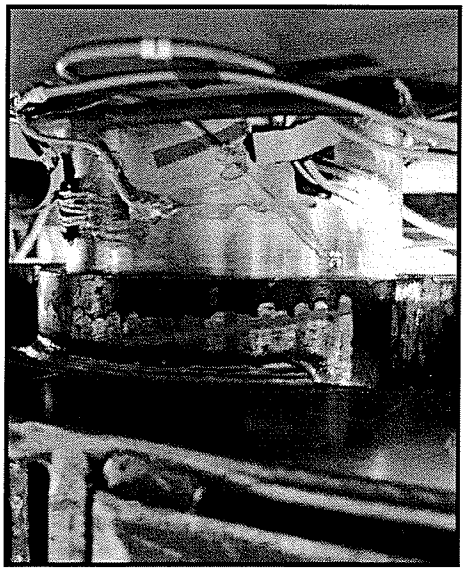

Figure 3-9: Installation of FBG

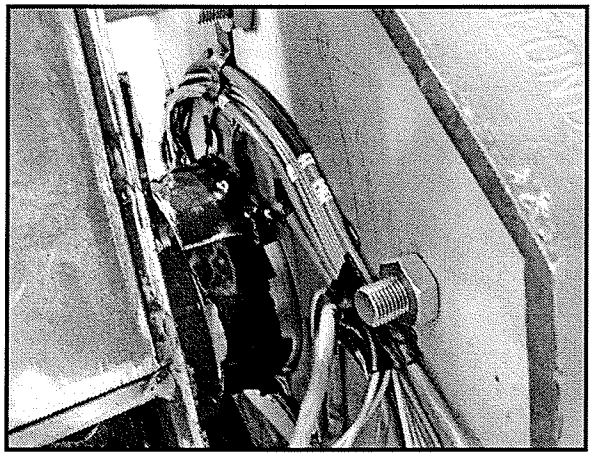

Figure 3-10: Protection of Gauges Around Shaft

3.2.2.3. Accelerometers

The installation of the accelerometers was completed at the end of May, 2002. The accelerometers were positioned in such a way that the y-axis is directly in line with North- South, x-axis in line with east-west and the z-axis up and down (parallel with the steel shaft). Two accelerometers were installed next to each other, at the top face of the steel shaft, which terminates at torso height of the Golden Boy as shown in Figure 3-11. The accelerometers were fastened by a set of screws and the lead cables feed through the interior of the lower part of the body. The cables were extracted through a hole near the bottom plate and tied together with the other leads.

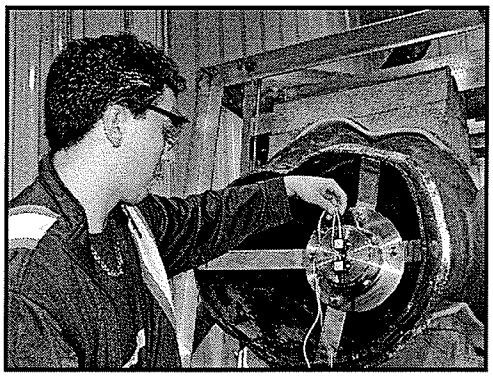

Figure 3-11: Installation and Location of Accelerometers

3.2.2.4. Electrical Box

The lead wires were pulled together through an electrical flextite inch conduit, six feet long. The conduit was used to guaranty the safety of the lead wires while being transported and re-furbished. Once all leads managed to pass through the conduit, an inch diameter hole was drilled through the side of the plastic electrical box, measuring 12 x 12 x 4 inches. The pulling of leads through the electrical box and fastening of the flexite conduit to the box by connectors was done. The wires were revolved in a loop, positioned in the box and secured by the lid, to ensure proper protection. The electrical box and conduit were fastened to the aluminium box frame of the Golden Boy shown in Figure 3-12.

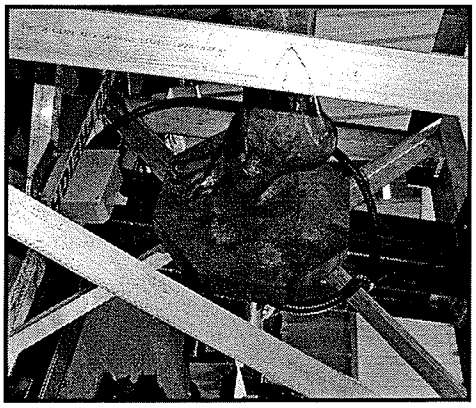

Figure 3-12: Box and Conduit Fastened to Frame

The work of the instrumentation on the stainless steel shaft of the Golden Boy was completed with the cooperation of all concerned parties (Picker,2002). Once the statue was assembled to its original shape and fastened to its aluminium frame box, it was moved to Bristol Aerospace for painting. In mid July, 2002 the Golden Boy was moved to the Forks Market in central Winnipeg, where it received its new 24-karat gold leaf as shown in Figure 3-13. In September, 2002 the Golden Boy was returned to its home atop the Manitoba Legislature Building.

Figure 3-13:The New Golden Boy at the Forks Market

3.3. STRUCTURAL HEALTH MONITORING PROCESS

The next phase of the preparation for remote monitoring took place at the Legislative Building. Just before the placement of the stainless steel shaft at the top of the dome to its fixity, the workers were allowed to accommodate the flex conduit and the plastic electrical box to be inside the dome. Approval was received from the government to establish a remote monitoring room inside the building. There were many questions and concerns about the establishment of the room. The first critical concern was the length of all lead wires. The signal through the leads couldn't extend more than 100 feet or the signal would be lost, therefore, the room had to be in close proximity to the statue. Would the room be properly equipped to house a structural health monitoring system? Would the room be properly heated throughout the years? If maintenance was needed, would it be easy to access the computer in the monitoring room and all leads ect.? These were the major concerns and questions which required review and after debate between all parties (Wiebe, Hawrylak and Mickalash, 2002), permission was granted to accommodate a monitoring room within the Legislature Building. It was agreed that the room was to be built at the bottom of the bigger dome which is directly below the smaller dome as shown in Figure 3-14. Figure 3-14 also shows the interior of the bigger dome.

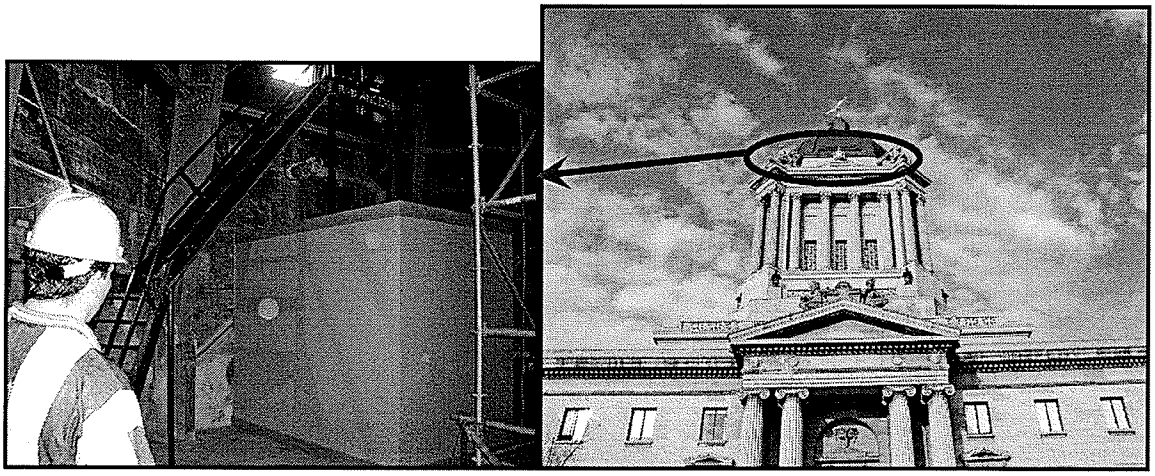

Figure 3-14: Location of the remote monitoring room inside and outside the legislature

3.3.1. Installation of the SHM Control Room

The remote monitoring room was installed at the bottom of the bigger dome at floor level, near the yellow wall shown in Figure 3-14. It is located about 80 feet vertically downwards from the top of the smaller dome, where the fixity of the Golden Boy is located. The yellow walls are part of the enclosure which prohibits heat from rising and encases the stairwells. The computer and the equipment system for monitoring couldn't be installed in the open area due to the lack of heating available at the location. Due to the lack of heating in the winter time the following materials were purchased: a sheet metal shed, insulation, epoxy, and 1500 watt utility heater. The shed was assembled and placed next to the yellow wall as shown in Figure 3-19. The insulation was installed inside the shed. The insulated shed was used for the remote monitoring room and the utility heater was used in the winter time for regulating the temperature inside the shed.

The plastic electrical box was detached from the Golden Boy's frame, placed through the top of the dome's opening and fastened to the interior of the small dome directly 6 feet below the Golden Boy's fixity. An inch hole was drilled on the adjacent side of the box to accommodate the inch diameter flextite conduit. The conduit spanned approximately ten feet to a junction box which was mounted at the bottom of the smaller dome. All lead wires (coming from the Golden Boy's sensors) were pulled through to the junction box. The distance from the bottom of the small dome to the bottom of the bigger dome (near the yellow wall) is approximately 80 feet. Due to the enormous amount of work involved in installing the conduit from one dome to another, the work was carried out by McCain electric subcontractor. The installation of two conduits next to each other run along side the steel beams and columns. One conduit was used for thermocouples, strain gauges and accelerometers where as the other was used for the FOS. With the same identification scheme mentioned previously, new wires were measured to approximately 100 feet in length, cut and labelled at both ends. The wires were then pulled through the 80 feet of conduit and pulled up to the junction box located at the bottom of the smaller dome as shown in Figure 3-15. In addition, the new strain gauge, accelerometer and thermocouple wires were stripped at the ends and spliced together at the top of the small dome as shown in Figure 3-16.

The fibre optic chord extensions (yellow) were also pulled through and labelled accordingly. The general plug adapter configuration mentioned in the

Design Manual I (ISIS Canada Corporation, 2001) was used. Figure 3-17 shows the adapter, the original FBG sensors (orange), the extending (yellow) fibre optic chords and their connections.

Shaw cable provided cable modem for internet access. The cable was extended from the third floor of the Legislature Building to the remote monitoring room (shed). Once all lead signal wires were completed, the computer equipment and the SHM system were carried up to the remote monitoring room. The preparatory work consisted of ordering the computer equipment, the SHM system and developing a program with Lab View which demonstrates proper output. A more detailed explanation of the SHM system will be provided in the following section. The SHM sensors are wired to the National Instrument Data Acquisition system or DAQ system that is connected to the resident computer in the Legislature Building as shown in Figure 3-18 and all wires and DAQ systems were tested. The final stage of the remote monitoring area at the top of the Legislature Building is shown in Figure 3-19.

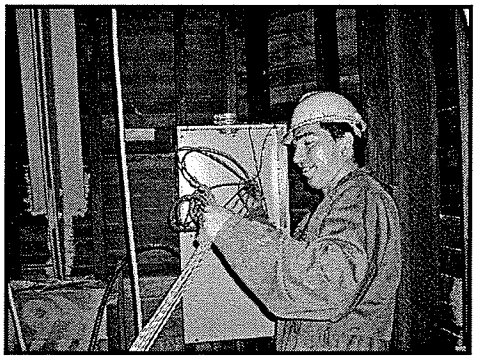

Figure 3-15: Pulling Wires up Through the Conduit to the Junction Box

Figure 3-16: Preparing Wires for Splicing

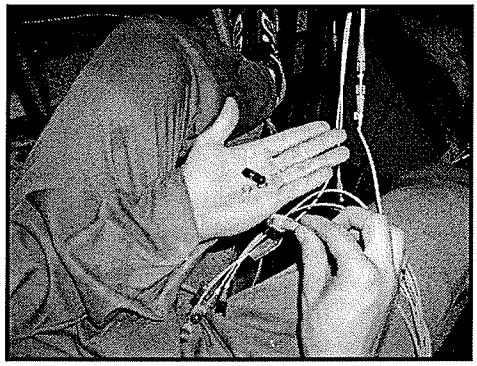

Figure 3-17: Adapters, Plugs and FOSs

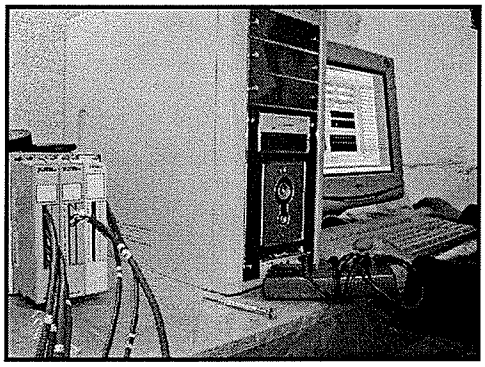

Figure 3-18: Connection of All Gauges to DAQ System (left) and Computer (right) Inside the Remote Monitoring Room

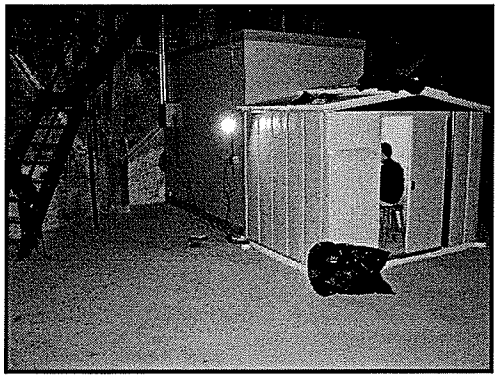

Figure 3-19: Remote Monitoring Area at the Floor of the Bigger Dome

3.3.2. Structural Health Monitoring System

An ideal structural health monitoring system should consist of the following components (ISIS design manual 2, 2001):

- Acquisition of data
- Communication of data
- Intelligent processing of data
- Storage of processed data
- Diagnostics and Data Interpretation
- Retrieval of data

These components are the backbone to a productive SHM system, and the schematic representation is shown in Figure 3-20.

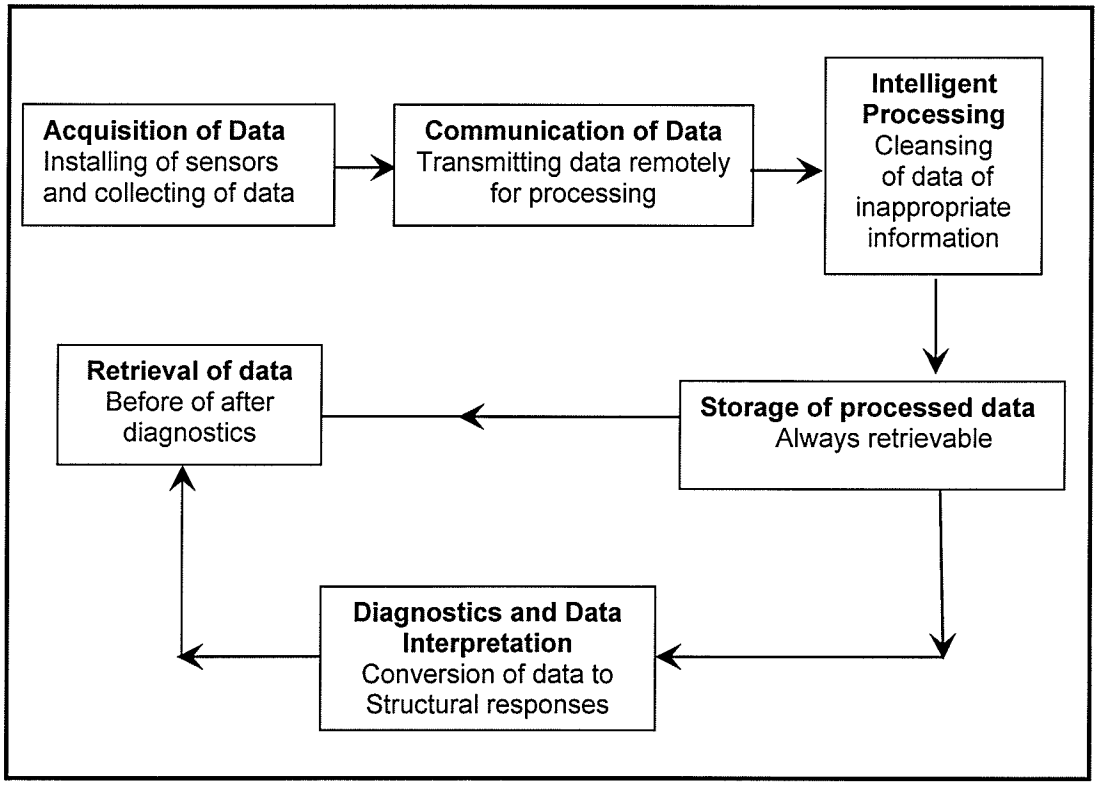

Figure 3-20: Components of a SHM System (ISIS design Manual2, 2001)

3.3.2.1. Acquisition of Data

The first component of an SHM system involves the acquisition of data. The first step is to accurately distinguish what type of instrument devices (sensors) are needed to measure the correct information of the structure (e.g. strain, deformation, acceleration, temperature etc). The sensors need to accurately and precisely measure the response of the structure and the installation of the sensors must be correctly done. Once the installation of sensors on a structure is performed correctly, the next important step is to assure that the data is properly collected by a Data Acquisition (DAQ) system. The task of collecting data is very complex and therefore adequate expertise is needed. Civionics Engineer, Liting Han is involved in administering and supervising the data acquisition aspect of the SHM system and works very closely with each member of the ISIS team.

The Golden Boy is equipped with multiple sensors that can measure strains, deformations, accelerations, temperatures, times, wind speeds, and pressures as previously discussed. Each one of these sensors is affixed to, or near the Golden Boy (eg, wind meter) and are connected to the National Instruments data acquisition unit through electrical cabling. The length of the cables is kept below 100 feet to reduce the noise level in the live sensor data. The term data acquisition system used in Structural Health Monitoring applies not only to the National Instruments acquisition board, but to the entire system including the computer that houses the National Instruments SCXI card, which will be discussed in more detail in Section 3.3.3. Before the data is obtained and viewed on a computer through the internet, it passes through three stages. Stage

I utilizes an advanced Lab View program that acquires signals from gauges and converts them to physical quantities. The electrical resistance or voltage values obtained by the sensor signals are converted by the DAQ to physical response quantities like strains, accelerations, etc. Although this process is considered a single stage, it does not happen simultaneously; rather, it occurs through complex equipment manufactured by National Instruments and an Lab View program.

3.3.2.2. Communication of Data

The communication of data is the next component of the SHM system. The word communicate is the essential component in the subdivision. The collected data is remotely sent out by wireless connections, telephone lines or cable modem (internet) connection. The communication method used in a particular SHM project depends on a number of factors including accessibility, volume and rate of data, and cost. The communication used in this project was via cable modem which was deemed the best choice considering the availability, cost and data rate.

3.3.2.3. Intelligent Processing of Data

The data retrieved from a sensor must be processed in a manner that is easy to read and economical to store. It is important to understand that the collected data be cleansed or intelligently processed. Efficient and good processing techniques make understanding of data easier, faster and more

precise (ISIS manual 2, 2001). The intelligent processing of data depends solely on the data processing program which is an essential component of a computer based DAQ system. The program allows the computer how often and when to scan the DAQ board, how to process the collected data, and what to save.

Once the numerical data is produced, the next stage, Stage II can start. At this stage, the data is transferred through a data socket mechanism developed by Labview program. This data socket is quite a unique piece of software for data transfer. Rather than creating and then transferring the data, it places the measured numerical data on a communication port that is then removed by an adjacent program, or in the case of Structural Health Monitoring a remote central data server. This does not imply that the data collected on the acquisition system or the onsite computer cannot be saved. It only suggests that the saving of data does not need to occur on site.

As implied in the above paragraph, the data socket mechanism can be used to transfer data from the on-site computer to the central data server located anywhere in the world through an internet connection (Stage III). The central data server currently used in Structural Health Monitoring of the Golden Boy is PC based, and runs a Lab View program similar to that running on the on-site computer. The Lab View program in Structural Health Monitoring is the key not only to web based monitoring, but to monitoring itself. The program can be set to obtain any data that is desired from a data socket located on any of the onsite acquisition systems. Once the Lab View program in the central server has obtained the data it can manipulate it and view it numerically, graphically and

even in an advanced dial gauge like manner. The Lab View program can also be set up to save the manipulated data in various ways that are dependant on time, magnitude and numerical range.

In the case of the Golden Boy, the sensor data collected by the data acquisition system; the Lab View program collects and compresses the data on the onsite remote monitoring computer and is sent via internet connection to the central main computer server at SHM laboratory located at the University of Manitoba. The central server also sends live data results to the web based monitoring system (The ISIS web site for live SHM projects). The whole sequence just explained, is shown in Figure 3-21. The data is decompressed into a text format file of approximately 300 Megs, zipped back to twenty percent of the original size and stored on the main server. The text format file is properly labelled and time stamped for future use and retrieval of data for diagnostic testing and analysis.

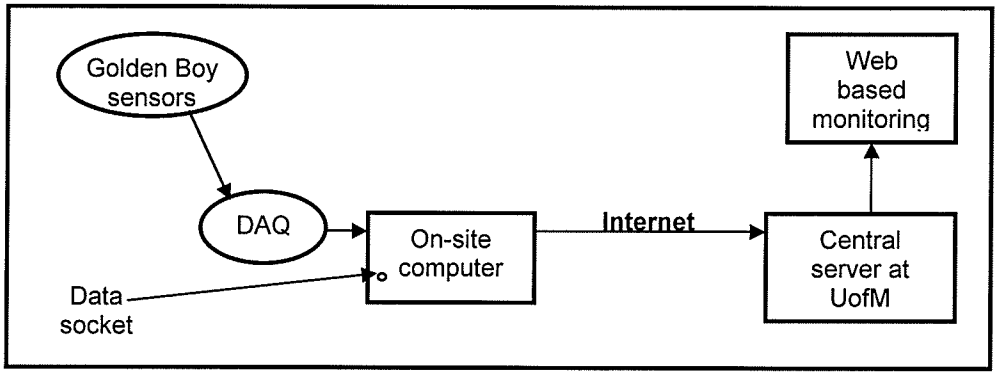

Figure 3-21: A Brief Sketch of Data Transfer Sequence

3.3.2.4. Storage of Processed Data

Once the data has been intelligently processed, it is stored on the central computer's server and is ready for retrieval and/or diagnostics. The central

computer located at the University of Manitoba, in the SHM laboratory at ISIS Canada is stored on the main server. In addition, the data is copied every month on to compact disc and stored for future use, if needed.

3.3.2.5. Retrieval of Data

The collected data which is intelligently processed and stored can be retrieved either before or after the diagnostics as shown in Figure 3-20. The engineer must make a decision in whether or not the data is important for retrieval and storage. The decision is based solely on the significance of the data, but also on the confidence of its interpretation (ISIS manual 2, 2001).

3.3.3. Data Acquisition (DAQ) System

The DAQ system is based on many components which form an integrated system. The DAQ system is by far the most important part of the SHM system. The system consists of the following:

- Sensor devices such as 4 bidirectional strain rosette, two accelerometers, two thermocouples and one ultrasonic wind sensor.
- Cables
- SCXI-1000 chassis
- SCXI modules
- SCXI front mounting terminal blocks
- A/D card

- SCXI cable
- Computer and PC
- Cable modem (Shaw cable)

The DAQ system is connected to a cable modem which is sent via internet to the central monitoring site located at the University of Manitoba. A schematic of DAQ system and the SHM network is shown in Figure 3-22.

All SCXI components and software (Lab View) are manufactured by National Instruments. The SCXI chassis is a rugged, rack mountable enclosure that provides power to the chassis and that route analog signals between modules and the DAQ board (A/D card). The chassis belongs to SCXI-1000 series as shown in the schematic diagram in Figure 3-22. Four modules were installed into the SCXI-1000 chassis. The first module is the SCXI-1520 which accommodates the signal from the strain gauge sensors. The second and third modules are the SCXI-1121 units which accommodate the signal from the accelerometer sensors and the sonic wind sensor respectively. The fourth module is the SCXI-2100 which accommodates the signal from the thermocouples. The SCXI front mounting terminal blocks shown in Figure 3-22 attaches directly to the front of the SCXI modules and provides a convenient method for connecting and disconnecting sensor devices to the system. The model SCXI-1314 front mounting terminal block was mounted to the SCXI-1520 universal strain gauge module. The SCXI-1320 block was mounted to the SCXI-1121 module. A front mounting terminal block was not needed for the SCXI-2100

module due to the easy connections feed available for the thermocouple sensors. An a/d card serial number PCI-MIO-6052 was installed into the PCI slot at the back of the computer modem on site. The SCXI cable (SH6868) was connected to the a/d card and to the back of the SCXI-1000 chassis. The a/d card allows the signal to change from analog to digital and also controls the SCXI system. The remote monitoring computer on-site uses the Lab View software and the SHM system is performed as mentioned previously.

A brief recap of the SHM system; first stage, the data acquisition, second stage, the data socket and the third stage, data transfer as mentioned in Sections 3.3.2.1 and 3.3.2.3, respectively. The Lab View software located in the onsite computer allows the data to be collected at a sampling rate of 32 Hz (32 points per second) which then compresses and moves the data every five seconds to the central server (ISIS SHM laboratory) via internet. The data which is sorted by time and date, is decompressed, zipped and saved on the central server. The central server computer also allows for real-time monitoring on a continuous basis through the ISIS Canada web site (www.isiscanada.com). A link was developed and constructed on the ISIS Canada web site (Page, 2003), labelled "Remote Monitoring LIVE DATA", which allows for real time monitoring of various projects around the ISIS Canada Network and can be viewed by any person around the world at any time. A brief outline on the web based monitoring system is discussed in the previous Section 3.3.4.

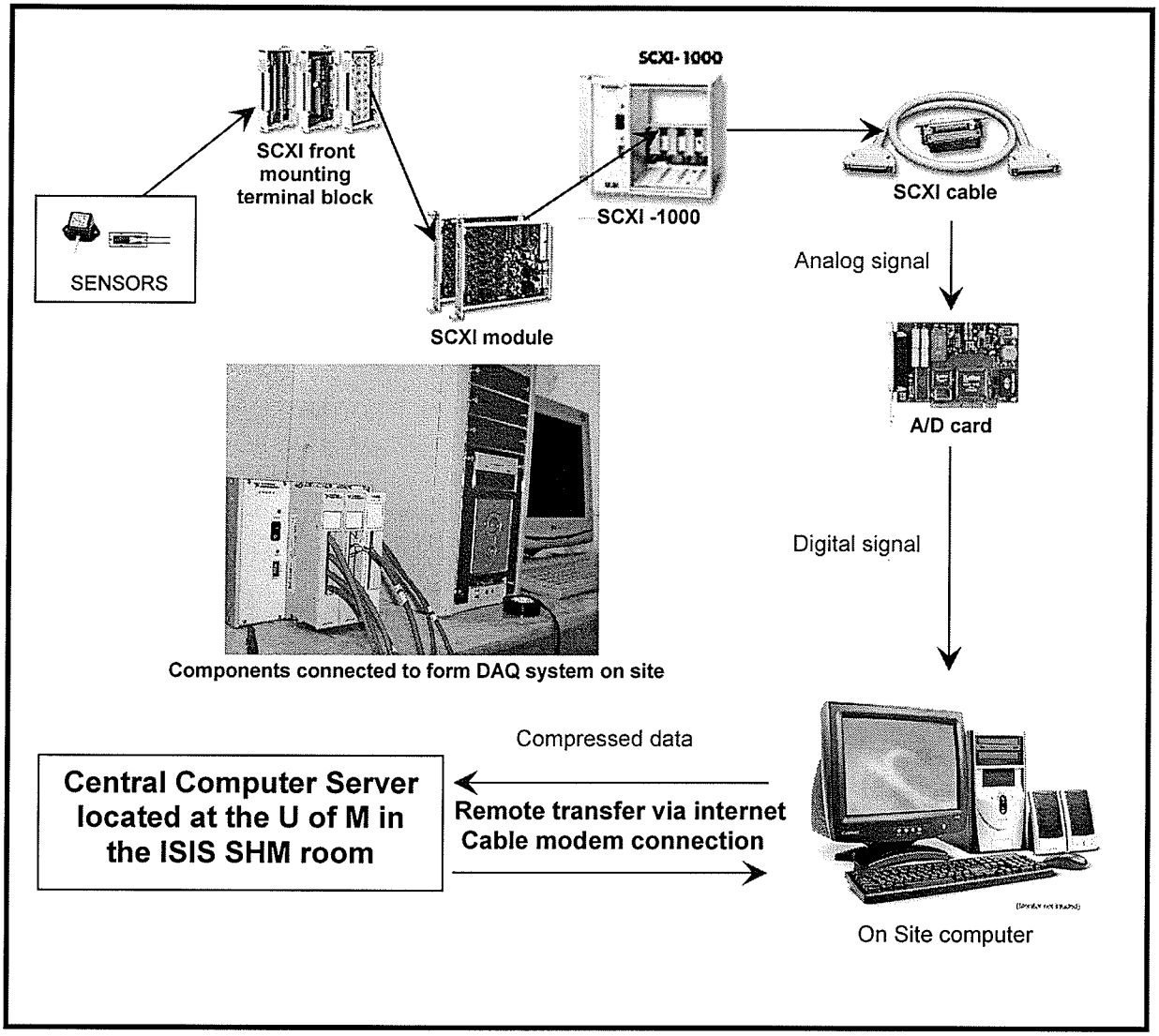

Figure 3-22: SHM Network

3.3.4. Web Based Monitoring

Web based monitoring systems although intricate and complex are no more complex in their final result than any globally accessible web page. They utilize two basic programming languages, HTML coding which provides static viewing and Java script which provides dynamic viewing. The web pages for SHM are primarily designed for Internet Explorer 6, with the allowed accessibility of secondary browsers like Netscape 6.1 or later versions.

These web pages allow the presentation of data in various forms including the graphical forms. The data viewed in a graphical form can be in JPG or GIF format. These images are produced by the Lab View program on the central server.

3.3.5. Installation of the Ultra Sonic Wind Sensor

The preparatory work consisted of selecting and ordering material needed to install the wind sensor on the North West corner of the Legislature's roof. A tripod was manufactured in the Structural Lab at the University of Manitoba. The following materials were needed:

- Two twenty feet long aluminium hollow structural section (dimension: 2"x2"x1/4"HSS)
- Two twenty feet long aluminium angles (dimension: L2"x2"x1/4")
- Box of 11/2" aluminium self tapping screws
- Eight solid concrete blocs
- Two ultrasonic wind sensors and components
- Miscellaneous accessories and materials for fabrication and installation

The tripod was assembled and the legs were bolted into the centre of each concrete block as shown in Figure 3-23. The ultrasonic wind sensors were purchased through Geneq Inc. located in Montreal, Quebec. Two sonic wind sensors of model 50.5 were procured. The wind sensor is a solid-state ultrasonic instrument capable of measuring wind speeds and wind directions. The wind sensor operates at a range 0-50m/s with resolution of 0.1m/s and the wind direction ranging from 0-359 degree with resolution of 1.0 degree. Some of the features are as follows: no moving parts, digital and analog output and operating

temperature between -40 to 70 degree Celsius. The ultrasonic wind sensor weighs 2.5kg and stands approximately 20 inches high and is 10 inches wide (Met One Instruments Inc., 2002).

The ultrasonic wind sensor was then assembled with its components. The sensor mount was aligned horizontally to the top of the rigid tripod and fastened correctly. The sensor mount was re-checked with a leveller and re-tightened for little or no movement. The key bushing was placed inside the sensor mounting fixture. The bushing was positioned and aligned to true North with the use of a portable compass and then fastened by set of screws to the sensor mount. The sensor was then placed correctly into the bushing slot and three captive machine screws were used to secure the sensor to the apparatus.

Once the wind meter was firmly secured onto the tripod, the signal cable was connected at the bottom of the wind sensor. The signal cable length couldn't be more than fifty feet in length as specified by the manufacturer. The signal cables output is in voltage and the signal would be lost if the cable length was exceeded. Since the dome (monitoring room) is located further away than fifty feet, a transformer was needed for converting the signal output voltage into current. The signal cable was pulled through a black flextite electrical conduit and plastic electrical box installed on the angle of the tripod. The conduit continued from the adjacent side of the box down along the roof's level as shown in Figure 3-24 and then through the ventilation shaft located approximately 10 feet away. The ventilation shaft leads to an attic.

The wind sensors also had an external heater provided for de-icing of the sensor arms and preventing the accumulation of ice. The heater consists of a laminated heater material that is custom designed and wrapped around the sensor arms and the sonic sensor element housings. The heater is connected to a temperature controller and is powered by a power supply unit. Both were installed inside the plastic electrical box for weatherproofing and protection.

The next phase was to run a 24 gauge electrical shielded wire from the attic to the remote monitoring room. The wire was routed through the attic along the ducts, up through the attic's roof, along the walls, through the door frame and finally along side of the stairwell up to the remote monitoring room. The transformer and the power supply for the sonic wind meter were placed and attached along the wooden frame inside the attic near the ventilation shaft. The wire was connected to the transformer which converts the signal from voltage to current. The other extremity of the wire was connected to the SCXI terminal box in the DAQ system located at the remote monitoring room. The signal is then converted back into voltage by an ohm resistor located in the SCXI terminal box. The sonic wind sensors were calibrated at the factory prior to shipment, therefore, there was no need for calibration. The operation manual (Met One Instruments Inc., 2002) does however mention a way to quick check the sensor (optional). The quick check was performed and consisted of covering the sensors, reading the voltage with a volt meter and then checking the table reference guide given in the operation manual of the wind sensor. The sampling

rate of the ultrasonic wind sensor is 1 Hz. All other instrumentations are sampled at 32 Hz.

The installation of a camera on the Legislature's roof was installed and connected to the computer server for continuous visual monitoring of the Golden Boy anytime during the day through the web page. The camera was installed next to the ultra sonic wind sensor and is shown at the bottom of Figure 3-24.

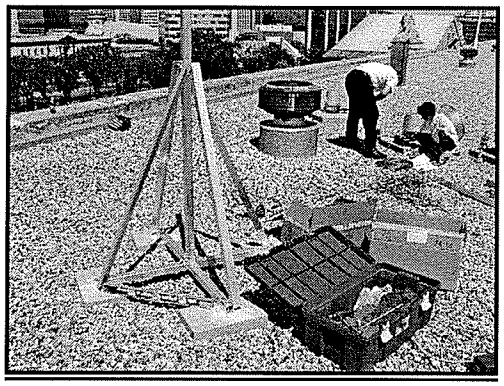

Figure 3-23: Levelling of Blocks and Tripod Installation on the Legislature's Roof

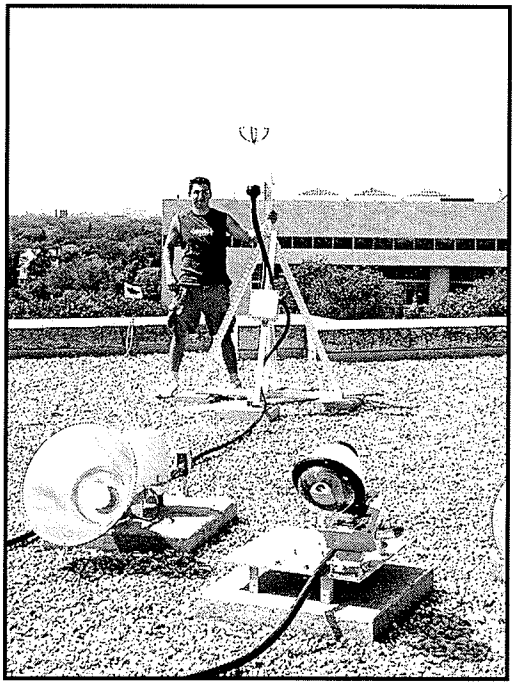

Figure 3-24: Wind Sensor and Camera on the North-West Corner of Legislature's Roof

3.4. LOCATION OF SENSORS

A schematic layout of the sensors on the shaft of the Golden Boy is shown in Figure 3-25. The location and orientation of the sensors were discussed in the previous section. The sensors are labeled correspondingly to the Golden Boy's global coordinate system. The Golden Boy faces true north and the sensors were installed relative to its directions. Plan views of the shaft are shown in Figure 3-25 along with the global coordinate system. The sensors will be referred by the identification labels as described earlier in this report. Note that S.G.N refers to the strain gauge located on the north axis of the shaft. S.G.E refers to the strain gauge located on the east axis of the shaft and vise versa. The odd numbered strain gauges refer to the horizontally, and the even numbered strain gauges refer to the vertically positioned sensors in the bi-directional strain rosettes. The two thermocouples are positioned directly underneath the west and east rosettes and are labeled by TC.1 and TC.2 respectively. The two accelerometers were positioned on the top of the shaft and placed on the north and south axis at an equal distance away from the centre of gravity of the stainless steel shaft as shown in Figure 3-25. The labeling of the FBG sensors begin with two letters, and then a digit. The two letters denote the global axis location on the shaft and the digit refers to the orientation angle of the FBG positioned to the face of the shaft. All of the odd numbered FBG sensors are orientated at forty-five degree angles and all of the even numbered FBG are orientated at zero degree angles. For example, "NW1" notation refers to the FBG located on the north-west axis of the shaft at an angle of forty-five degree and "SE2" refers to the FBG located on

the south-east axis of the shaft at an angle of zero degree as shown in Figure 3-25.

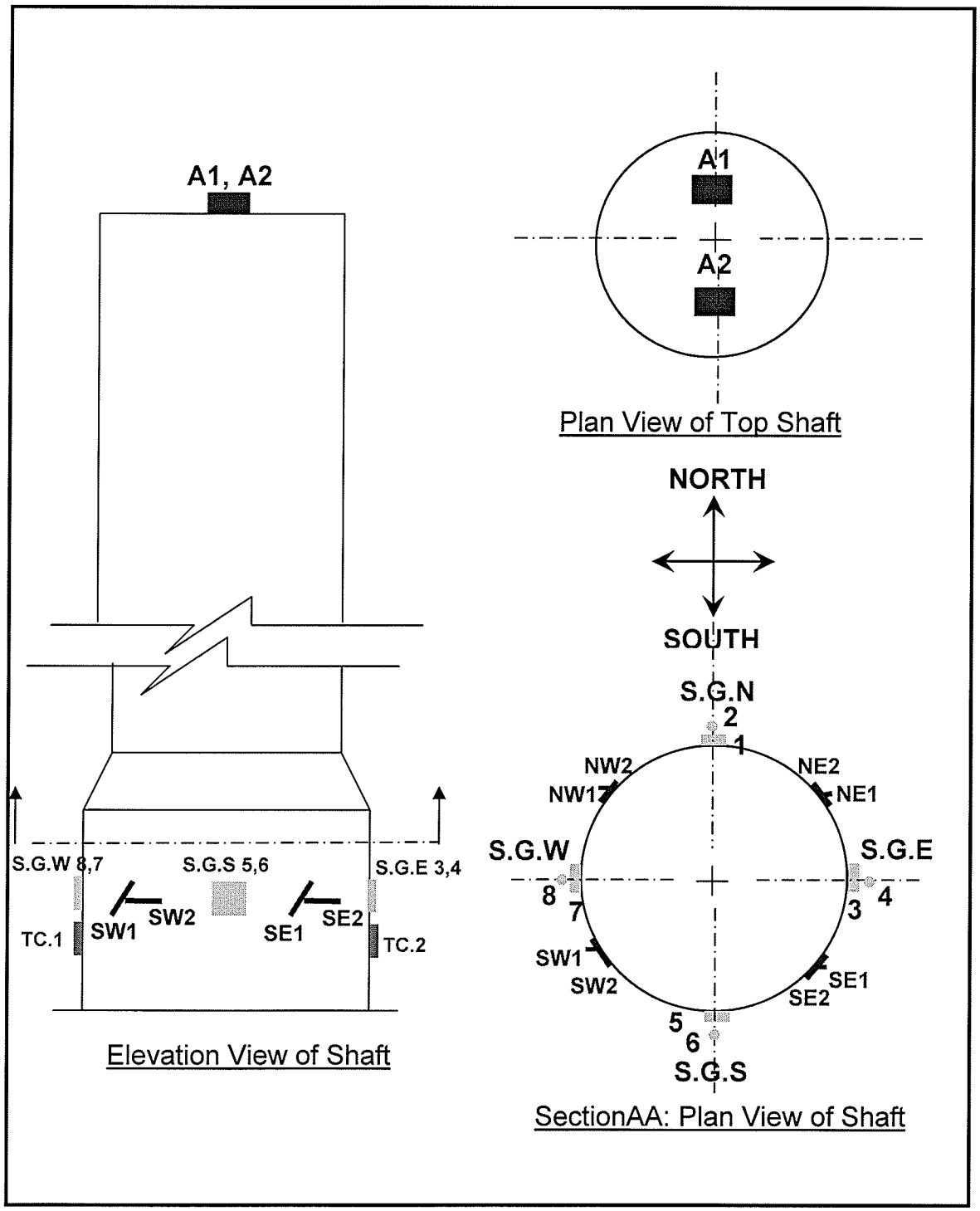

Figure 3-25:Location and Identification of Sensors

3.4.1. Damaged Instrumentations

As the restoration and instrumentation process was completed, the Golden Boy made its way back to the top of the Legislature's dome, where it will remain for many years to come. All instrumentations were safely secured and protected. A team of workers preformed the difficult task of placing the Golden Boy at the top of its perch. The six inch diameter shaft was to be secured at a distance approximately three inches away from the sensors but due to an unfortunate mishap the Golden Boy's shaft descended further than expected. The sensors covered approximately six inches around the circumference of the shaft and were heavily protected. The protection around the shaft was able to save some sensors, but unfortunately most of the protective coating was damaged and slipped slightly upwards (one inch) towards the bottom of the Golden Boy's plate. The extent of the damage was not known because the sensors were not visible. The repair did not include the relocation and replacement of the sensors due to the lack of time and resources. Repair consisted of adjusting the instrumentation as close to the original position and re-applying a protective covering over the damaged one. The Golden Boy's shaft was then placed correctly into the fixity of the dome, fastened and tightened with bolts. In addition, the sensors were re-checked and unfortunately not all sensors were in working order. The following gauges were confirmed to be damaged and the identifying labels can be used to locate them in Figure 3-25:

1. North axis, vertical rosette strain gauge, S.G.N.2
2. South axis, horizontal rosette strain gauge, S.G.S.5
3. West axis, horizontal rosette strain gauge, S.G.W.7
4. Bragg grating sensors, NW1, NW2, SW1,SW2, NE1, NW2, SE1, SE2

3.4.2. Role of Civionics Specifications

As indicated in the previous sections in this report, correct installation and protection of sensors are crucial for a successful SHM system. Based on past experience, where sensors were not installed correctly, maintained properly, and wiring was not secured, ISIS Canada developed some guidelines to avoid such problems. The guidelines on the sensor installation (ISIS Design Manual 1,2001) and the upcoming design manual on Civionics Specifications would be very helpful for future SHM projects by ensuring proper installation, protection of the instrumentation, wires, conduits etc.

4. THEORITICAL ANALYSIS

4.1. STRUCTURAL MODEL

The Golden Boy sculpture is a very unique and complicated structure that has many different angles and curvatures around its perimeter. The formation of a mathematical model of the structure is an important stage of any engineering analysis. The model will help to idealize the structure so that a practical dynamic and static analysis can be performed. For the present study, the Golden Boy structure is modeled with a number of assumptions which are explained later. The model allows theoretical predication and behaviour under externally applied loadings.

The Golden Boy is illustrated in Figure 4-1. The sculpture is hollow and is attached at two locations. The first location is near the bottom, directly above the plate and below the Golden Boy's left heel as shown below. The brass plug connects the Golden Boy's left foot to the circumference of the stainless steel shaft. The second location is at the top of the stainless steel shaft which terminates at torso height of the Golden Boy as shown in Figure 3-6.

The mathematical model of the structure has been constructed based upon the following assumption. The connection at the bottom is very near the point of fixity, therefore it will not be treated as a point which transfers the external forces. Both surface areas can be modeled by a rectangular cross section as shown below in Figure 4-2. The front and rear of the Golden Boy corresponds to north

and south face respectively and the sides to the east and west. The surface area is $3.8m^2$ and $3.23m^2$ respectively. The centre of gravity (c.g) of the statue was estimated visually at Pritchard machine shop. Measurements were taken from the bench-mark located at the c.g of the steel armature, directly beneath the left foot to a fictitious point inside the sculpture. The north and south face plane had an eccentric c.g whereas the east west face plane lied directly in line with the armature's centre of gravity as shown below in Figure 4-2. The top connection is attached at torso height which is near the vicinity of the centre of gravity of the Golden Boy structure. Therefore the centre of pressure due to the wind action will be take directly at the centre of gravity of the structure and all external forces will be transferred through the centre of gravity.

The internal mechanism involved in holding up the statue consists of a 3556mm (140 inch) stainless steel shaft, with an actual diameter of 152.4mm (6 in.). The stainless steel characteristic consists of 17-4 chromium nickel precipitation/age hardening martensitic double aged (Dillon Consulting Ltd., 2002). The shaft had modification done at the shop; it consisted of bending the steel armature slightly to accommodate the internal structure and machining to the appropriate cross-section. The length of the shaft from tip, directly vertical to the top measures 3505.2mm (138 in.). The bottom 755.65mm (29 ¾ in.) has a diameter of 152.4mm (6 in.) which then has a transition of 40mm to a diameter of 127mm (5 in.) to the top of the steel shaft. A schematic representation of the armature and dimension is shown in Figure 4-3.

The theoretical model for the structure is represented best by a cantilever beam so that the forces in the structure may be determined with reasonable accuracy. The cantilever beam is assumed to be vertical with a length of 2750mm and constant cross-sectional diameter of 5.5 inches (139.7mm) shown in Figure 4-3.

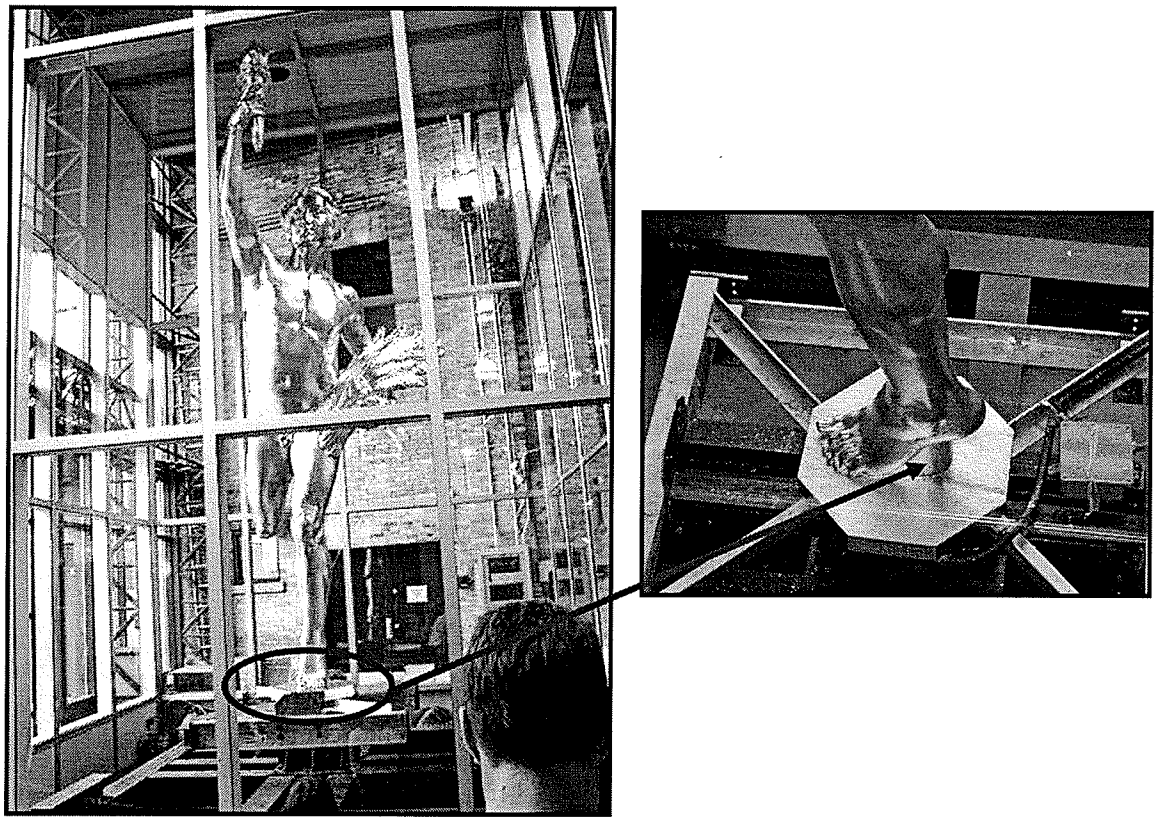

Figure 4-1: The Golden Boy and the Brass Plug

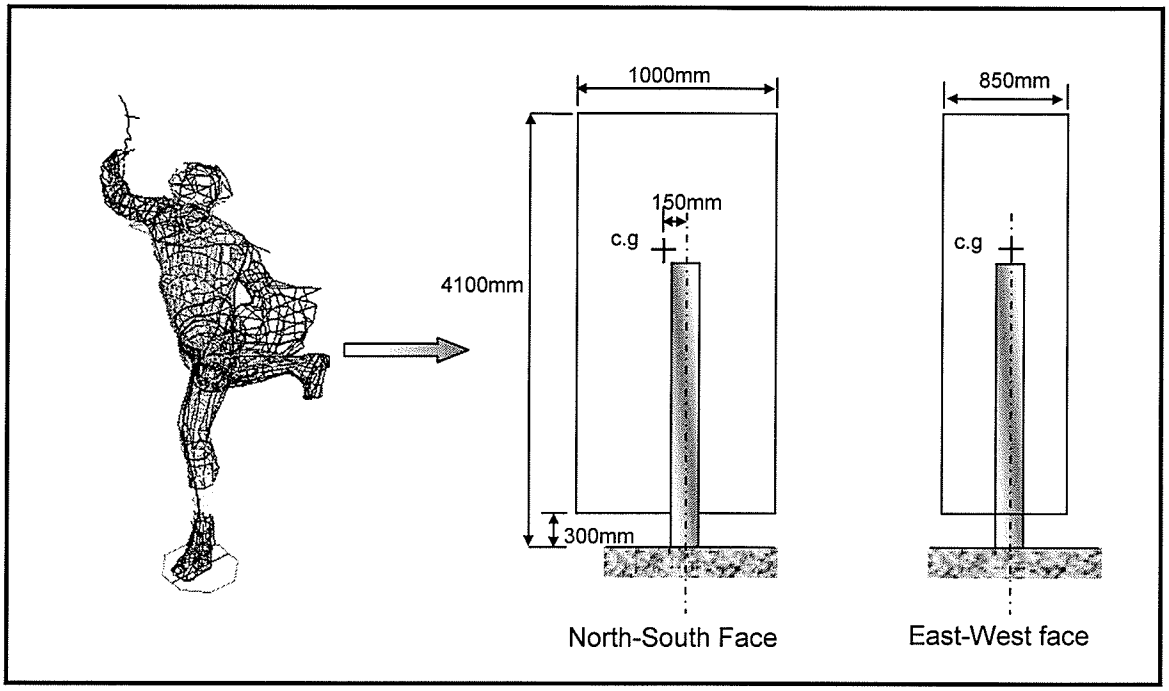

Figure 4-2: Schematic Representation of the Golden Boy with Rectangular Cross Section

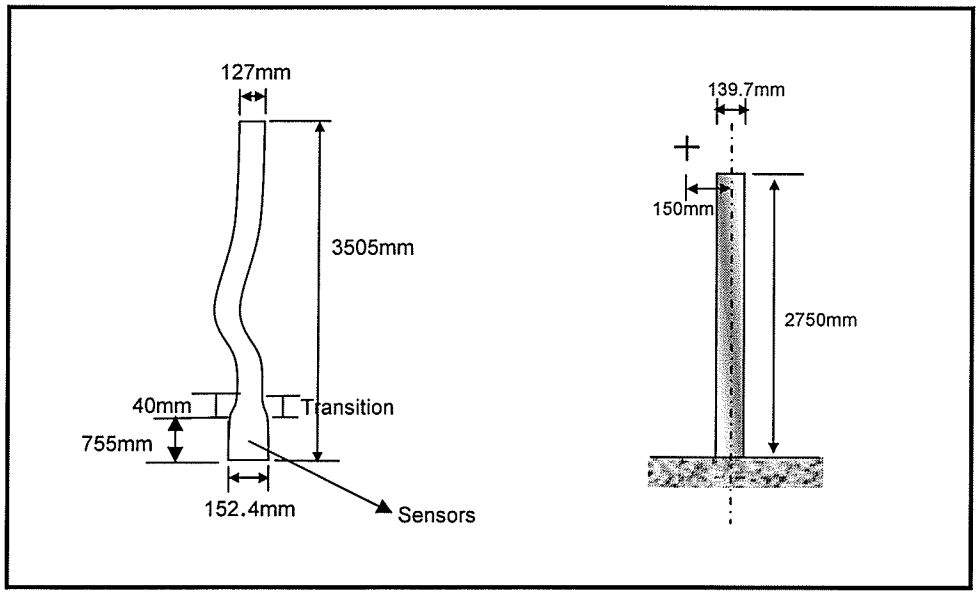

Figure 4-3: Actual Dimension and Theoretical Representation of the Shaft

4.2. NOTATION AND SIGN CONVENTION

The following notations will be used in this report. The sign for the cross sectional face is determined by the direction of the outward normal vector as shown in Figure 4-4. The moment (M_{yz}) first subscript y defines the direction of the outwardly directed normal vector to the face of the cross section and the second subscript z defines the coordinate directions of the force or moment component (Lardener & Archer, 1994).

The following sign convention will be used in the report. Figure 4-5a) shows the positive directions of the internal normal, shear force and moments on the cut member. In the left hand face of the cut member, the normal force N acts to the left, the internal shear force V acts downwards and the moment M acts counterclockwise. According to Newton's third law, the forces and moment on the right hand face of the cut member must be equal in magnitude but opposite in direction. Figure 4-5b); positive normal force tends to elongate the member, Figure 4-5c); positive shear force tends to rotate the member clockwise, Figure 4-5d); positive moment tends to bend the member concave upward, which elongates the bottom chord in tension and shrinks the top chord into compression.

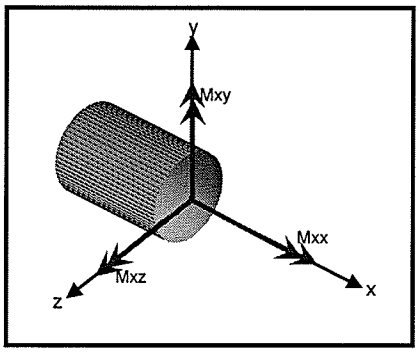

Figure 4-4:Positive Moment Vector Notation(Lardener & Archer, 1994)

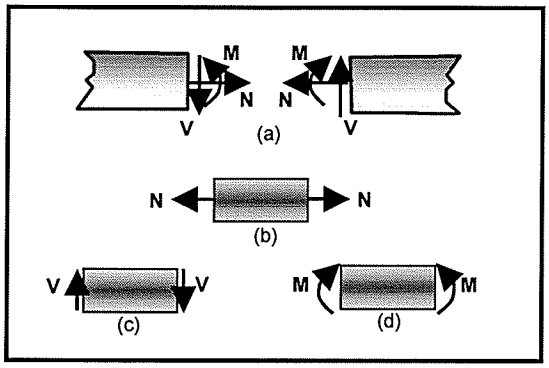

Figure 4-5:Positive Sign Convention (Hibbeler, 1998)

4.3. STATIC ANALYSIS

An elastic section analysis for predicting the response of a stainless steel cantilever beam, loaded dynamically and statically is presented. Schematic representation of the 3D structural model, the external loading applied on the centre of gravity of the Golden Boy and the dimensions is shown in Figure 4-6a).

The cantilever beam can be seen as a great load-carrying member, which is classified as a slender member. A slender member is a member whose length is much greater (at least 5 times) than either of its cross-sectional dimensions (Lardner & Archer, 1994). The north wind direction will be used, since it is the most critical, most dominant wind and acts on the largest surface area (North or South). An analysis of any wind direction would follow the same process. Figure 4-6a) shows the resultant component due to the wind (W) acting along the surface area of the Golden Boy's north face (wind coming from North), along with the dead load (D). The cantilever is considered as having a fixed support at the base and allows no relative rotation and translation between the connected members, therefore the support exerts two force components and a moment

(Hibbeler, 1999). Figure 4-6b) shows the north face of the structure in the y-x plane, the external dead load (parallel to the plane) and reactions. The eccentric dead load can be due to the weight of the structure, any other live load (snow, ice, rain ect..) or a combination of both. Figure 4-6b) can be reduced to a force couple system at an arbitrary point O as shown in Figure 4-7. In addition, the internal forces and moments which vary along the length of the beam are present as well as the reactions.

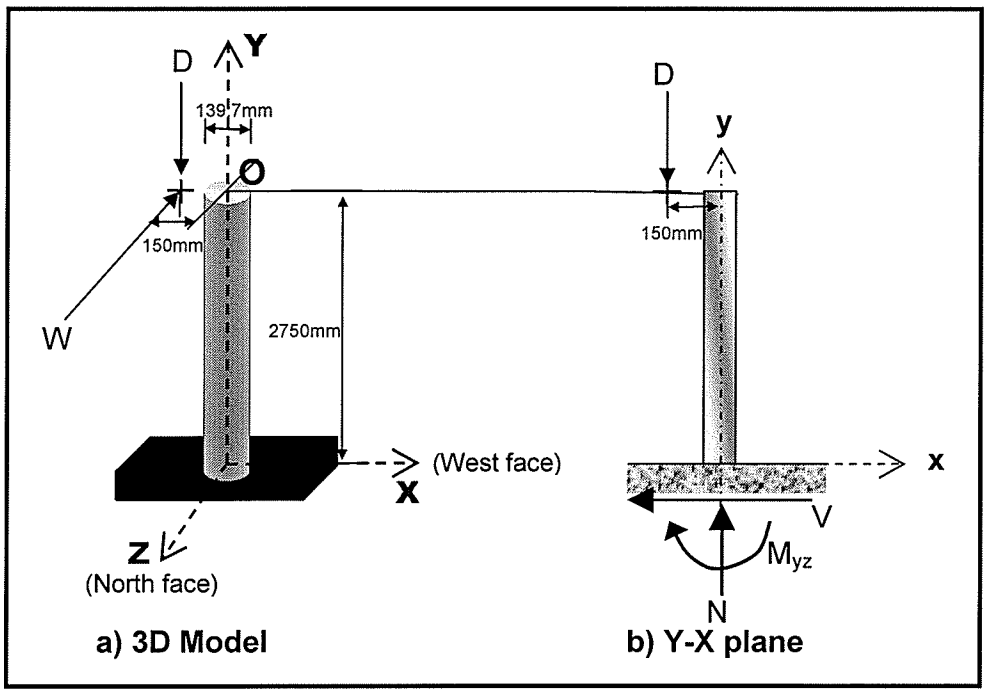

Figure 4-6:Free Body Diagram

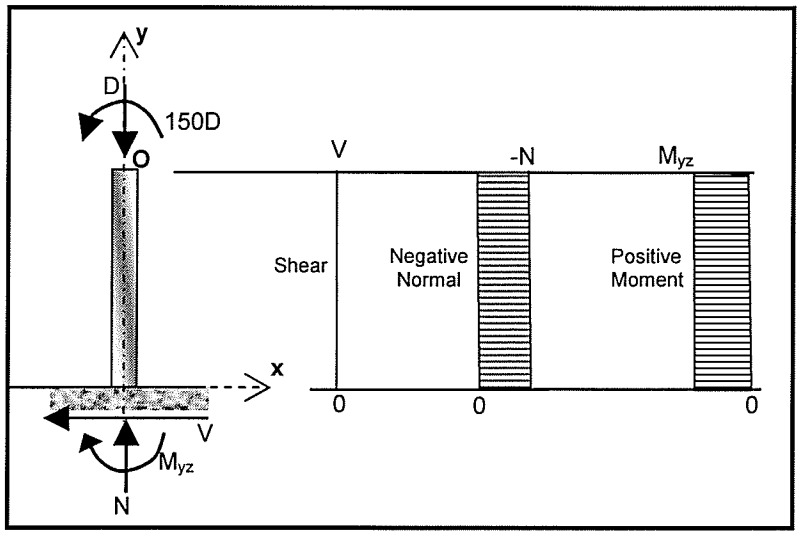

Figure 4-7:Force Couple System with Forces and Moment Distribution

It is important to note that the free body diagram shown in Figure 4-7 is at a state of equilibrium therefore is given by:

$\sum Fx = 0$ (summation of forces in X); V=0

$\sum Fy = 0$ (summation of forces in Y); N=D

$\sum M = 0$ (moment about the fixity); M_{yz}=150D

A two-dimensional loading in the y-z plane (west face) on the cylindrical cantilever beam and the shear and moment diagrams is shown in Figure 4-8. The wind force W acts at a distance of 150mm away, parallel to the y-z plane as shown in Figure 4-6a). It creates a force couple system which is shown in the Figure 4-8 at location O. The double headed vector (T_{yy}) denotes a twisting moment or Torque. The same subscript notation and sign convention is used as previously mentioned.

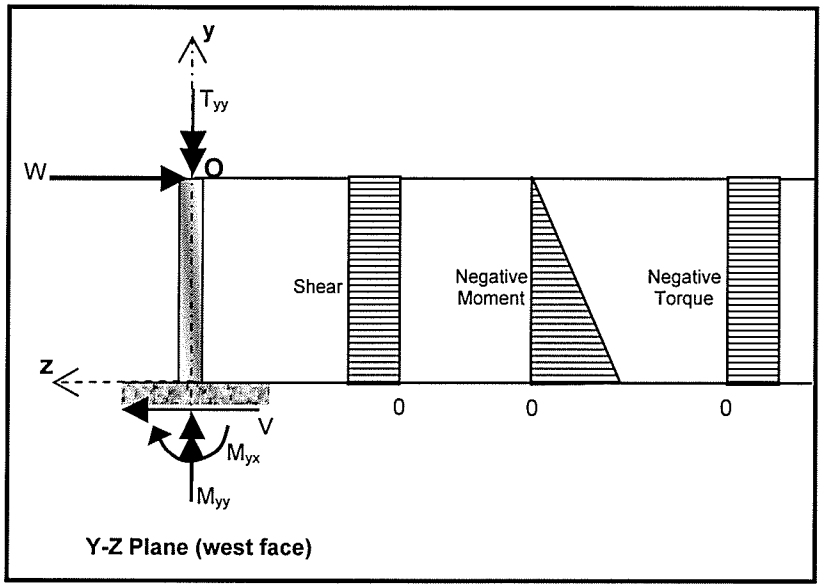

Figure 4-8: Free Body & Internal Distribution

The free body diagram shown in Figure 4-8 is in the state of equilibrium therefore the following is true:

$\sum Fz = 0$ (summation of forces in Z); V=W

$\sum Fy = 0$ (summation of forces in Y); N=0

$\sum Mx = 0$ (moment about the X-axis from the fixity); M_{yx}=2750W

$\sum My = 0$ (moment about the Y-axis from the fixity); M_{yy}=T_{yy}=150W

4.4. STRESSES

4.4.1. Axial Stress

The force couple shown in Figure 4-7 produce two types of stresses on the circular shaft, axial stress and bending stress. The axial stress is given by:

$$\sigma_A = \frac{-D}{A} \tag{4.1}$$

where: σ_A = Axial stress D = Axial force A= cross-sectional area

The axial force tends to shorten the member due to the compressive force therefore it is said to produce a negative stress.

4.4.2. Bending Stress

The moment at the free end of the cantilever beam shown in Figure 4-7 produces a constant moment distribution throughout the length of the beam. The bending stress is given by:

$$\sigma_{yz} = \frac{(M_{yz})x}{I_z} \tag{4.2}$$

where:

σ_{yz} = normal stress
I_z= moment of inertia of the cross section about the z-axis passing through the centroid
x= distance from the centroid of the cross section to an extreme point along x-axis
M_{yz} = bending moment

The maximum bending moment occurs at the base of the cantilever beam shown in Figure 4-8 and the stress distribution at the cross section is shown in Figure 4-9 and the bending stress is given by:

$$\sigma yx = \frac{M_{yx} * Z}{Iy} \tag{4.3}$$

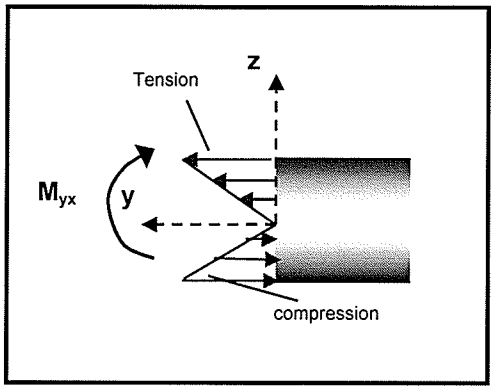

Figure 4-9: Two Dimensional Representation of Stress Distribution and Bending Moment

4.4.3. Shear Stress

The Torque (T_{yy}) is constant throughout the length of the beam and the shear stress distribution is shown in Figure 4-10. The shear stress distribution is linear and maximum at the outer part of the cylinder. The shear stress is given by:

$$\tau = \frac{Tyy * r}{J} \tag{4.4}$$

$$J = \frac{\pi * r^4}{2} \tag{4.5}$$

where;

τ = shear stress
J = polar moment of inertia
r = radial distance from the axis

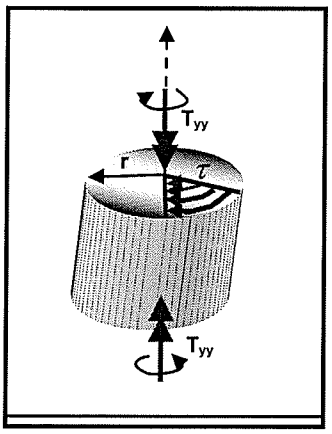

Figure 4-10: Shear Distribution

4.4.4. Combined Stresses

The cantilever beam acts as a slender member and is an important structural component for the Golden Boy. At different angles or directions of wind acting on the surface of the structure, the stainless steel shaft experiences many different types of combined stresses caused by axial, torsional and transverse bending loads. At any given point on the cantiliver beams cross-section we are able to combine the different stress states. The most critical location is near the point of fixity of the cantiliver beam. A schematic representation of the different states of stresses acting near the point of fixity is shown in Figure 4-11.

The combined state of stress corresponds to the addition of all four stress resultants, torsion, bending about the x-axis, bending about the z-axis and axial force as shown in Figure 4-11. The cross sections are taken near the fixity of the shaft and their corresponding tensile and compressive stresses are indicated by arrows pointing down for compressive stresses and arrows pointing up for tensile stresses.

The maximum value of the shear stress due to torsion occurs at all points of the outside surface where radius is maximum in Eq.(4.4). The maximum value of bending stress occurs at the extreme points where the radius is at its maximum. Bending about the x-axis, the maximum value of bending stress can be calculated by Eq.(4.3), and it occurs along the lines on the outer surface where z= ± (diameter)/2. Also, the maximum bending stress about the z-axis can be calculated using Eq.(4.2) which occurs along the lines on the outer surface where x = ± (diameter/2). The maximum axial stress is uniform over the cross-sectional area and can be obtained from Eq.(4.1). Combining the stresses at appropriate segments, we are able to calculate the principle stresses and the maximum shear stress at any given point by using Mohr's circle.

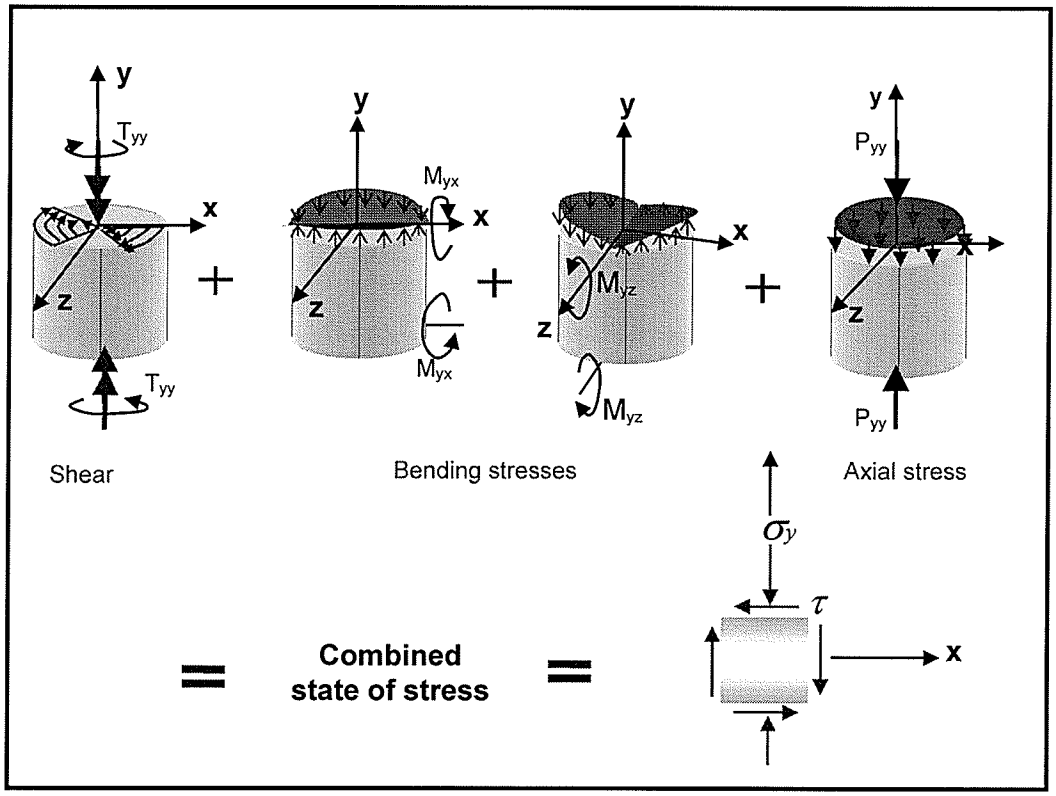

Figure 4-11: Combined States of Stress

4.4.4.1. Mohr's Circle Representation

The Mohrs circle representation will be based on the axis orientation that has been followed throughout this report; the Y-axis pointing directly upwards to the sky, the Z-axis along the north- south orientation and the X-axis along the east-west orientation of the Golden Boy.

The construction of the Mohr's circle for plane stress is shown in Figure 4-12, with the corresponding equations 4.6-4.9. The compresive normal stresses are plotted to the left and the tensile stresses are plotted to the right of the vertical shear stress axis. Shear stress τ is shown along the vertical axis and normal stress σ, along the horixontal axis. This sign covention is adapted from T.J Lardner and R.R Archer (1994). σ_1 and σ_2 denote the principle stresses.

$$\sigma_{AV} = \frac{\sigma x + \sigma y}{2} \tag{4.6}$$

$$\tau_{\max} = \sqrt{\left(\frac{\sigma x - \sigma y}{2}\right)^2 + \tau^2} \tag{4.7}$$

$$\sigma 1 = \sigma_{AV} + \tau_{\max} \tag{4.8}$$

$$\sigma 2 = \sigma_{AV} + \tau_{\max} \tag{4.9}$$

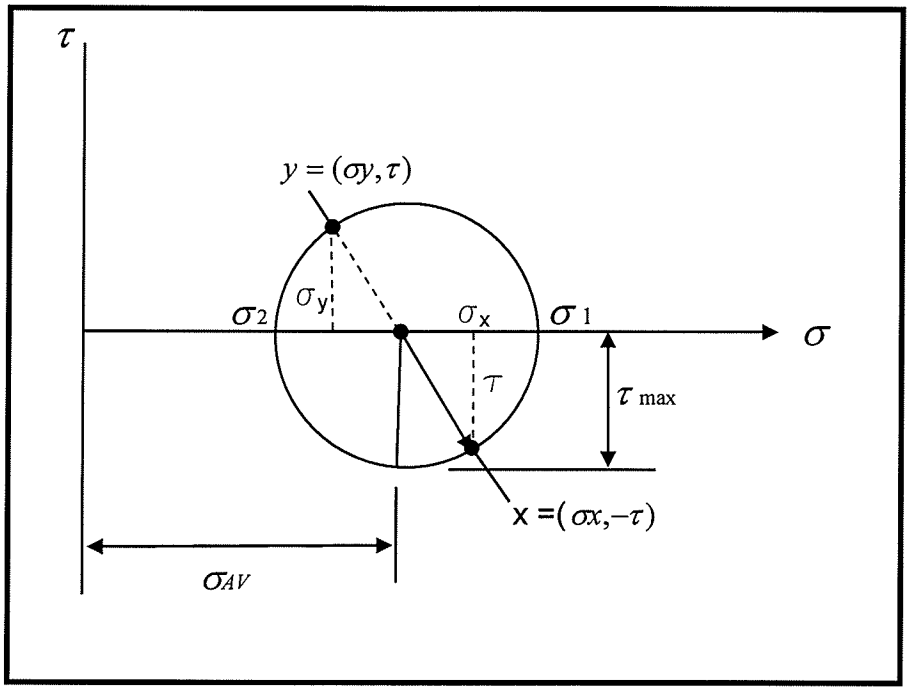

Figure 4-12: Mohr's Circle (Lardner & Archer, 1994)

4.5. STRAIN

The stress-strain relationship in the elastic region of the material is linear and is often a one-dimensional Hooke's law for stress and strain (Lardner and Archer, 1994).

Two types of strain, normal and shear strain are directly related to the linear elastic stress-strain curve, and they are given by Eq. 4.10 and 4.11, respectively.

$$\varepsilon = \frac{\sigma}{E} \tag{4.10}$$

$$\gamma = \frac{2 * \tau(1+\nu)}{E} \tag{4.11}$$

Where;

ε is the normal strain in the shaft.
σ is the normal stress in the shaft.
E is the elastic modulus of the material.
γ is the shear strain in the shaft.
τ is the shear stress in the shaft.
ν is poisson's ratio of the material.

4.6. WIND LOADING OF 100 YEAR WIND STORM (NBCC,1995)

The full scale modelling of the wind climate was utilised for the Golden Boy. The purpose was to obtain a representative wind velocity and direction for the wind tunnel model. Due to the lack of wind climate information available for Winnipeg, the wind climates for Regina and Minneapolis for a 100 year return period were used. The direction characteristic for the two cities depict the stronger winds coming from the North and Northwest as previously mentioned (D.A Kopp and D.Surry,2001). The NBCC 95 reports that for a 100 year mean hourly wind speed, 10 meters above ground in open country terrain (e.g., airport), the wind pressure is q=0.49 kPa. For suburban terrain, the mean hourly wind speed at height of 72 meters above ground (Golden Boy) is q=0.485 kPa. The equation 4.12 provides design wind loads for bridge substructures and superstructures. All winds loads based on the reference wind pressure, q, shall be treated as equivalent static loads (CAN/CSA-S6-00, 2001). The NBCC loading provisions for external pressure due to wind are as follows

$$p = q * Ce * Cg * Cp \qquad (4.12)$$

where:

q= wind pressure in NBCC $\left(\frac{1}{2}*\rho*\overline{V}^2\right)$

Ce=exposure factor
Cg=gust factor
Cp=external pressure coefficient
ρ = mass density of air ($100x10^{-6}$ KN/m^3)
$\overline{V}$ =Velocity of winds (0.1,0.033,0.01 probability of exceedance)

Analysis for the 100-year wind storm.

The 3D model is shown in Figure 4-6a) with the appropriate dimensions and wind direction approaching from the North. The 100 year wind acting at the worst wind direction at a height above ground of 72 meters is q=0.485Kpa.

The corresponding wind speed is calculated by the following equation:

$$q=\left(\frac{1}{2}*\rho*\overline{V}^2\right)\Rightarrow\overline{V}=\sqrt{\frac{2q}{\rho}}=\sqrt{\frac{2*0.485}{100x10^{-6}}}$$ =98.5 Km/hr

The following factors were used, the exposure factor Ce=1.5 (NBCC 95,table 4.1.8.1), gust factor Cg=2.5 (NBCC 95, sec 4.1.8) and external pressure factor Cp=1.3 (NBCC,sec 4.1.8). The external wind pressure is calculated by Eq.4.12

$p=q*Ce*Cg*Cp$ =0.485*1.5*2.5*1.3=2.37 Kpa

The resultant force W acting at the centre of pressure shown in Figure 4-6 is calculated by:

W=p*A

where; A=surface area of the Golden Boy according to the direction

north face of the Golden Boy has an approximate surface area of 3.8m^2 as shown in figure 3.3.

W=2.37*3.8=9.0kN=9000N

The weight of the Golden Boy and the internal shaft is approximately 1575Kg. It was obtained by subrtracting the weight of the cradle from the overall weight of the structure and the cradle. The crane erection company, Litz, was responsible for the weighing procedure on the scale.

The dead load D is calculated using Newton's Second law.

F=ma where; F=force, m=mass, a=acceleration(gravity)

D=1575kg*9.81m/s^2=15450N=15.45KN

The cross-sectional properties of the cylindrical cantilever stainless steel beam are shown below; d=139.7mm (5.5 inch diameter).

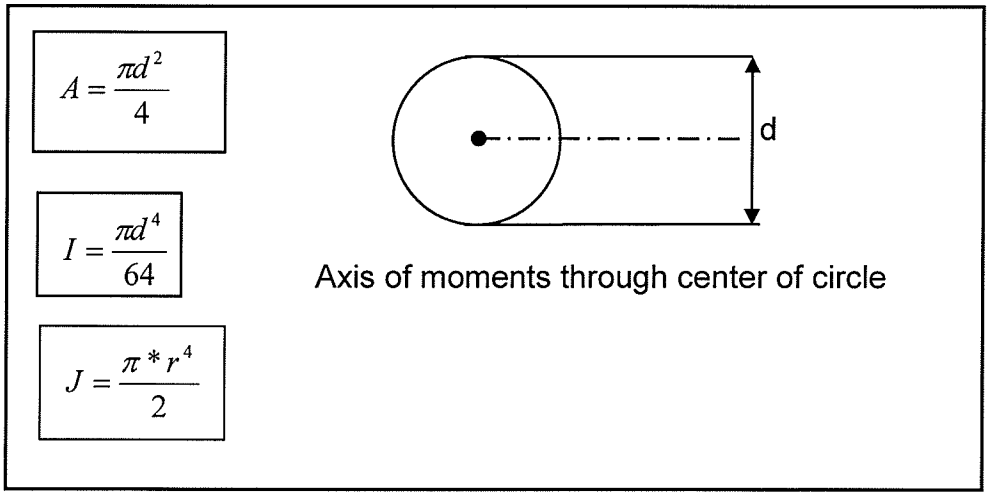

Figure 4-13: Geometric Properties of the Shaft

The cross-sectional area and moment of inertia are calculated

$$A = \frac{\pi d^2}{4} = \frac{\pi * (139.7)^2}{4} = 15328 mm^2$$

$$I = \frac{\pi d^4}{64} = \frac{\pi * (139.7)^4}{64} = 18.696 \times 10^6 \ mm^4$$

The bending moments M_{yz} and M_{yx} are calculated from the free body diagrams and the state of equilibrium shown in Figure 4-7 and Figure 4-8, respectively.

M_{yz}=150*D=150*(15450N)= 2,317,500 Nmm

M_{yx}=2750*W=2750*(9000N)= 24.75×10^6 Nmm

The torque moment T_{yy}, as shown in Figure 4-8 is calculated by

$M_{yy}=T_{yy}$=150*W=150*(9000N)=1,350,000Nmm

The axial load D gives rise to a compressive normal stress distributed uniformly over the cross section of the shaft, represented in Figure 4-7 and is calculated according to Eq.4.1

$$\sigma_A = \frac{-D}{A} = -15450/15328 = -1.01 \text{ Mpa}$$

The torsional shear stress, τ, distribution across the shaft is a result of the twisting moment T_{yy} , and is calculated according to Eq.4.4 and Eq.4.5

$$J = \frac{\pi * r^4}{2} = \frac{\pi * (139.7/2)^4}{2} = 37.39 \times 10^6 \ mm^4$$

$$\tau = \frac{Tyy * r}{J} = \frac{1350000 * (139.7/2)}{37.39x10^6} = 2.54 \text{ Mpa}$$

The shear stress, f_v, is due the shear (wind) load of 9KN and is calculated as follows:

$$f_v = \frac{4W}{3A} = \frac{4 * 9000}{3 * 15328} = 0.78 \text{Mpa}$$

Both bending moments act on a positive y face and are bending about two different axes, one being the x axis and the other the z axis as shown in Figure 4-11. The normal bending stresses are calculated by Eq.4.2 and Eq.4.3.

$$\sigma_{yz} = \frac{(M_{yz})x}{I_z} = \frac{2317500 * \left(\frac{139.7}{2}\right)}{18.696x10^6} = 8.7 \text{ Mpa}$$

$$\sigma yx = \frac{M_{yx} * z}{Iy} = \frac{24.75x10^6 * \left(\frac{139.7}{2}\right)}{18.696x10^6} = 92.5 \text{ Mpa}$$

The combined state of stresses corresponds to the addition of the four separate states of stress on any point or segment on the outer surface of the shaft. The four segments which are important are the north, south, east and west segments of the outer surface. The north-south elements lie along the line $z = \pm d/2$ and the east-west segment lie along the line $x = \pm d/2$. The north and south segment are critical due to the higher normal bending stress (σ_{yx}) which has a value of ± 92.5 Mpa. The north side of the shaft, the bending stress is tensile and the opposite side (south) the bending stress is compressive as shown in Figure 4-11. Since the axial stress is compressive (-1.01Mpa) throughout the cross section, it will add to the compressive stress (-92.5Mpa) on the south segment and

decreases the tensile stress on the north segment of the shaft. Therefore the south segment is the critical one, and is shown below in Figure 4-14.

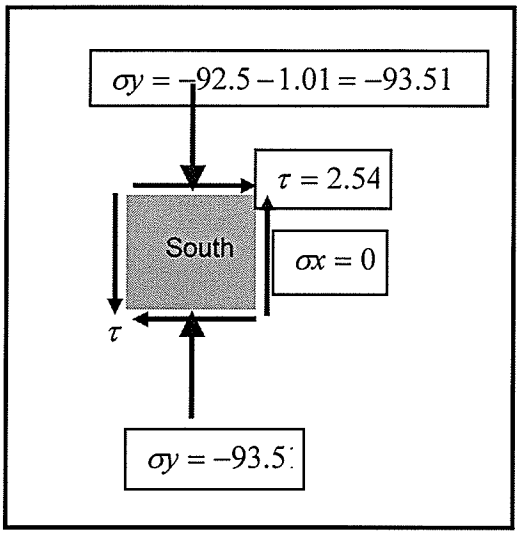

Figure 4-14:Critical Section(South)

The principle stresses and the maximum shear stress are found by using the Mohr's circle representation as shown in Figure 4-12. Therefore,

$$\sigma_{AV} = \frac{\sigma x + \sigma y}{2} = \frac{0 + (-93.51)}{2} = -46.76$$

$$\tau_{max} = \sqrt{\left(\frac{93.51}{2}\right)^2 + (2.54)^2} = 46.82\text{Mpa}$$

$$\sigma_1 = \sigma_{AV} + \tau_{max} = -46.76 + 46.82 = 0.06\text{Mpa}$$

$$\sigma_2 = \sigma_{AV} - \tau_{max} = -46.76 - 46.82 = -93.58\ \text{Mpa}$$

Discussion

The maximum principle stresses due to the combined stresses are calculated. It is seen that due to the very small eccentric loading of the shaft, a very small torque moment (1.35KNm) or shear stress (2.54Mpa) is produced. The torque moment amounts to only 5.4% of the bending moment. The axial stress (-1Mpa) is also very small which amounts to only 1.1% of the bending stress (92.5Mpa). The bending stress is the most significant part. The maximum combined bending stress is 93.5 Mpa which is very close to the maximum principle stress of 93.58 Mpa, which is marginally higher (0.08%). The shear stress is only 2.75% of the normal bending stress. Therefore it is fair to say that the analysis of combine stresses is no longer needed. Our main objective is the dynamic analysis of the wind on the Golden Boy. The effects of the eccentric loading and dead loads to the Golden Boy has no significant effect on the outcome of the maximum principle stress.

4.7. DYNAMIC ANALYSIS

The Golden Boy is one of many different types of structures. Many structures possess different numbers of degree of freedom (DOF) and there exists a natural frequency (or natural period) of vibration corresponding to each mode of vibration. The most important step in analysis procedures is defining a mechanical model that accurately represents the physical problem. The Golden Boy may be subjected to dead load and a disturbance due to wind or gust. Due to the geometry, the wind or the gust of wind may induce forces in several directions. The wind forces naturally produce a deflection in the direction parallel

to the wind. It may also produce vibration perpendicular to the wind which is induced by a phenomenon known as vortex shedding. This chapter discusses the procedure by which the dynamic response is evaluated on the model previously mentioned and as shown in Figure 4-15a).

There are two types of vibration associated with structures, being either free vibration or forced vibration.

The natural frequency of a structure is directly related to the mass and stiffness of it. If we assume that some energy is applied to the structure suddenly, such as kinetic or potential energy, and then removed shortly after that, the vibration experienced by the structure in the absence of external excitation is known as the free vibration. The free vibration will eventually dissipate or damped out with time since there are no external loads being applied.

The forced vibration is induced directly by a disturbance such as an external excitation. The forced vibration consists of the superposition of steady-state response and a transient response. The steady-state response is directly related to the external loading and the transient response is due to the initial stored energy in the structure.

4.7.1. Free Vibration

When a system is displaced from its static equilibrium position and then released, it vibrates freely around its equilibrium position with a behaviour that depends on the mechanical model (mass and stiffness of the system). The mechanical model of the Golden Boy is represented by a Single Degree of Freedom (SDOF) vibrating system which is attached to a lumped mass element

that is connected to a rigid support through a linear elastic spring as shown in Figure 4-15b). The purpose of a free vibration analysis is to determine this behaviour in terms of the frequency, known as the natural frequency, ω_n. The natural frequency plays a very important role in the vibration analysis and will be extremely important for the structural health monitoring of the Golden Boy's well being.

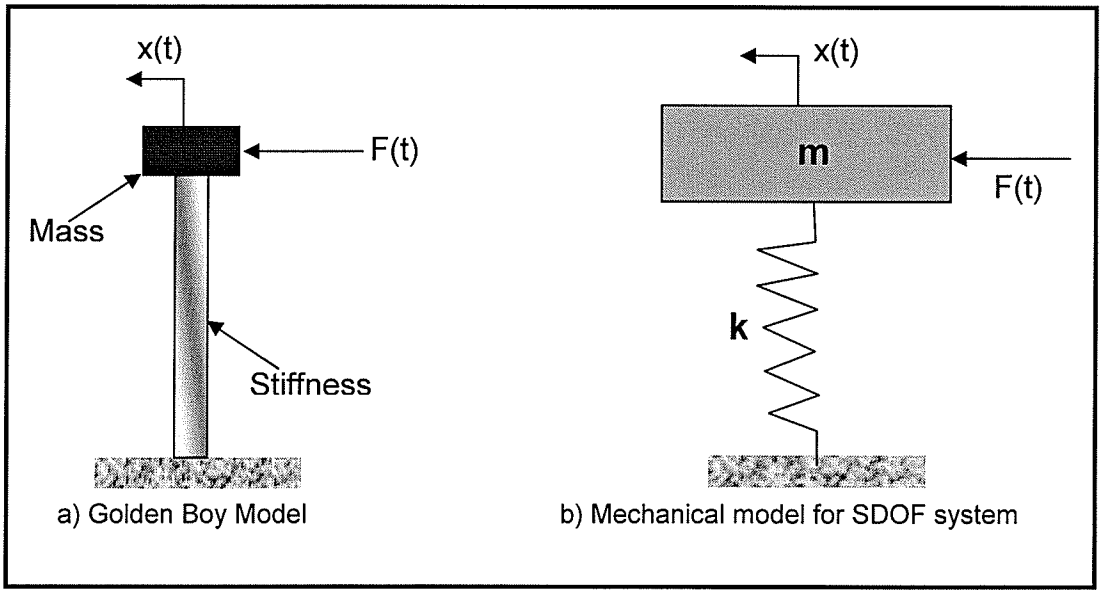

Figure 4-15: Schematics Representation of Static and Dynamic Analysis

The equation for SDOF system can be expressed by D'Alembert's Principle of Dynamic Equilibrium which is directly related to Newton's second law of motion to the system. Newton's second law states if the resultant force on a body is not zero then the body will move with an acceleration which is proportional to the resultant forces in the direction of the force (M. Frye, N. Rattanawangcharoen and A.H. Shah, 2003). Therefore, d'Alembert's principle of dynamic equilibrium is given by:

$$\sum (forces)_x - m\ddot{x} = 0 \qquad (4.13)$$

A free body diagram for a SDOF system is in a state of equilibrium and the dynamic problem can be reduced to an equivalent problem of statics shown is Figure 4-16 (Tedesco, Mcdougal &Ross, 1998).

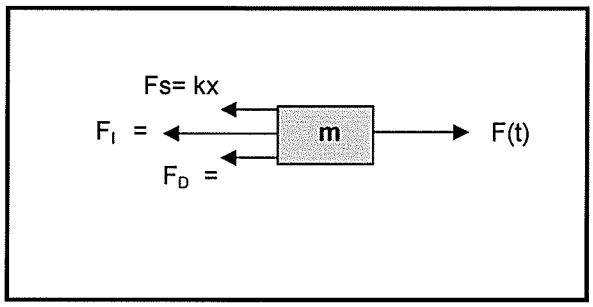

Figure 4-16: Free Body Diagram for SDOF System

The equation of motion for the system is given by applying Eq.(4.13)

$$F(t) - kx - c\dot{x} - m\ddot{x} = 0 \qquad (4.14)$$

where;

F_I= inertia force represented by the product of mass (m) and acceleration $(\ddot{x})$
F_S= mechanical force represented by the product of spring constant (k) and displacement (x).
F_D= damping force represented by the product of viscous damping coefficient (c) and velocity $(\dot{x})$.
Rearranging Eq. (4.14) and dividing through by m gives an end result

$$\ddot{x} + \frac{c}{m}\dot{x} + \frac{k}{m}x = \frac{F(t)}{m} \qquad (4.15)$$

The natural circular frequency is given by:

$$\omega_n = \sqrt{\frac{k}{m}} \qquad (4.16)$$

Eq. (4.14) can be defined simply by the system's mass and stiffness characteristics, if the damping is negligible, and hence ignored. For the case of the Golden Boy model system (Figure 4-15a) it is assumed to be undamped, free

vibration. The viscous damping force (F_D) and the external force (F(t)) are removed therefore from the equation of motion, which is then reduced to

$$m\ddot{x}+kx=0 \quad \text{or} \quad \ddot{x}+\omega_n{}^2 x=0 \quad \text{where;} \quad \omega_n=\sqrt{\frac{k}{m}} \tag{4.17}$$

The solution for a general undamped free vibration system where the mass is in motion and in terms of the prescribed initial conditions is shown by equation 4.18 (Tedesco, McDougal & Ross, 1999) and is used to evaluate the impulsive response function.

$$x(t)=\frac{\dot{x}_o}{\omega_n}\sin\omega_n t+x_o\cos\omega t \tag{4.18}$$

4.7.2. Equivalent Stiffness

The Golden Boy model is represented by a cantilever beam with an elastic stiffness (EI), and end load, F, applied at its free end as shown in Figure 4-17. The applied load F is a consequence of the dynamic effect of the wind on the structure.

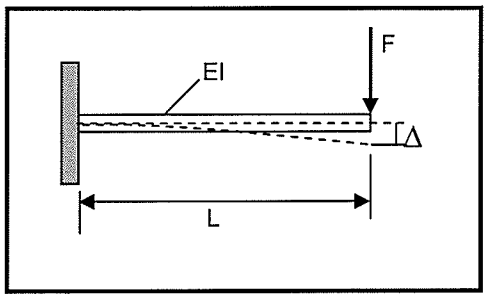

Figure 4-17: Cantilever Beam with Tip Load (CSA-S16.1-94)

The deflection, Δ, at the free end of the cantilever beam from an applied load, F, is given by:

$$\Delta = \frac{FL^3}{3EI} \tag{4.19}$$

Where;

E= Young's Modulus for stainless steel
I= moment of inertia of the beam's cross-sectional area about the neutral axis
L= length of the beam

The equivalent stiffness for the cantilever beam is the ratio of the applied load to the deflection at the free end of the beam (Tedesco, McDougal & Ross,1998), therefore:

$$k = \frac{F}{\Delta} \tag{4.20}$$

Substituting Eq.(4.19) into Eq. (4.20) and rearranging the equation in term of spring stiffness constant, k, yields the following:

$$k = \frac{3EI}{L^3} \tag{4.21}$$

Moment of inertia for a circular cross-section is given by

$$I = \frac{\pi r^4}{4} \tag{4.22}$$

4.7.3. Forced Vibration

As mentioned in the introduction, the forced vibration consists of two different types of motion. The first is the transient response which is related to the stored energy in the structure when set in motion instantaneously by an initial displacement and/or an initial velocity to the mass shown by Eq.4.18. The stored potential energy in the spring will be converted to kinetic energy to the mass which will continue to vibrate pass its natural equilibrium position, until it comes to rest due to damping. If no damping is present, the rate of energy transferred between the spring and mass, is the natural frequency.

The steady state response is related to the external excitation on the system. The response can be due to periodic (harmonic) or nonperiodic (arbitrary) exciting force. Periodic excitation repeats itself at equal time intervals or periods. Nonperiodic excitation does not repeat itself at equal time intervals and can consist of a short blast or of long duration. The wind is categorized as a nonperiodic force due to the continuous change in wind speed, gust and direction.

The response to a nonperiodic exciting force makes use of the solution for a unit impulse. Consider a simple system as shown in Figure 4-16 with a force response to unit impulse shown in Figure 4-18.

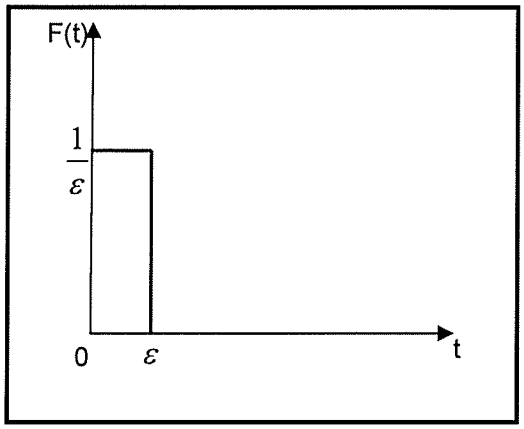

Figure 4-18: Unit Impulse (Anderson, 1967)

The equation of motion for the system is given by Eq.4.15 and the solution can be written as

$$\ddot{x} + \frac{c}{m}\dot{x} + \frac{k}{m}x = \frac{1}{m\varepsilon} \tag{4.23}$$

The assumption is that the system is initially at rest and that the time increment for the force is very small $\varepsilon \to 0$. The function which describes the exciting force with $\varepsilon \to 0$ is commonly referred to as a delta function or a unit impulse function (Anderson, 1967). Integration of Eq.4.23 over the duration of the force leads to

$$\dot{x} + \int_0^{\varepsilon} \frac{c}{m}\dot{x}dt + \int_0^{\varepsilon} \frac{k}{m}xdt = \int_0^{\varepsilon} \frac{1}{m\varepsilon}dt \quad \Longrightarrow \quad \dot{x} = \frac{1}{m} \tag{4.24}$$

The second and third term on the left hand side will also approach zero and the right hand side will become (1/m) as shown above. The velocity is finite and change in displacement will be very small (infinitesimal) at the end of the unit

impulse force, therefore the motion at the termination of the exciting force is given by (Anderson, 1967):

$$x = 0$$
$$\dot{x} = \frac{1}{m} \tag{4.25}$$

Equation 4.18, the transient response for an undamped system with an impulsive response function and with the initial conditions, Eq.4.25 is given by

$$x(t) = \frac{\dot{x}_o}{\omega_n}\sin\omega_n t + x_o \cos\omega t \quad \Longrightarrow \quad \boxed{h(t) = \frac{1}{m\omega_n}\sin\omega_n t} \tag{4.26}$$

The impulsive response function h(t) Eq.4.26 will be used to evaluate the dynamic response of non periodic motion of the Golden Boy.

4.7.4. Nonperiodic Excitation

The SDOF system is subjected to an arbitrary nonperiodic forcing function, as depicted in Figure 4-19.

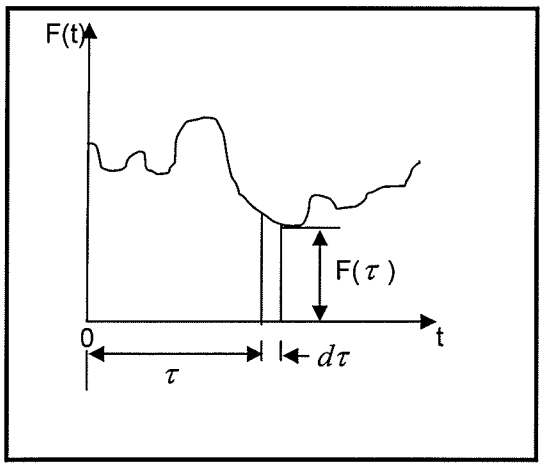

Figure 4-19: Incremental Component of An Arbitrary Force

Assuming that this excitation is a sequence of impulses such as the impulse of magnitude $F(\tau)d\tau$ over a very small time interval $d\tau$, then the displacement response to each impulse is valid for all time $t > \tau$ (Tedesco, McDougal & Ross, 1998). Thus the motion resulting from the single impulse can be expressed as

$$x(t) = F(\tau)h(t-\tau)d\tau \tag{4.27}$$

The motion for the single impulse can be superimposed for the total displacement response over the entire time interval t, integrating resulting in

$$x(t) = \int_0^t F(\tau)h(t-\tau)d\tau = \frac{1}{m\omega_n}\int_0^t F(\tau)\sin\omega_n(t-\tau)d\tau \tag{4.28}$$

Equation 4.28 is commonly known as Duhamel's Integral or the convolution integral (Tedesco, McDougal & Ross, 1998).

The excitation force must be a set of discrete points which are connected by a straight line so that a Duhamel's integral can be evaluated numerically. Therefore Duhamel's integral can be represented by a simple replacement of the integral by a summation

$$x(t) = \frac{\Delta t}{m\omega_n}\sum_{t=0}^{t=t_1} F(t)\sin\omega_n(t_1 - t) \tag{4.29}$$

It should be noted that it is usually necessary to determine values of the displacement, x, at a number of different times, t_1. It is thus advantageous to be able to calculate the results form previous time in a current calculation, but the summation formula (4.29) preclude this because times t_1 and t are intermixed in

the sine term. Therefore to separate them, we substitute a simple trigonometry relationship

$$\sin(\omega_n t_1 - \omega_n t) = (\sin \omega_n t_1 * \cos \omega_n t) - (\cos \omega_n t_1 * \sin \omega_n t),$$

giving

$$x(t_1) = \frac{\Delta t}{m\omega_n}\left[\sin\omega_n t_1 \sum_{t=0}^{t=t_1} F(t)\cos\omega_n t - \cos\omega_n t_1 \sum_{t=0}^{t=t_1} F(t)\sin\omega_n t\right] \quad (4.30)$$

Equation 4.30 is the steady state response which allows for dynamic displacement of the Golden Boy subjected to a loading F(t) at different time intervals (time step). The equation 4.30 will be evaluated with the forcing function of the live wind meter data (sampled at 1 Hz.) to obtain the dynamic displacement of the Golden Boy and then simple static analysis will be used to evaluate the strain at the fixity of the statue. The procedure will be discussed in section 5 of the report.

5. PROCESSING AND INTERPRETING THE SHM DATA

The DAQ system is continuously recording, collecting and displaying live data on the ISIS web page (ISIScanada.com). The web page was constructed for the purpose of graphically displaying the stresses, strain, temperature and movement of the Golden Boy over the internet.

The SHM system as mentioned previously, is the backbone to the monitoring of any structure. The DAQ system plays an important role in the acquisition of the data. A cable modem is used for the transfering of data from the onsite location to the main computer server located at the University of Manitoba. However, prior to the transfering of data, the DAQ program software (Labview) must be properly configured and must intelligently process data in a manner suitable for storage and retrieval. Once the data is transfered to the main server for storage, it may be retrieved at any time for diagnostic testing. The diagnostic testing of data will establish many important ideas and future consideration for the monitoring of any structure. The goal is to achieve a safe and reliable method for predicting the future health of the Golden Boy and to detect possible damage before any catastrophic event occurs. In doing this it enables establishing boundary limits for possible health concerns and allows adequate interpretation of live data. It will also enable proper decision making regarding the health of the Golden Boy structure.

5.1. WIND RETRIEVAL INFORMATION CENTRE

Environment Canada predicts and informs the public of future or present weather conditions throughout the continent. Weather conditions have an impact on the lives and decisions of everyone. The weather allows people to accommodate to their every day lifestyles. It is fair to say that the weather conditions heavily influence everyone and everything within our universe. The Golden Boy is one of the many objects which are influenced by weather conditions including winds. More so than the humidity or temperature, the wind or gust of wind is what impacts the movement and constant vibration of the statue. The Environment Canada website (www.ec.gc.ca/weather) allows for constant viewing of present and past weather conditions. The weather conditions are shown on a daily basis and can be retrieved for the whole year. The daily weather information is divided up into twenty-four hourly subsections. Each subsection displays the wind speed, direction, temperature, wind chill, visibility, relative humidity and dew point for the complete day. Environment Canada updates the wind speed every hour on the hour. The wind speeds and directions are taken from a wind meter located at the Winnipeg International Airport, ten meters from ground level. The wind information for each hour is based on the strongest gust of wind encountered during the full hour. An example of weather results for a complete day is shown in Figure 5-1. The Environment Canada website serves as a very important tool. It intelligently allows to pin point the exact day and time interval for different wind velocities, which guides the retrieval and analyses of the live data.

Hourly Data Report for February 22, 2004										
Time	Temp °C	Dew Point Temp °C	Rel Hum %	Wind Dir 10's deg	Wind Spd km/h	Visibility km	Stn Press kPa	Hmdx	Wind Chill	Weather
00:00	-4.2	-5.6	90	17	15	6.4	98.28		-10	Snow
01:00	-4.3	-5.6	91	17	11	3.2	98.30		-9	Snow
02:00	-4.4	-5.7	91	18	7	6.4	98.34			Fog
03:00	-4.4	-5.9	89	18	7	6.4	98.36			Fog
04:00	-4.6	-5.9	91	17	4	6.4	98.33			Fog
05:00	-4.8	-6.0	91	34	6	24.1	98.38			Cloudy
06:00	-4.6	-5.7	92	36	7	3.2	98.43			Fog
07:00	-4.2	-5.3	92	3	11	3.2	98.48		-9	Fog
08:00	-4.7	-5.7	93	2	15	6.4	98.56		-10	Fog
09:00	-4.8	-6.1	91	3	17	11.3	98.60		-11	Mostly Cloudy
10:00	-4.5	-5.9	90	2	17	16.1	98.67		-10	Cloudy
11:00	-4.3	-6.0	88	1	19	16.1	98.73		-10	Cloudy
12:00	-3.9	-5.5	89	35	15	16.1	98.80		-9	Cloudy
13:00	-3.1	-4.9	87	2	17	9.7	98.81		-9	Snow, Fog
14:00	-3.0	-4.9	87	2	24	19.3	98.83		-10	Cloudy
15:00	-2.9	-5.2	84	2	17	24.1	98.88		-8	Cloudy
16:00	-2.8	-5.4	82	1	15	24.1	98.94		-8	Cloudy
17:00	-2.6	-5.4	81	36	17	24.1	98.99		-8	Cloudy
18:00	-2.9	-4.9	86	34	11	24.1	99.04		-7	Cloudy
19:00	-3.1	-5.2	85	1	13	24.1	99.09		-8	Cloudy
20:00	-3.3	-5.5	85	33	11	24.1	99.12		-8	Cloudy
21:00	-3.6	-6.2	82	34	19	24.1	99.16		-10	Cloudy
22:00	-3.6	-6.4	81	1	11	24.1	99.21		-8	Cloudy
23:00	-3.9	-6.1	85	34	7	24.1	99.23			Cloudy

Figure 5-1: An Example of Weather Climate Information on Environment Canada Website.

The Golden Boy's movement is solely depicted by the speed and direction of the prevailing wind. A search was conducted through the use of the Environment Canada website as previously mentioned, to locate different wind speeds recorded for any given hour during the past months. An in depth analysis was administered for wind velocities ranging near the vicinity of 0, 10, 20, 30, 40, and 50 km/hr. The maximum wind speed (59Km/hr) occurred on September 24, 2003 between 10am to11am and on March 10, 2004 between 11am to 12pm as shown in Table 5-1.

Shown in Table 5-1 are wind velocities ranging from 0-59 Km/hr with their corresponding wind direction and the day/time of the occurrence. The wind speed and direction shown in the time interval is recorded by Environment Canada

corresponding to the greatest gust of wind encountered during that hour interval. The velocities are shown in descending order starting with the highest gust of wind.

Table 5-1: Weather Climate Data for Specific Days

DATE	TIME INTERVAL	WIND SPEED (km/hr) (GUST)	WIND DIRECTION (degrees)
September 24,2003	10am-11am	59	355
March 10,2004	11am-12pm	59	357
January 21,2004	8am-9am	54	355
January 2,2004	9pm-10pm	50	10
October 27,2003	2pm-3pm	43	185
October 22,2003	4pm-5pm	43	355
November 20, 2003	8am-9am	43	355
March 1,2004	2pm-3pm	39	10
February 26, 2004	3pm-4pm	32	180
March 20,2004	3pm-4pm	30	350
February 11,2004	6pm-7pm	20	350
December 22,2003	5am-6am	20	340
March 28,2004	2am-3am	19	345
December 10,2003	12pm-1pm	19	350
February 22, 2004	7pm-8pm	12	10
November 3,2003	11pm-12am	9	15
December 14,2003	2pm-3pm	11	265
October 26,2003	8pm-9pm	0	–
December 22,2003	11pm-12am	0	–

The days and one hour intervals shown in Table 5-1 will be used to acquire the corresponding live data files, which are being collected at the University of

Manitoba main computer server. The live data files will be extracted by the dates and modified to obtain correct time intervals as above in Table 5-1. A brief recap of the retrieval and modification of stored data is discussed in the next section of the report.

5.2. STORAGE, RETRIEVAL AND MODIFICATION OF DATA

As discussed in Section 3.3.2, the live data is compressed by the Labview program onsite and transferred via modem connection to the central main computer server located at the University of Manitoba. The data is decompressed and zipped to twenty percent of the original text file (.dat) and stored on the hard disk drive. The hard drive stores the daily data in text files for up to one month and then the data is saved to secondary storage during regular maintenance. The whole month's worth of data is saved onto compact disc, and the hard drive is cleaned for the storage of the next month's data.

Each stored data file is labelled according to the start date of the collection period. For example, the file labelled as Jan2-2004(8:13:46 Pm).dat would contain data starting from January 2, 2004 at precisely 8:13:46 p.m and collected continuously for approximately twenty-four hours (one day). The main computer server is continuously collecting and saving live data from the onsite DAQ system. Therefore, a second computer in the Structural Health Monitoring Lab was needed to process the data. The PC Anywhere software was installed on the computer allowing direct connection to the main server. The data files were located by dates shown in Table 5-1 and transferred onto the computer.

Once data transfer is completed, the files are unzipped (WinZip software) to their original size (300 Mb.). The Labview software has an option called dataextract.vi which breaks down the original data file into smaller files (size of approximately 12Mb.), which are suitable for processing by other programs such as the Excel spreadsheet program. The smaller files (12 Mb) are stored with identifiers to match the exact time interval previously mentioned in Table 5-1. A 12 Mb. file as mentioned above accommodates approximately 60,000 data points (sensor data, strain gauges, accelerometers, and thermocouples). The data is sampled at 32Hz (32 points per second), and one file of 60,000 points relates to approximately half of an hour duration (1800 seconds). Therefore, two succeeding files are used to represent the data for one full hour. Both files are opened with an individual Excel spreadsheet that ranges in the same hour time interval that Environment Canada encountered its gust of wind. The information contained on the files consists of the actual strain gauges, temperature and the accelerometers output data readings. Some Excel files are shown in the Appendix D of this report.

The complete procedure of SHM data processing and interpretation include the following steps:

a) locating different ranges of wind speeds (Environment Canada website).

b) retrieval of the original live data files from the main server.

c) the brake down of original data files into individual excel files (duration of approximately 30 minutes).

d) Modifying consecutive excel files (same hour interval as table 5.1) for the purpose of obtaining the actual strain gauge and accelerometer data for analysis, and finally

e) interpreting the strain and other data to answers the health of the structure .

5.3. ANALYSIS OF THE STRAIN GAUGE DATA

It is assumed in the analyses that all wind speeds are approaching approximately from the north or south as shown in Table 5-1 of the report. Therefore the vertical strain gauge rosettes positioned at either the north or south side would be able to obtain the correct strain gauge readings for comparison purposes. Unfortunately, the north vertical strain gauge (S.G.N.2) is malfunctioning, hence, the south vertical strain gauge rosette (S.G.S.6) will be used throughout the report. Before the pair of files are plotted, corresponding to an hour, the actual strain gauge data is corrected for thermal effects. The actual strain gauge data is dependent on bending strain due to wind (dynamic affect), axial strain (weight of the Golden Boy) and thermal strain (change in temperature of the material). The instrumentation devices were zeroed prior to the collection of SHM data eliminating the axial strain component. Therefore the live data recorded by the strain gauges consists of both bending and thermal strains. The following techniques are used to eliminate the thermal component, leaving the strain solely due to wind (dynamic motion).

Method1: This method deals with the theory of pure bending of a cantilever shaft. If we assume that the wind is approaching from the north or south, one side will be in tension and the other in compression, therefore it is safe to say that the vertical strain gauge on the south side will experience pure bending and thermal expansion. The vertical strain gauge positioned on the east and west face of the shaft will experience no bending theoretically. Therefore the values recorded on the east and west side should only be due to thermal strain. The values depend solely on temperature change from a reference value (usually room temperature) and in this case, the day the Golden Boy's instrumentation were zeroed, and the coefficient of thermal expansion of the material of the shaft. Therefore, theoretically the change in length or deformation of a shaft due to temperature change is given by :

$$\delta_T = \varepsilon_T L = \alpha(\Delta T)L \tag{5.1}$$

where;

L= is the initial length of the shaft

α=coefficient of thermal expansion

ΔT=change in temperature from the reference temperature

ε_T= thermal strain

The total strain in the shaft of the Golden Boy is given by

$$\varepsilon = \frac{\sigma}{E} + \alpha\Delta T \tag{5.2}$$

where now the total strain ε consist of the internal bending strain and the thermal strain in the shaft. The temperature change (ΔT) is positive for temperature

increase and negative for temperature decrease, indicating that the shaft has increased or decreased in length, respectively.

All vertical strain gauges on the shaft of the Golden Boy experience both bending strain and thermal strain which relate to the instantaneous dynamic wind effect and temperature changes. The average of strain at opposite faces should represent the thermal strain. Thus the east (S.G.E.4) and west (S.G.W.8) values were averaged to obtain the thermal strains and subtracted from the south (S.G.S.6) strain gauge for each corresponding point and plotted. The plots were examined and the plot which demonstrated the largest peak during the duration of 30 minutes was selected. The window of time is only 30 minutes that is why we must select one of the two for These plots are presented for the days shown in Table 5-1. The figures 5.2 through 5.20 show the plots of Micro-strain versus time, having duration of approximately 30 minutes (1800seconds) and are shown in decreasing order of wind velocities, starting with the maximum.

Method2: This method is based on simple intuition and common sense. The temperature change in the shaft is slow and the thermal strain should remain reasonably unchanged for a short period of time. The thermocouples temperature readings are shown in the Appendix E of this report for various days. The temperature outside may change fairly dramatically from day to day but as the thermocouples demonstrate, the temperature change on the stainless steel shaft is quite slow. This may be a consequence of the stainless steel shaft at the top of the Legislature being well protected and insulated by the dome. Given that the time intervals being compared are no greater than a half an hour (1800 seconds),

it is safe to say that the previous file strain gauge readings (S.G.S.6) will not have a huge change in thermal strain. Therefore, the baseline or the average of the data points for a small window of time proceeding the period of interest would correspond to the thermal strain of the shaft and is subtracted from each data point. The effectiveness of this method is quite comparable to the previous one (method 1). The Appendix E of this report demonstrates both methods for September 24, 2003 and illustrates how similar they are in output. Therefore, it is appropriate to choose either one for the analysis of the strain gauge results. Method 1 was used throughout this thesis for consistency.

The entire hour intervals for each specific day (table 5.1) includes two excel files as mentioned previously. Both files were corrected (method 1) and plotted (Micro-strain vs. time). The plot which contained the absolute maximum strain peak at any given instant was selected because it indicates the maximum gust of wind encountered during that hour. Figure 5.2 through 5.20, are labeled by their corresponding dates, placed in descending order of wind velocity, starting with the highest. The two highest wind (gust) speeds (59Km/hr) occur on September 24, 2003 and March 10, 2004 and are shown below in Figure 5.2 and Figure 5.3, respectively. The remaining figures are placed in the Appendix A of the thesis.

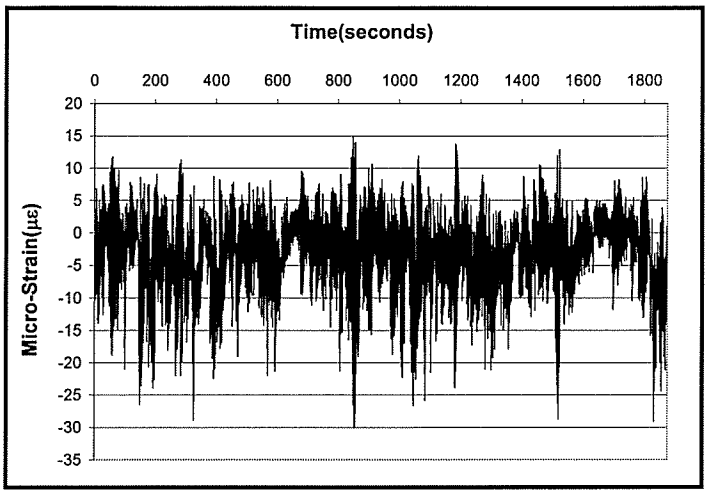

Figure 5-2: Strain vs. Time of Actual Strain Gauge South (S.G.S.6) on September 24, 2003

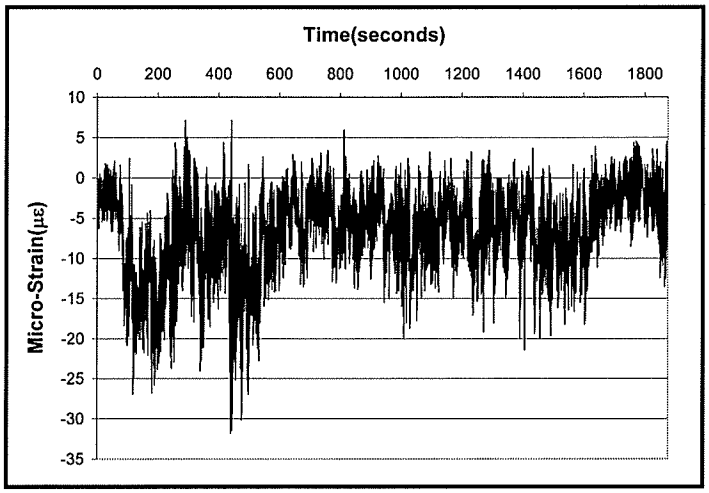

Figure 5-3: Strain vs. Time of Actual Strain Gauge South (S.G.S.6) on March 10,2004

5.4. ANALYSIS OF THE ACCELEROMETER DATA

Two accelerometers were installed at the top of the shaft inside the Golden Boy as discussed in Section 3.2.2.3. The location of the accelerometers is shown in Figure 3-25. The same procedure as mentioned in Section 5.2, was followed to obtain the appropriate data for analysis. The analysis of data was done on the same time frame and day as the actual strain gauge (S.G.S.6) results for comparison purposes. The accelerometers data output is expressed in g's (g is

the acceleration due to gravity) and the range of the accelerometer spans ±4g's. For comparison reasons the Y-accelerometer data was used in the analysis, because it is oriented parallel and in line with the North-South axis of the shaft of the Golden Boy.

5.4.1. Analysis Results

The accelerometer is located at the top of the shaft and in very close proximity to the centre of gravity of the shaft. The movement of the accelerometer is directly related to the force which moves the object. The accelerometers are recording the actual dynamic movements (vibrations) of the statue. Therefore, the force will be calculated using Newton's second law (F=ma) and will be applied at the same location as the force W on point O as shown is Figure 4-8. At point O the force represents the dynamic forcing function which alternately will be used to determine the strain at the bottom of the cantilever stainless steel shaft. The force calculated at each instant can use the static, bending stress and strain theory as described in section 4.3, section 4.42 and section 4.5 respectively. The accelerometer analysis is demonstrated using an actual data point obtained from the September 24, 2003 file. The procedure shown above is used for all data points and then plotted using an Excel spreadsheet. The plots or numerical results are shown in Figure 5.21 through Figure 5.39 and are in descending order, starting with the maximum wind velocity (September 24,2003). Figure 5.21 and Figure 5.22 are shown below and correspond to the two highest wind (gust)

speeds, September 24, 2003 and March 10, 2004, respectively. The remaining figures are placed in the Appendix B of the thesis.

Sample calculation

The accelerometer data corresponding to a=0.053g was chosen for calculation:

F=ma

g = acceleration due to gravity (9.81m/s^2)

m = mass of the object which is the total mass of the golden boy statue along with the internal shaft (1575 Kg).

F=ma= (1575)*(0.053*9.81)= 818.9 N where F=W referring to Figure 4.9

Static equilibrium gives the following moments at the fixity of the cantilever shaft and is calculated by the following equations:

Myx= 2750W= 2750(818.9)= 2,251,975 Nmm

The stress are calculated by Equation 4.3 of the report

$$\sigma yx = \frac{M_{yx} * Z}{Iy} = \frac{2251975 * 69.85}{18.69x10^6} = 8.42 \text{ MPa}$$

Normal strain is calculated by Equation 4.10 of the report

$$\varepsilon = \frac{\sigma}{E} = \frac{8.42}{200000} = 42.1X10^{-6} = 42.1\ \mu\varepsilon$$

The value of 42.1 micro-strain is shown in Figure 5-21 at time 860 seconds of September 24, 2003, which is the instant of the maximum gust of wind experienced by the statue at that time interval.

5.4.2. Numerical Results

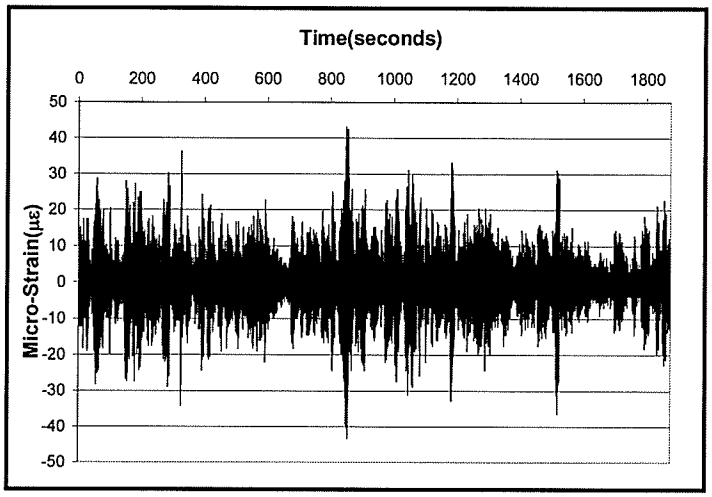

Figure 5-21:Strain vs. Time of Y-Accelerometer Analysis on September 24, 2003

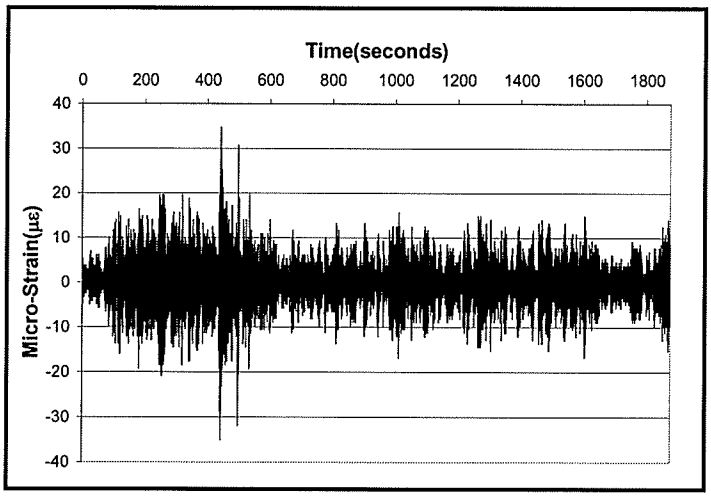

Figure 5-22: Strain vs. Time of Y-Accelerometer Analysis on March 10,2004

5.5. DIAGNOSTIC DYNAMIC ANALYSIS AND RESULTS

This section discusses the natural frequencies obtained by the theoretical and FFT analysis of the accelerometer as well as their comparison. It also discusses the procedures needed to obtain a representation of the dynamic response of the Golden Boy using the live data of the ultrasonic wind sensor

located on the roof of the Legislature. In addition, it is necessary to check if there is any correlation between the results of the dynamic analysis of the structure using the wind meter data and the actual strain gauge readings.

5.5.1. Natural Frequency

Theoretical Calculation:

The mechanical model representing the Golden Boy's structure is illustrated in Figure 4.15b) and the free body diagram is shown in Figure 4.16. The application of D'Alembert's principle of dynamic equilibrium yields the equation of motion given by Equation 4.15 as discussed in Section 4.7 of this report. The natural circular frequency (Equation 4.16) of the system is obtained directly from Equation 4.15 and is calculated as follows:

m=1575Kg; The mass of the system (Golden Boy and shaft)

The equivalent stiffness, discussed in Section 4.7.2 of the report, is expressed as

$$k = \frac{3EI}{L^3} = \frac{3*200000*18.69x10^6}{2750^3} = 539.2 \text{ N/mm}$$

Therefore, from Equation 4.16

$$\omega_n = \sqrt{\frac{k}{m}} = \sqrt{\frac{539.2}{1.575}} = 18.5 \text{ rad/sec}$$

The theoretical natural frequency is

$$f = \frac{\omega_n}{2\pi} = \frac{18.5}{2\pi} = 2.95 \text{ Hz.}$$

As mentioned in Section 3.3.4, the web base monitoring system is displayed on the ISIS Canada web site. The web page allows for continuous viewing of the data. The Lab View program located on the on-site data

acquisition system can be set to obtain the sensor data that is desired from a data socket. The program allows the data to be viewed numerically and graphically on the web site. The Lab View program has many different functions. One function used is the Fast Fourier Transformation (FFT) of accelerometer data, which extracts the frequency contents of the data which can be used to determine the natural frequencies of the Golden Boy Structure. Figure 5-40 and Figure 5-41 show the Y-accelerometer's data (acceleration in g's) and the natural frequencies of the Golden Boy, respectively.

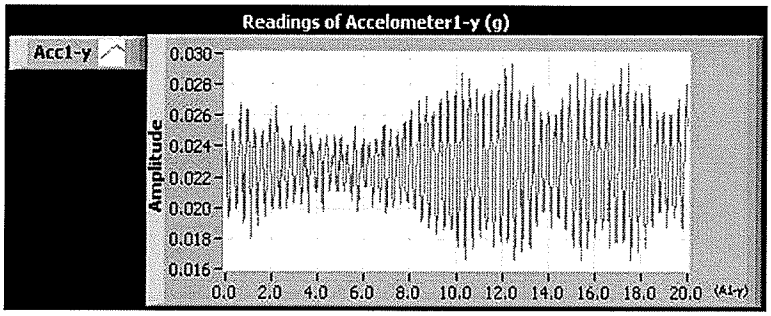

Figure 5-40: Accelerometer Data as Displayed on the Website

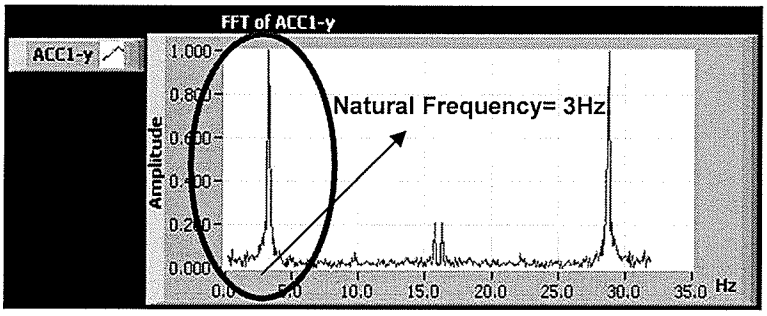

Figure 5-41: Natural Frequencies as Displayed on the Website

Throughout the 10 month study the natural frequency (3Hz) of the Golden Boy has been observed continuously on the website. The natural frequencies have demonstrated a slight variation of 3.5% (3.05 Hz. to 2.95Hz.), but overall has been very consistent throughout the study. The theoretical and FFT analysis

shows that the natural frequency of the Golden Boy structure is about 2.95 Hz., therefore the natural frequency of 2.95 hertz is considered a healthy structure. If the natural frequency changes in any way, this can be cause for concern, and what would be a reasonable amount of change before the health of the structure comes into question. Figure 5-42 shows the decrease in natural frequency as the shaft's diameter is reduced. If the structure frequency reduces by 5% the diameter looses about 3.7 mm around the circumference of the shaft which may be due to corrosion. A baseline (Figure 5-42) is established to identify the value of natural frequency of the Golden Boy which would alter his state of health from healthy to unhealthy structure.

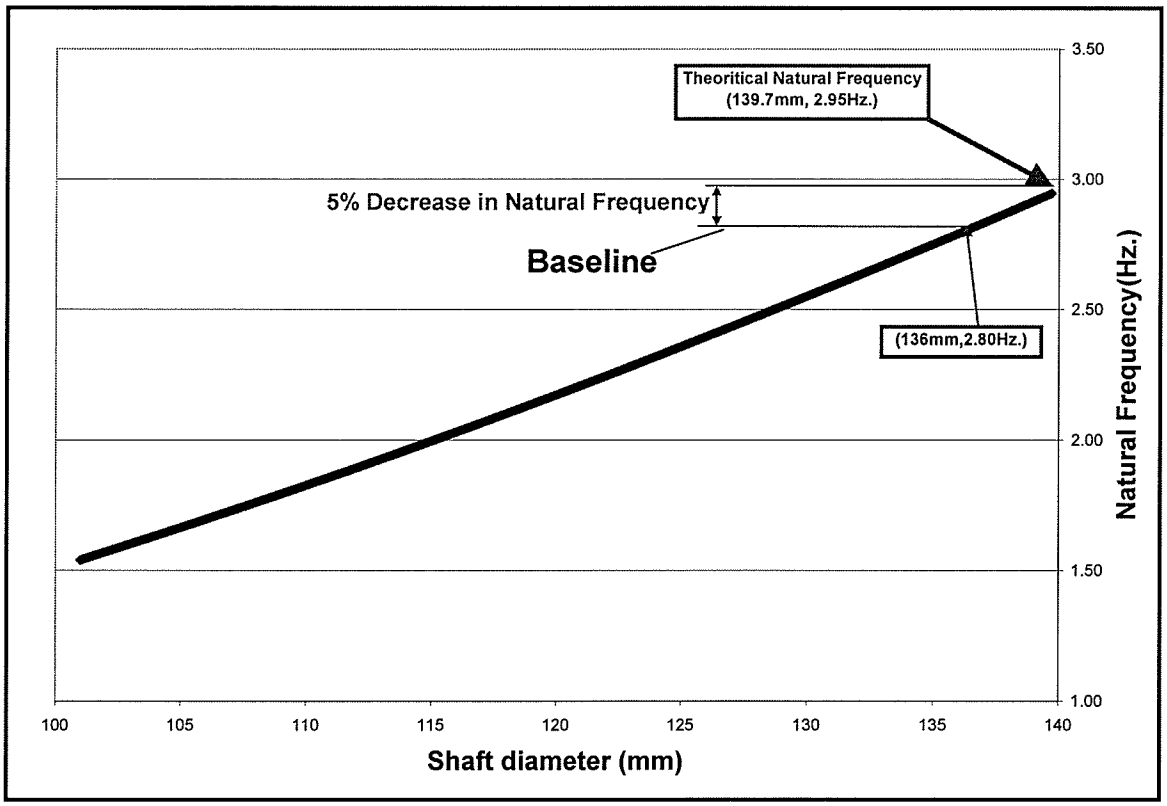

Figure 5-42: Change in Natural Frequency Due to Decrease of the Shaft

If the Golden Boy's frequency from the FFT analysis of the accelerometer would ever demonstrate a result of 2.80Hz or smaller an in-depth analysis of the Golden Boy structure should be done immediately to see what is the cause for this change.

5.5.2. Dynamic Analysis on Wind Meter Data

Due to restriction and safety concerns, it was not possible to place the ultrasonic wind sensor on the Golden Boy's dome. It was installed on the north-west corner of the Legislature's roof top. The roof top is approximately 25 meters from ground level. The ultransonic wind sensor positioned at seven feet from roof level is high enough to record the wind velocities' patterns experienced at the Legislature Building's roof top. The wind velocities and directions are sampled by the ultrasonic wind sensor at one Hertz (one point per second), recorded and stored in data files on the on- site server at the Legislature Building.The wind data files are stored in the same manner as previously disccussed in section 5.2 of this report. The wind data files are transferred from the on-site server to a computer at the SHM laboratory within the University of Manitoba. A search is conducted to locate appropriate files according to the time/day as referred in Table 5-1 of this report. The wind velocity profile on September 24,2003 is shown in figure 5.43. The half an hour interval (1800 points sampled at 1Hz.) corresponds to the same time frame which the absolute maximum strain occurred in the strain gauge analysis, shown in section 5.3 of this report.

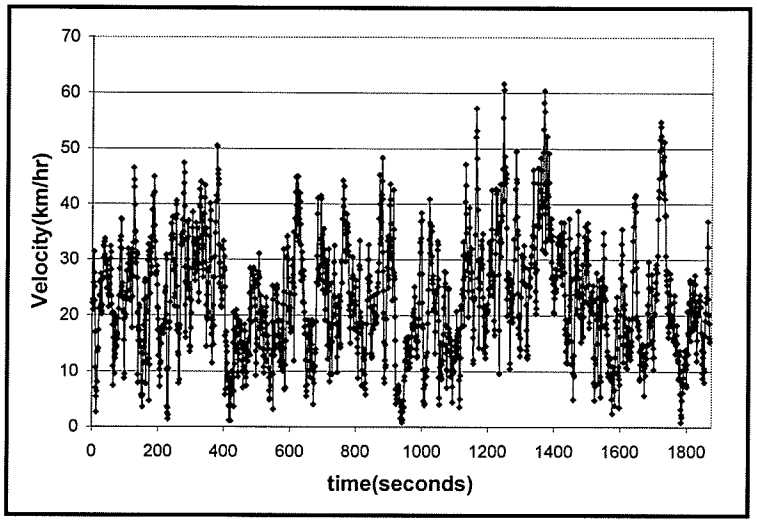

Figure 5-43: Wind Velocities Data Recorded at the Legislature's Roof Top

Next, the file is modified in an Excel spreadsheet. The winds data is converted into external pressure by using the wind loading provisions of the National Building Code of Canada and Canadian Highway Bridge Design Code. In addition, an approximate projection area of the Golden Boy at 15 degree increments was performed. The results are shown in Table 5.2. The Golden Boy's north face relates to the projection area of zero degrees and so on. The external pressure is multiplied by its corresponding projection area, resulting in the force being applied at the same location as the force W on point O as shown is Figure 4-8. Finally, the force is seperated into its north, south, east, and west components which creates the North-South and the East-West forcing functions. A sample calculation is performed below, to better understand the procedures involved in modifying the excel spreadsheet, which results in the forcing function for the entire 30 minute interval.

Table 5-2: Projected Area of the Golden Boy

Angle (degrees)	Projected Area (m^2)
0	3.19±0.1
15	3.24±0.1
30	3.22±0.1
45	3.22±0.1
60	3.17±0.1
75	3.13±0.1
90	2.98±0.1
105	2.90±0.1
120	2.85±0.1
135	2.86±0.1
150	2.91±0.1
165	3.08±0.1
180	3.19±0.1
195	3.24±0.1
210	3.22±0.1
225	3.22±0.1
240	3.17±0.1
255	3.13±0.1
270	2.98±0.1
285	2.90±0.1
300	2.85±0.1
315	2.86±0.1
330	2.91±0.1
345	3.08±0.1
360	3.19±0.1

Sample calculation :

Let us assume that the wind approaches the Golden Boy at 20km/hr from the North-East at 45 degrees. The pressure is calculated by Equation 4.12

$$p = \frac{1}{2}\rho * V^2 * C_e C_p C_g$$

The coefficient C_e, C_p and C_g shall be taken from section 3 of the Canadian Highway Bridge Design Code (CAN/CSA-S6-00).

The exposure coefficient (C_e = 1.5) shall be taken from ground level to the top of the Golden Boy, a height of approximately 75 meters as shown in table 3.10.1.3 of the code. The gust effect coefficient (C_g = 1) shall be used due to the actual representation of the wind velocities data being used in the analysis. Therefore there is no need to estimate the gust effect because the data file already includes all gust and dynamic effects of wind. The loads will be applied directly to the

structure. The external pressure coefficient (Cp=0.7) shall be used as the surface of the statue is smooth and there are no sharp edges, resembling more a circular pier than a rectangular pier.

$$p = \frac{1}{2} * 100X10^{-6} * 20^2 * 1.5 * 0.7 * 1 = 0.021\text{Kpa}$$

The projection area of $3.22m^2$ (table 5.2) is used to obtain the force vector. The force vector will be applied at point O as shown in the 3D model (Figure 4-7a). The force vector was geometrically decomposed to the North-South components (F_{NS}) and East-West components (F_{EW}).

F =p*A=0.021*3.22=0.06762 KN at 45 degrees

Force components are determined

F_{NS}= Fcosθ=0.06762 cos45= 0.0478 KN (North component)

F_{EW}=Fsinθ= 0.06762sin 45= 0.0478KN (East component)

Note: south and west components are taken with their negative values.

The excel file containing the forcing function is then called by a matlab program and is discussed next.

5.5.2.1. Matlab Program

As discussed earlier in Section 4.7.4, the Duhamel's summation formula is based on incremental component of arbitrary force which is represented by very small time intervals or time step. It is necessary to find out what time step will ultimately optimize the dynamic displacement of the structure? The forcing function is assumed to be connected by a straight line therefore the simplest form

of interpolation is used to obtain a point between the connected line. This technique, called linear interpolation, is depicted graphically in Figure 5-44 and the linear interpolation formula shown in Equation 5.1. The forcing function file which is called by the matlab program has a time step of one second (Δt=1s). Equation 5.1 re-evaluates new forcing functions for a time step of Δt=0.5s, Δt=0.25s, Δt=0.125s, Δt=0.0625s and Δt=0.03125s. The forcing functions are applied to Duhamel's equation (4.30) which calculates the dynamic displacement of the Golden Boy. Due to the size of the force function and complexity of the equation, excel was not able to perform such tasks of summing all incremental points (time step) continuously. Additionally due to, the number of points and complexity of the analysis, hand calculations were done for the first ten force increments only, to verify results. The program written was also verified with a numerical example, taken from the section 3.4 of the book by Kenneth Medearis (1976). Furthermore, the programs running time to execute the dynamic analysis with a time step of 0.03125 second, is approximately one hour.

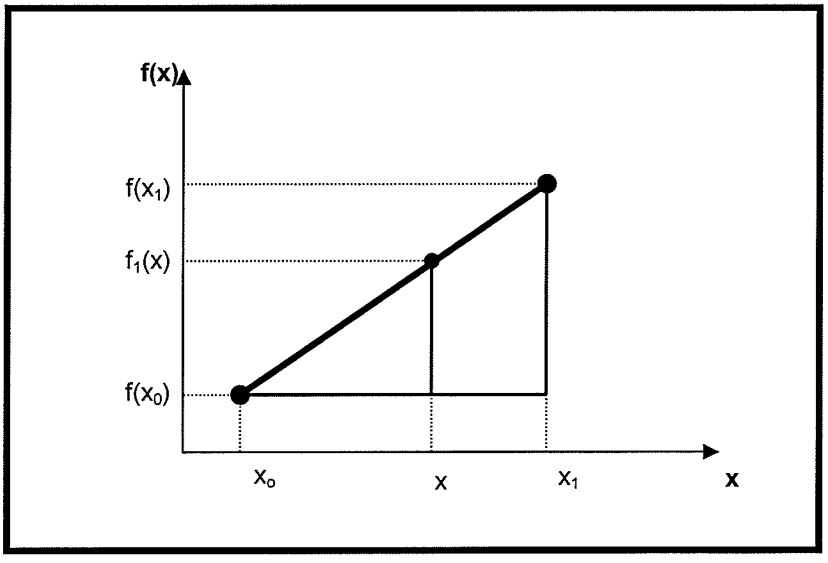

Figure 5-44:Linear Interpolation (Chapra and Canale, 1998)

$$f_1(x) = f(x_0) + \frac{f(x_1) - f(x_0)}{x_1 - x_0}(x - x_0) \qquad (5.1)$$

The dynamic displacement analysis was performed to all dates listed in Table 5-1 of this report. Figure 5-45 through Figure 5-50 are two different dynamic displacement results shown in decreasing order of time step, starting with the greater (Δt=1s) and ending with the smaller time step (Δt=0.03125s), respectively and is shown in the Appendix F of the report. The figure to the left correspond to the day of September 24, 2003 and the figure to the right correspond to the day of March 10, 2004. From these figures it is clear the time step Δt=0.0625s and Δt=0.03125s as shown in Figure 5.49 and Figure 5.50, respectively achieve similar results. Thus, by reducing the time step further then Δt=0.0625 second, will not have any affect on the results. Therefore the optimal dynamic displacement is obtained using a time step of Δt=0.0625 second.

Next the program calculated the corresponding static force P for each optimal dynamic displacement. The static force was calculated using the maximum deflection equation for a cantilever beam loaded at the end by a concentrated load as shown below

$$\partial \max = \frac{PL^3}{3EI} \Rightarrow P = \frac{3 * \partial_{\max} * EI}{L^3}$$

The static force P is applied at the top of the cantilever shaft (point O) and the maximum bending moment, stress and strain were calculated using the same procedure described in the sample calculation of Section 5.4.1. The matlab program is shown in Appendix G of the thesis.

5.5.2.2. Numerical Results

Figure 5-51 through Figure 5-65 are arranged in decreasing order of wind velocity starting with September 24,2003 (maximum wind speed) and ending with October 26,2003 (zero wind speed), the same sequence as in Table 5-1 of this report. In addition, the figures use the optimal time step of Δt=0.0625 second. The two higher gust speeds are shown below (Figure 5-51 to 5-52) and the remaining figures are placed in the Appendix C of the thesis.

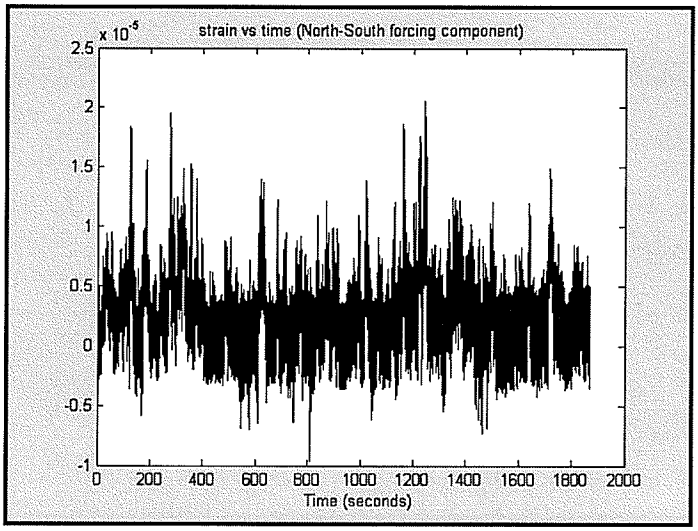

Figure 5-51:Strain vs Time (Dynamic Analysis on September 24,2003)

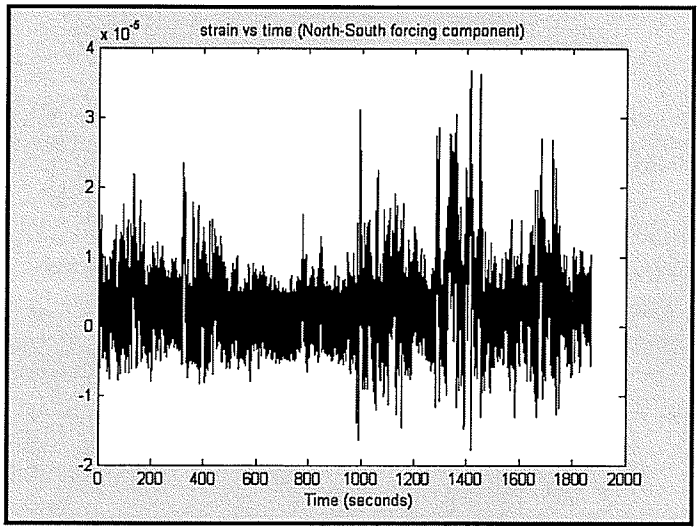

Figure 5-52: Strain vs Time (Dynamic Analysis on March 10,2004)

5.5.2.3. Effect of Damping

The Golden Boy structure is a lightly damped system experimental study shows (A. Kopp and D.Surry, 2001) that damping in the Golden Boy structure is about 1%. It can be observed in Humar et al (1998) that for lightly damped multi degree of freedom building frames subjected to constant forcing function for a given period of time, the response is not affected significantly by damping. As the damping is low in the Golden Boy structure, the response due to wind is calculated by assuming no damping in the system.

As the system is loss-less, there is a chance that when the frequency of the exciting force matches the natural frequency, the structure would go into resonance and the response will grow out of bound. The FFT analysis of the wind pattern of the most windy day (Figure 5-66) shows that the energy of the wind forces related to the natural frequency of the structure is not high compared to other frequencies. That's why the response may not keep on growing if the wind pattern persists. Wind gust is generally short lived and structures goes into steady state of vibration soon after the gust ends. To prove that the solution is stable and it does not depend on the time window for which the Duhamel's integration is evaluated, sample analyses is performed with wind duration of one hour and two hours periods. The peak response of these two analyses does not differ much. 22 micro-strain and 24 micro-strain for the duration of one and two hours periods, respectively.

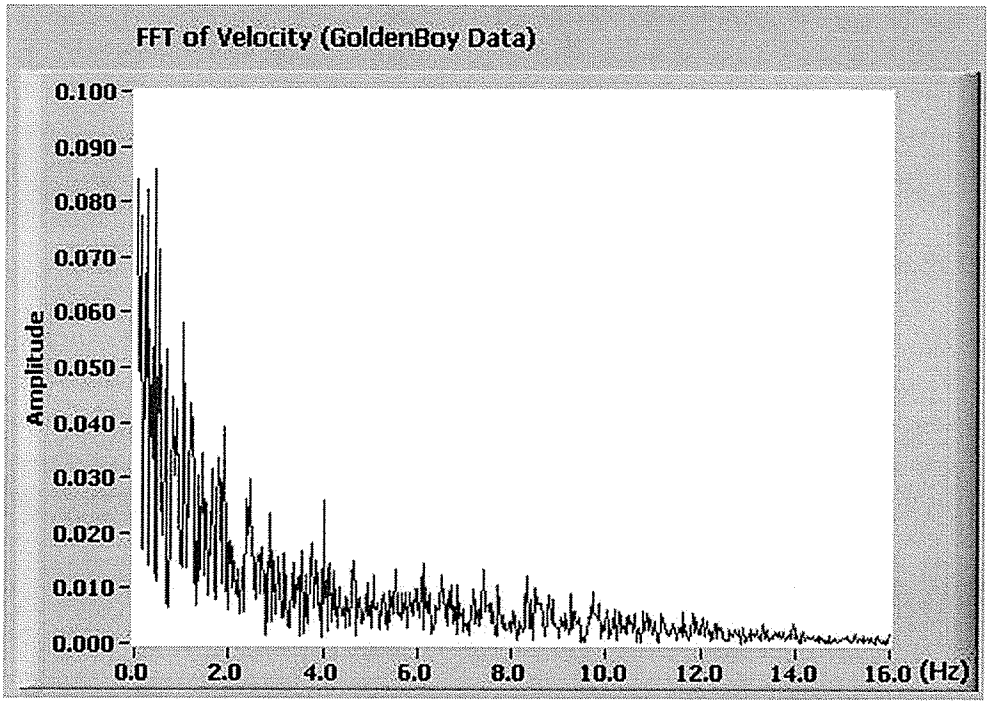

Figure5-66: FFT Analysis on the Windiest Day

The total response of the Golden Boy neglects the contribution of the free part (transient response) since the response is negligible after a few cycles, therefore we consider only the steady-state, or forced, part of the response. The expression for duhamel integral for the forced vibration of a damped system is shown below:

$$x(t) = \frac{1}{m\omega_d} \int_0^t F(\tau) e^{-\zeta w(t-\tau)} \sin \omega_d (t-\tau) d\tau$$

It can be observed in J.M. Biggs (1964) that for a forced vibration with 10% of critical damping the maximum response (displacement) is 13.5 percent less than an undamped system, therefore it is fair to conclude that damping has little effect on the maximum response of a structure. Now consider the same argument but with the damping of 1% (ζ=0.01) on the Golden Boy structure,

system initially at rest and subjected to a suddenly applied constant force (F_1). For an undamped Golden Boy structure the maximum displacement is given by

$$X_{max} = \frac{2F_1}{k}$$

and for a damped system the maximum displacement is given by

$$X_{max} = \frac{F_1}{k}(1 + e^{-\pi\zeta}) = \frac{1.97F_1}{k}$$

Hence the reduction due to the amount of damping experienced on the Golden Boy structure is 1.5%. Therefore by ignoring the effect of damping on the structure will not affect the dynamic response of duhamel integral formula used in the study. That is why the damping is neglected throughout the dynamic analysis.

5.6. DISCUSSION AND COMPARISON

The events chosen in Table 5-1 represent different gusts of wind between the hour intervals. All plots are shown in decreasing wind speeds, starting with the highest gust. The actual strain gauge results for S.G.S.6 have been modified by either technique which eliminates the temperature effects, as discussed earlier in the report. The techniques explained are adequate for modification of data and can be used for analysis of the actual strain gauge results. The results are very similar and may vary within a couple of micro-strain. Figure1 and Figure2 as shown in Appendix E demonstrates the two different techniques used for thermal correction of strain data for September 24,2003.

The actual strain gauge results all have their own unique trend of dynamic motion which is expected due to the diverse nature of wind behavior. The wind patterns for any given instant are different from all others. The strength, intensity, direction, duration, gust are some factors which makes the wind patterns quite random. Therefore it is very difficult to estimate the wind pattern for any given instant for a period of time making the task of Structural Health Monitoring very interesting and challenging. The dynamic oscillation of the actual strain readings is not symmetrical as demonstrated in Figures 5.2 through Figures 5.20. The unsymmetrical results may be a consequence of the asymmetry of the statue about the east-west axis. The theoretical analysis does not account for this asymmetry which is why the accelerometer and wind analysis results are symmetric. Winds approaching dominantly from the North experience the higher peaks of strain in compression as shown in Figure 5.2 through 5.5, Figure 5.7 through 5.9 and Figure 5.11 through 5.17. In addition, wind blowing dominantly from the South causes the higher peaks of strain in tension as shown in Figure 5.6 and Figure 5.10. This behavior is expected since the strain gauge (S.G.S.6) is placed on the south face of the shaft. Theoretically speaking, north winds should shorten and south winds should elongate the south face of the shaft under pure bending assuming that the force is applied at the top of the cantilever shaft.

The accelerometer analysis results are symmetric along the horizontal axis which is expected since the theory doesn't include the asymmetry of the statue. For comparison, all corresponding plots with the same date shown throughout

this report are taken from the same time frame. Therefore, the plots can directly be compared. The results of the actual strain gauge are compared to strains obtained from wind and accelerometer analyses. The results of both strain gauge and accelerometer analysis demonstrate different ranges of peak strains occurring at the same instant of time throughout the strain-time relationship plots. For example, November 20,2003, can be categorized as a windy and very gusty day. This is demonstrated by a large peak on both plots at time 200, 426, 550, 850, 1000, 1200, 1350, 1600, 1750 and 1810 second. In addition, the maximum peak occurring at time 426 seconds which may be due to the largest gust at this time interval. The peaks are less evident and the vibrating motion tends to reassemble a narrow bandwidth as the gust approach 10km/hr is shown in Figure 5.16 to Figure 5.20 and Figure 5.35 to Figure 5.39, respectively. The maximum peak in the strain-time plots are compared by time and numerical value and are summarized in Table 5-3.

Table 5.3 reveals an apparent trend in which the maximum strain recorded by the strain gauge and that obtained from the accelerometer occurs at the same instant for a given day. The strain values for the actual strain analysis are approximately within a couple of micro-strain of the accelerometer analysis with the exception of September 24,2003 and November 20,2003 being 10 micro-strain and 6.5 micro-strain off, respectively. The curves for both analyses tend to have a distinct pattern. Not one curve is identical, but as the gust velocity decreases, the curves tend to lose oscillatory motion which tends to reassemble a narrow bandwidth. Observing the actual strain analysis, gust velocities ranging

from 59 km/hr to 50 km/hr, 43Km/hr to 39Km/hr, 32Km/hr to 19Km/hr and 12Km/hr to 0Km/hr (table 5.1) have an average absolute maximum strain of 30 micro-strain, 15.4 micro-strain, 6.5 micro-strain and 2.6 micro-strain, respectively. Each range of velocities contains a maximum value of strain which is relatively close and as the range decreases the strain is approximately divided in half.

The actual strain gauge analysis and dynamic analysis are being compared. Table 5.4 shows the occurrence of the maximum peak during the same time frame and it's apparent that it does not happen at the same instant. The values are all within approximately 10 micro-strain of the actual analysis with the exception of January 2, 2004 which is exceptionally high. This may be due to an anomaly in wind data. The velocity profile of the wind of January 2, 2004 is shown in Figure 5-67. The velocity reaches 135 km/hr (unrealistically high) at the time of 1200 seconds which is the exact location were the maximum strain (150micro-strain) occurs. The ultrasonic wind sensor must have malfunctioned; therefore the results of dynamic analysis for this set of data should be ignored. The curves for both analyses have no resemblance. The dynamic analysis seems to over predict the results and may have to be improved in the future. The wind behavior on the roof may not be the same near the Golden Boy, and the factors applied in the analysis may need to be fine tuned. The factors should be modified and adjusted to better fit the actual strain curves by analyzing the behavior of wind at the corner of the roof and the top of the dome in a wind tunnel test.

Table 5-3:Maximum Peaks of Strain

DATE	Occurrence of the Maximum Peak (gust)				% difference in strain
	ACTUAL STRAIN GAUGE ANALYSIS		ACCELEROMETER ANALYSIS		
	Time (second)	Absolute max. strain (με)	Time (second)	Absolute max. strain (με)	
September 24,2003	854	31	854	41	32
March 10,2004	441	30.5	441	33	8
January 21,2004	1189	27	1190	28	3
January 2,2004	104	30.5	104	28.9	5
October 27,2003	765	15.3	765	14.4	5
October 22,2003	1689	16.9	1689	16	5
November 20, 2003	426	14	426	20.5	46
March 1,2004	1660	15.3	1660	17.5	14
February 26, 2004	100	7.4	100	7.9	6
March 20,2004	150	7.2	150	6.5	9
February 11,2004	1050	5.6	1050	5.0	10
December 22,2003	1000	6.6	1000	8.2	24
March 28,2004	1510	7.0	1510	8.0	14
December 10,2003	200	5.0	200	4.0	20
February 22, 2004	1000	3	1000	2.8	6
November 3,2003	1150	4.1	1150	5.3	29
December 14,2003	1460	2.6	1460	3.2	23
October 26,2003	*	1.5	*	2.1	40
December 22,2003	*	1.5	*	2.8	85

* note that the asterisks mean that the wind velocity is none existent and have a quite broad band width associated with the intior time frame and no apparent peaks are observed.

Table 5-4:Maximum Peaks of Strain

DATE	Occurrence of the Maximum Peak (gust)				
	ACTUAL STRAIN GAUGE ANALYSIS		DYNAMIC ANALYSIS		
	Time (second)	Absolute max. strain (με)	Time	Absolute max. strain (με)	% differenc e in strain
September 24,2003	854	31	1280	21	32
March 10,2004	441	30.5	1400	38	24
January 21,2004	1189	27	1600	33	22
January 2,2004	104	30.5	1200	150	391 **
October 27,2003	765	15.3	1000	18	18
October 22,2003	1689	16.9	1040	17.5	35
November 20, 2003	426	14	80	9.9	29
March 1,2004	1660	15.3	200	16	5
February 26, 2004	100	7.4	1840	12	62 *
March 20,2004	150	7.2	1300	14	94 *
February 11,2004	1050	5.6	680	7	25
March 28,2004	1510	7.0	1450	8.4	20
December 10,2003	200	5.0	1150	8.7	74
February 22, 2004	1000	3	1000	12	300 *
October 26,2003		1.5		0.12	920 *

*for low values of velocity the data is noisy **Possible malfunction of wind meter

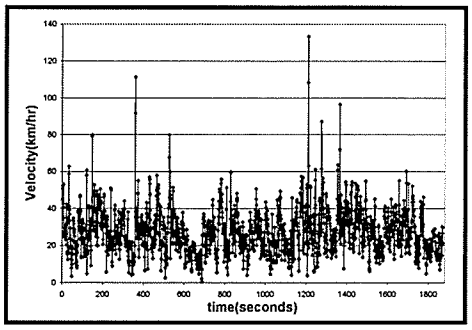

Figure 5-67 :Velocity Profile for January 2,2004

The wind meter's maximum wind velocity during the hour time frame compares quite closely to the gust recorded from the airport by Environment Canada. The results are summarized in Table 5-5. The wind meter is recording reasonable values and the values are all greater than registered by Environment Canada. This may be due to an increase of turbulence around the building, if any, or some kind of effect relating to the surrounding terrain such as buildings and trees. Also, the wind profile increases parabolically with height. Since the wind meter at the airport is at a lower elevation than the Legislature Building this may account for the difference. It seems that there is approximately 10 km/hr difference for the maximum wind velocity readings.

Table 5-5: Comparison of maximum velocity

DATE	Maximum velocity(km/hr)	
	Wind Meter	Environment Canada
September 24,2003	62	59
March 10,2004	70	59
January 21,2004	70	54
January 2,2004	135 **	50
October 27,2003	54	43
October 22,2003	50	43
November 20, 2003	50	43
March 1,2004	46	39
February 26, 2004	39	32
March 20,2004	41	30
February 11,2004	29	20
March 28,2004	30	19
December 10,2003	30	19
February 22, 2004	13	12
October 26,2003	4	0

**malfunction of the wind meter

The Root Mean Square (RMS) coefficient was calculated for the actual strain gauge data and the strain calculated from the accelerometer data for the higher wind speeds. The RMS coefficient ratio of the strain gauge to the accelerometer is compared. The RMS ratio for the entire interval (1800 second) as well as a 20 second time interval where the maximum gust of wind (peak) occurred were calculated. The results for both time intervals are summarized in table 5.6.

Table 5-6:Mathematical comparison of strain and accelerometer

DATE	RMS RATIO= ($RMS_{S.G}/RMS_{ACCELEROMETER}$)		Correlation coefficient for entire interval	Correlation coefficient for Max.peak interval 20sec
	Entire interval of 1800second	Max.Peak interval of 20 second		
September 24,2003	0.60	0.75	0.14	0.685
March 10,2004	1.65	1.08	0.37	0.628
January 21,2004	1.59	1.20	0.11	0.662
January 2,2004	1.75	1.24	0.10	0.658
October 27,2003	0.85	0.99	0.39	0.621
October 22,2003	0.75	0.99	0.12	0.674
November 20, 2003	0.61	0.71	0.13	0.673
March 1,2004	0.71	0.89	0.43	0.615
February 26, 2004	1.3	0.94	0.10	0664
March 20,2004	1.5	1.10	0.10	0.659
February 11,2004	0.78	1.15	0.08	0.601
December 10,2003	1.59	1.16	0.06	0.613
March 28,2004	1.35	0.96	0.37	0.601

The RMS ratio tends to have a greater significance for the smaller interval around the maximum peak, since the ratios are all closer to unity. This could only mean that both curves have significant correlation between the maximum gusts. This also reinforces the issue that the maximum absolute values of strain are similar in both analysis and that either one of the analysis will prove valuable for future prediction. The correlation between the curves for the entire interval is quite insignificant and is demonstrated by the larger skew.

The correlation analysis attempts to measure the strength between two different types of variables by means of a single number called the correlation coefficient (Walpole & Myers,1998). The correlation coefficient values range between -1 and +1, value of ±1 indicate a perfect correlation between both variables. Values near zero signify no apparent correlation between variables. A correlation coefficient was calculated for the entire time interval and is shown in Table 5-6. The variables consist of the actual strain gauge data and the strain obtained from the accelerometer data. The correlation coefficient ranging from 0.06 to 0.47 only means that there is no essential regression between the curves (entire interval). The correlation coefficient range is quite small and consistent (0.601 to 0.685) for the smaller interval of 20 seconds, meaning that we have two positive correlations and somewhat stronger correlation than the entire interval. The curves can not be correlated mathematically for the entire interval, but have some kind of correlation at smaller intervals (20 sec) shown in Table 5-6. The correlation coefficients are consistent for 20 seconds intervals around the maximum strain peaks.

5.7. SIMPLIFIED FORMULA

The simplified method is constructed with the maximum wind velocities recorded by Environment Canada shown in Table 5-5 and the maximum strain values obtained from the analysis of the strain gauge data. The corresponding points for the each day were plotted and are symbolized by the blue dots shown in Figure 5-68. A curve fitting technique was used in Excel to produce the best

fitting curve which is shown in Figure 5-68. The curve is a second degree polynomial and is represented by the equation below:

$$\varepsilon_{sg} = 0.0073\nu^2 + 0.1053\nu$$

where

ε_{sg} corresponds to the vertical axis in Micro-strain($\mu\varepsilon$) and ν corresponds to the horizontal axis in Velocity (Km/hr) as shown in Figure 5-68.

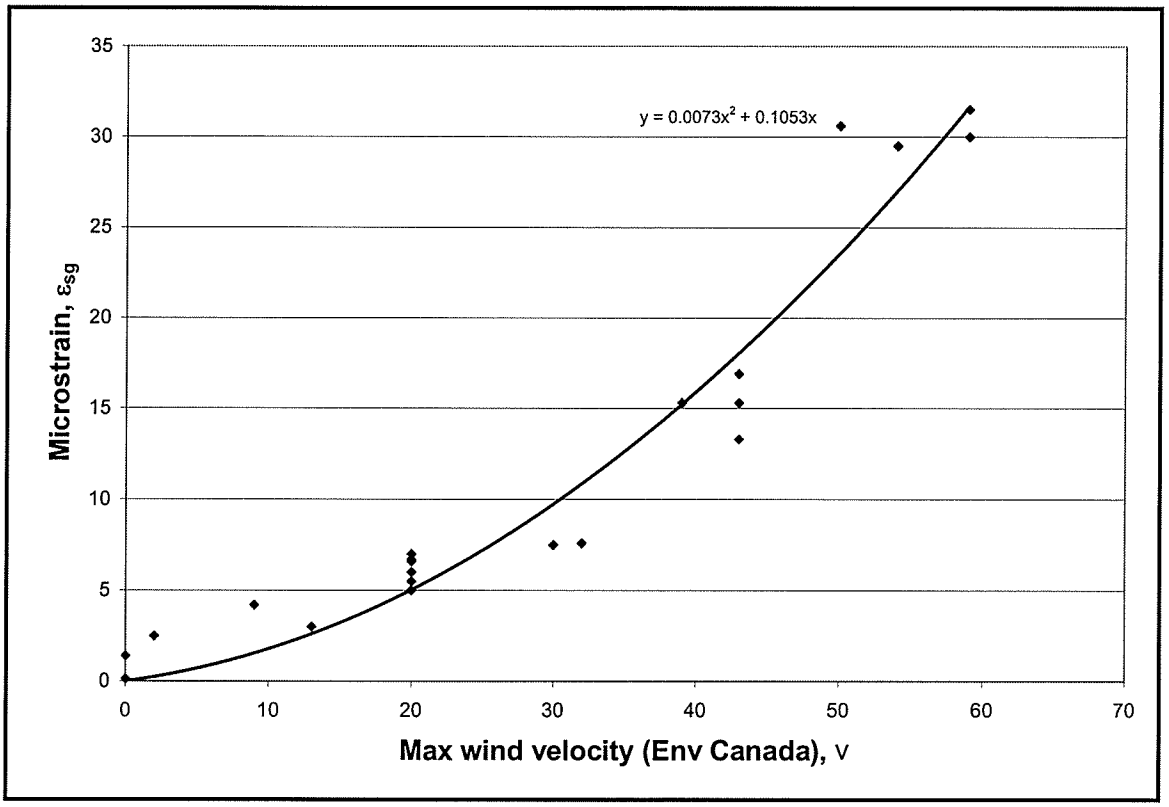

Figure 5-68: Simplified Analysis

The simplified analysis under predicts the strain at lower wind velocities. As the velocity increases past 20 Km/hr, the curve (formula) becomes more useful in predicting strain values. People may argue that the curve may be far too

conservative for wind velocities over 20 Km/hr, however, realistically the curve may be used as an upper boundary limit for higher velocities. The maximum strain gauge points should never reach the curve on very windy days as shown in the plot. If for some reason the strain exceeds the simplified formula, it should be of immediate concern and the appropriate actions must be taken.

6. CONCLUSIONS

Based on the findings of this study, the following conclusion can be drawn:

The wind and accelerometer data have been used to calculate the peak strains at the base of the shaft and compared with the strain gauges data. The results are found to be in good agreement. The SHM system of the Golden Boy thus provides some redundancy which could be useful in predicting the strains even in the event of possible malfunction of any sensors. The instrumentation sensors installed for the SHM of the Golden Boy is of great importance. The instrumentation devices are recording useful information which can be used for evaluating the structural health condition of the statue. Since the monitoring of the statue is in the early stages and the Golden Boy has been reinforced properly, it is fair to conclude that the data collected within the first year will serve as the baseline for a very healthy structure. Everything beyond the first year will be compared to the baseline on a continual basis which will indicate the health or other concerns of the statue.

Note that the analysis in the report doesn't assess the amount of change in the material properties or strength of the stainless steel shaft, if any, but sets a baseline for strain expected for the different types of wind speeds. The focus of the report is based on the dynamic movement of the statue due to the winds. The

study indicates winds between 59-50 Km/hr, 43-39Km/hr, 32-19Km/hr and 12-0Km/hr experience maximum strain values of approximately 30 micro-strain, 15.4 micro-strain, 6.5 micro-strain and 2.6 micro-strain, respectively. This relates to a stress of 6 MPa, 3.1 MPa, 1.3 MPa and 0.52 MPa at the fixity of the shaft, respectively. If those strains are ever exceeded by a huge amount for a known wind velocity there is a definite state of concern to the statue's health. In that event some type of action must be taken by the engineer to determine the cause of change.

The simplified formula should be used as an upper case boundary for very windy days. This may be the ultimate tool for a fast check to see if the real data strain is in an acceptable range. The empirical relationship formula can be a useful tool to the owner of the structure to get a ball-park estimate of the strain in the shaft based on the wind velocity and detect possible malfunction of the sensors or deterioration of the structure.

.

Another important feature of the traditional rosette strain gauge instruments installed is that they record both thermal and dynamic strain together. In other words, the dynamic strain due to bending is solely dependent on wind behaviour and the thermal strain is dependent on temperature changes to the material. It is necessary to eliminate the thermal strain component from the total strain recorded by strain gauges. Several techniques discussed in Section 5.3 of the report can be used for this purpose. It is also possible to obtain a history of the thermal strain profile for an entire year, which can serve as a baseline or bench

mark for thermal strain. This will help in the future to asses the mechanical properties and strength in the steel for years to come.

The accelerometer analysis when compared to the actual strain gauge analysis has some kind of correlation. For the entire time frame of 1800 seconds the linear correlation between both analyses is not very good as the signals look unrelated, while the strain histories by the correlation coefficient for a shorter time span around the peaks appear to be reasonably good. The correlation coefficient ranged from 0.06 to 0.43 confirming the curves are independent and diverse, which is expected, because the theoretical analysis of the accelerometer doesn't include the asymmetry or the irregularity of the Golden Boy's structure whereas the strain gauge does. On the other hand, both analyses show overall similarities throughout the entire time frame. The spontaneity of the gusts incorporated in the wind's pattern was revealed in both curves at the same instance of time by producing larger peaks. In addition, gusts of wind occurring at the same time (table 5.3) and the absolute value were comparable (table5.3). Overall, the absolute maximum strain values between both analyses at high gust (approx. 50Km/hr) differ by 9% on the average, with 3% being the lowest and 32% being the highest difference. For high gust this is reasonable since the micro-strain range is quite small, generally speaking. The correlation between both variables at 20 second intervals where the maximum peak occurred is quite good. The RMS ratio ($RMS_{S.G}/RMS_{ACCEL}$) ranging from 0.71 to 1.24 (Average 0.94) provided a sense of comfort in establishing that the data points are similar and correlate

well with one another (table 5.6). Therefore, the biggest advantage is that if the strain gauge rosettes were to fail due to environmental effects such as lightning causing electrolysis, di-bonding of epoxy due to temperature or just aging, the accelerometer would still be able to demonstrate live strain profiles for any given day with reasonable accuracy.

The ultrasonic wind sensor records the wind patterns as indicated in table 5.5. The maximum gust within the hour time frame is quite close to the velocity (max. gust) recorded by Environment Canada at the Winnipeg airport. The difference may be a result of the extra height or additional turbulence on the roof of the Legislature Building as compared to the airport where it is located a distance of 10 meter from ground level in open terrain. The wind patterns as recorded using the wind meter near the statue are used in the dynamic analysis which uses the Duhamel integral formula. The results of the Duhamel's integral depends on the following two criteria, the forcing function (wind meter) and the time step used in the integration. The time step needs to be small enough for obtaining correct output (dynamic displacement). The Forcing Function for each different time step (Δt=1, 0.5, 0.125, 0.0625 and 0.03125s) was prepared with linear interpolation. The time step, Δt=0.03125 s, yields the displacement which is quite close that was obtained using the larger time step (Δt=0.0625 s). Therefore the correct solution is using Δt=0.0625s as evident from Figure 5-49 and Figure 5-50. A time step of Δt=0.0625s is used throughout the study. The dynamic and the actual strain gauge analysis of the maximum peak (gust) do not occur at the same instant as shown in table 5.4 of the report. The percentage

difference between both analyses is quite high. Therefore the wind meter analysis is not as accurate in predicting the response of the actual maximum strain in the structure, but serves as a good starting point. It must be kept in mind that the factors used in calculating the forces due to wind are based on the formula in NBCC 1995 which may need to be modified in future research to obtain the appropriate or acceptable values. The procedure used here for calculating the dynamic displacement of the structure, given the forcing function due to wind, serves as an alternate way of monitoring the structural health of the Golden Boy.

The accelerometer's live data is continuously being monitored for the Golden Boy's dynamic characteristics, such as natural frequency. A Fast Fourier Transformation (FFT) of the data is endlessly showing 3.05 hertz to 2.95 hertz. The web page has been constructed to view the live data on a continuous basis (updated every 5 seconds). The theoretical natural frequency of the statue is 2.95Hz which can be used as the reference value for a healthy structure. If the natural frequency changes below the baseline frequency (2.80 Hz or 5% decrease of the reference frequency) in any way, this would be a signal to be taken very seriously. Immediate action should be taken for any change in the health condition of the structure and must be, in that event, dependent on the degree of change. Factors that may affect the natural frequency of the Golden Boy are the total mass, elastic modulus and the geometric properties of the shaft. The theoretical analysis performed with the mathematical model achieved good correlation of natural frequency.

The early stage of SHM of the Golden Boy was accomplished correctly by installing the instruments and monitoring system. In addition, the data collected by the system were analysed for the interpretation of what the values actually mean to an engineer. The gust of wind at any given instant can be used to obtain the maximum strains or stresses of the statue. The accelerometers can also serve to monitor the health of the Golden Boy should the strain gauge ever malfunction. The data analysed here should give some confidence in the SHM process and overall well being of the statue.

6.1. RECOMMEDATION FOR FUTURE RESEARCH

In order to achieve full understanding of the SHM of the Golden Boy, research is required in the following areas:

1. The refinement of the mathematical model to accurately predict the results more precisely.
2. A system which allows recovery of recorded data in a manner very simplified and easy to access through our server.
3. Some boundaries and limits should be applied to the system which would give engineers a signal of the statue's health.
4. Investigation of a wind tunnel test for the entire Legislature Building and top of the Golden Boy statue which should help modify the factors used in the wind meter analysis.
5. The possible development of a temperature strain profile for the entire year which should be used for a baseline to future trends.
6. Evaluating the possible changes in material properties and strength of the steel once a baseline as been established.

REFERENCES

Lardner, T.J. and Archer, A.A., "Mechanics of Solids: An Introduction", McGraw-Hill, Inc., 1994.

Simiu, E., "Wind Effects on Structures", John Wiley & Sons, Inc. New York,1986.

Rivera, E., Mufti, A.A., and Thomson, D.J., (2004) "Civionics Specifications", ISIS Canada Design Manual, 2004.

Kopp, G.A. and Surry, D., "A Study of Wind Effects On the Golden Boy, Winnipeg", The Boundary Layer Wind Tunnel Laboratory, The University of Western Ontario, November 2001.

Canadian Highway Bridge Design Code, A National Standard of Canada, CAN/CSA-S6.00, 2001.

Mufti, A.A., "Structural Health Monitoring of Manitoba's Golden Boy", ISIS Canada, 2003.

Gilles, M., 2001. Street of Dreams, The Story of Broadway. Heartland Associates Inc., Winnipeg, MB, pp.82-113.

Chapra, S.C. and Canale, R.P., "Numerical Methods for Engineering", McGraw-Hill, Inc., 1998.

Medearis, K., "Numerical-Computer Methods for Engineers and Physical Scientists", KMA Research, Denver-Fort Collins, Colorado, 1974.

Frye, M.J., Rattanawangcharoen, N. and Shah, A.H., "130.135 Engineering Statics", The University of Manitoba, 2003.

Tennyson, R.C., "Installation, Use and Repair of Fibre Optic Sensors", Design Manual No. 1, ISIS Canada Corporation, September 2001.

Mufti, A.A., "Guidelines for Structural Health Monitoring", Design Manual No. 2, ISIS Canada Corporation, September 2001.

Hibbeler, R.C., "Structural Analysis", Fourth Edition, Prentice-Hall, Inc., 1999.

Anderson, R.A, "Fundamentals of Vibrations", The Macmillan Company, New York, Collier-Macmillan Limited, London, 1967

Mufti, A.A.,"CIVIONICS Expanding the Limits of Civil Engineering", Innovator Newsletter of ISIS Canada Research Network, August 2003

Rivera, E., Mufti, A.A., and Thomson, D.J., "Civionics Specifications", ISIS Canada Design Manual, 2004.

Mufti, A.A, and Tadros, G, Manitoba Legislative Building, Golden Boy-Review and Comments, report submitted to Dillion Consulting , Winnipeg, Manitoba, November, 2001.

Doncaster, A.M., "An Evaluation of Fibre Optic Sensors for Monitoring of Civil Structures", Research Report No.1-1997, Nova Scotia CAD/CAM Centre, Nova Scotia, Canada.

Mufti, A.A., Bakht, B., and Limaye, V., "Instrumentation of Portage Creek Bridge", Project Report T-3.3.10, Nova Scotia CAD/CAM Centre, Nova Scotia, Canada.

Qureshi, H.T., "Archival and Processing of Structural Health Monitoring Data", Master of Applied Science, Carleton University, Ottawa, Ontario, Canada, June 2001.

Vo, P.H., Haldar, A., and Ling, X., "Experimental Verification of a Novel System Identification Technique", 8th ASCE specialty Conference on Probabilistic Mechanics and Structural Reliability, 1997.

Dillon Consulting Ltd., Stainless steel mechanical properties, 2003.

Met One Instruments Inc, Operation Manual, Document No. 50.5-9800, 2002.

Wiebe, B., Hawrylak, M., and Mickalash, T., Private Meetings at the Legislative Building, 2002.

Picker, P., Pritchard Machine Shop, Conversation and meetings for installation of instrumentation, 2002.

Tedesco, J.W., McDougal, W.G. and Ross, C.A., "Structural Dynamics Theory and Application", Addison Wesley Longman, Inc., 1999.

http://www.ec.gc.ca/weather, Official web site of Environment Canada.

http://www.isiscanada.com, 2002. Official web site for ISIS Canada, a federally funded network of centres of excellence.

Biggs, J.M., "Introduction to Structural Dynamics", McGraw-Hill, Inc., 1964.

Humar, J.L., Bagchi, A., Xia, H., "Frequency Domain Analysis of Soil-Structure Interaction", Computers & Structures Vol.66 Nos2-3. pp.337-351, 1998.

Appendix A

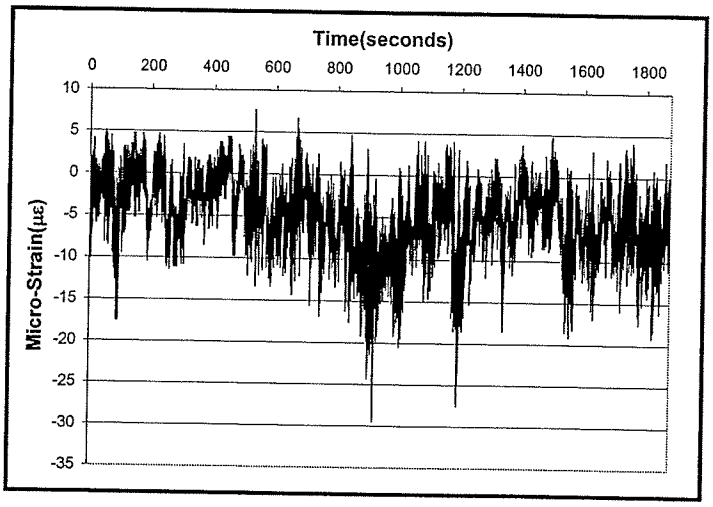

Figure 5-4: Strain vs. Time of Actual Strain Gauge South (S.G.S.6) on January 21, 2004

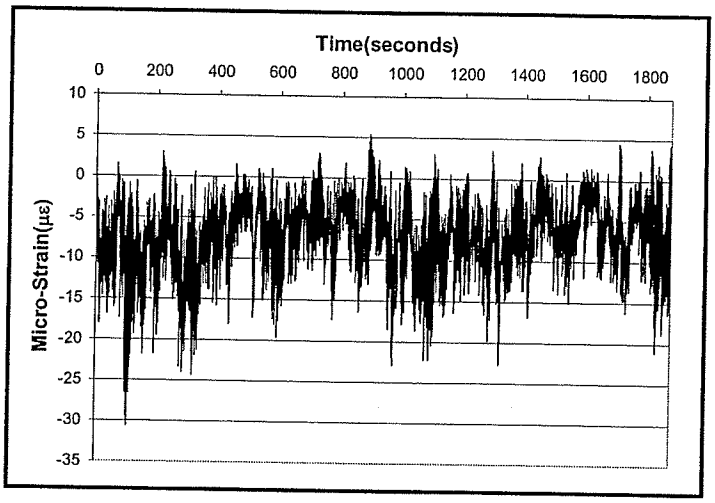

Figure 5-5: Strain vs. Time of Actual Strain Gauge South (S.G.S.6) on January 2, 2004

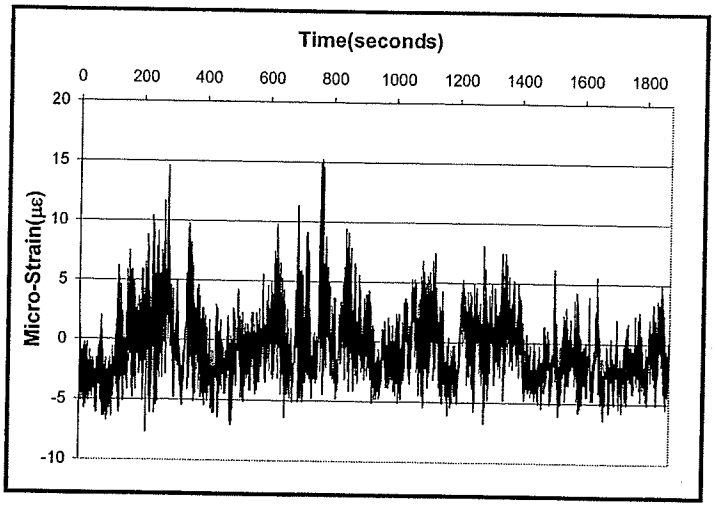

Figure 5-6: Strain vs. time of actual strain gauge south (S.G.S.6) on October 27, 2003

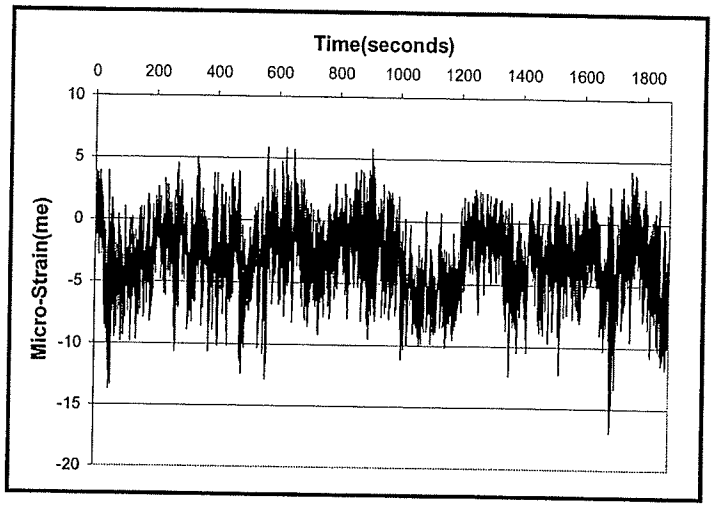

Figure 5-7: Strain vs. time of actual strain gauge south (S.G.S.6) on October 22, 2003

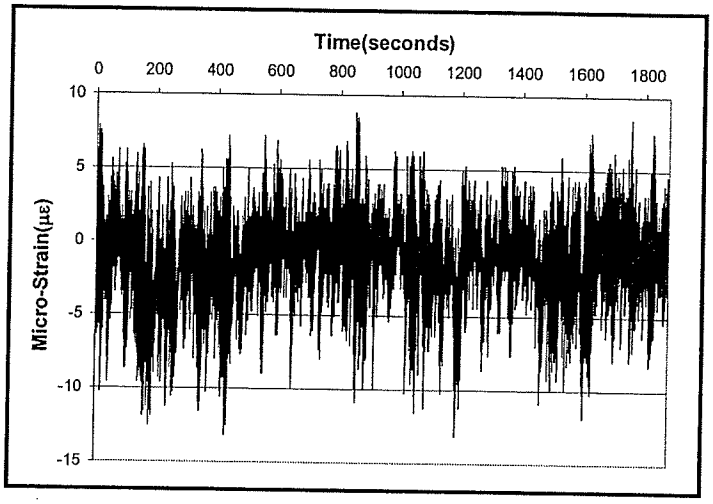

Figure 5-8: Strain vs. time of actual strain gauge south (S.G.S.6) on November 20,2003

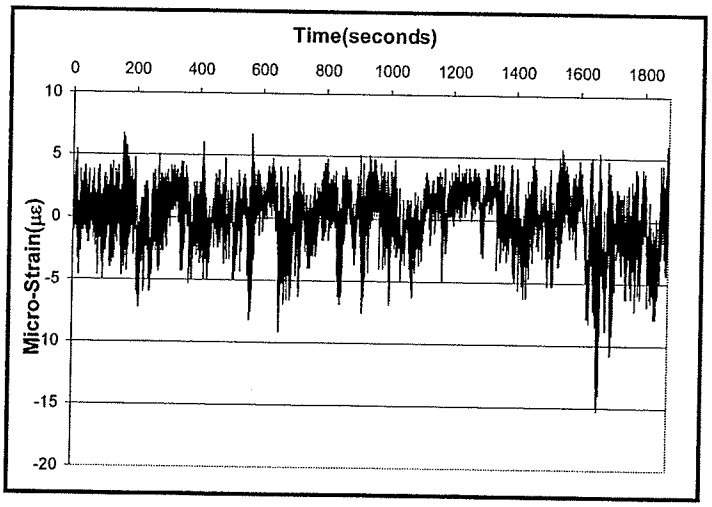

Figure 5-9: Strain vs. time of actual strain gauge south (S.G.S.6) on March 1, 2004

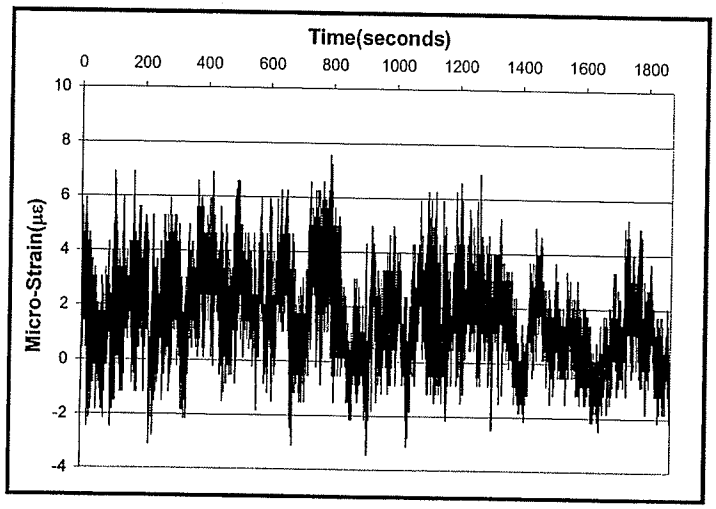

Figure 5-10: Strain vs. time of actual strain gauge south (S.G.S.6) on February 26, 2004

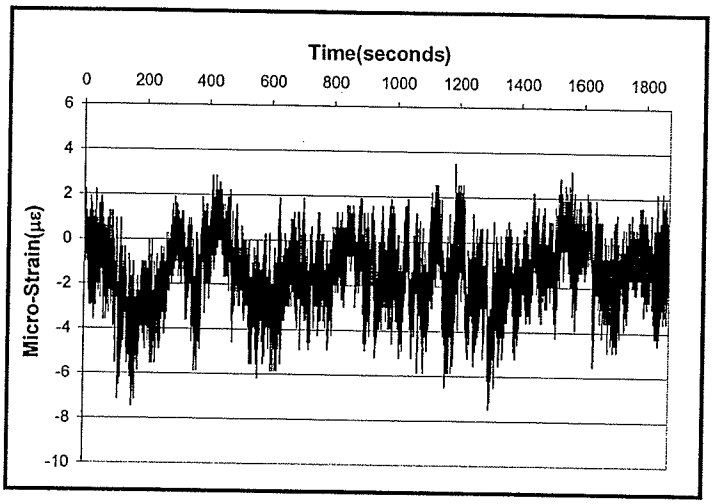

Figure 5-11: Strain vs. time of actual strain gauge south (S.G.S.6) on March 20, 2004

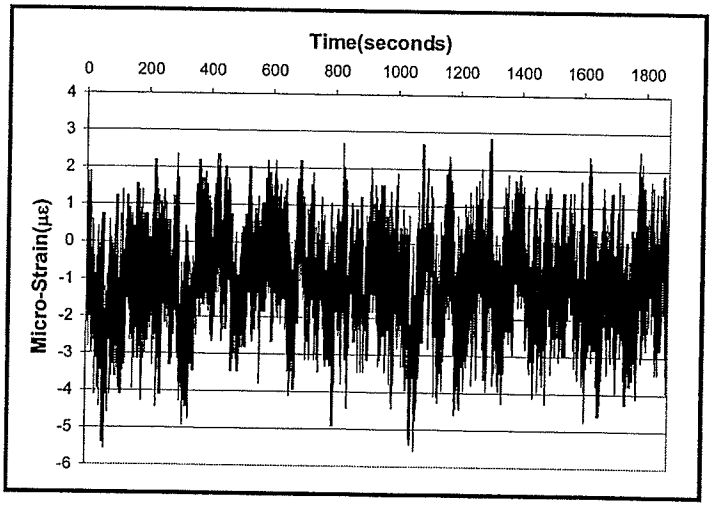

Figure 5-12: Strain vs. time of actual strain gauge south (S.G.S.6) on February 11, 2004

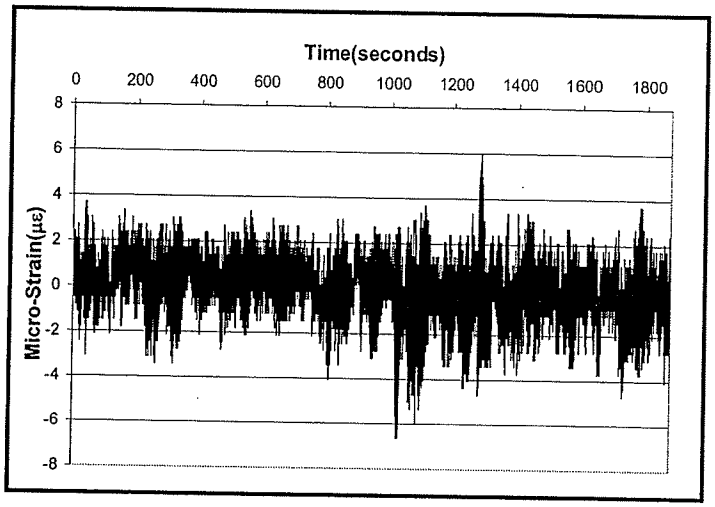

Figure 5-13: Strain vs. time of actual strain gauge south (S.G.S.6) on December 22, 2003

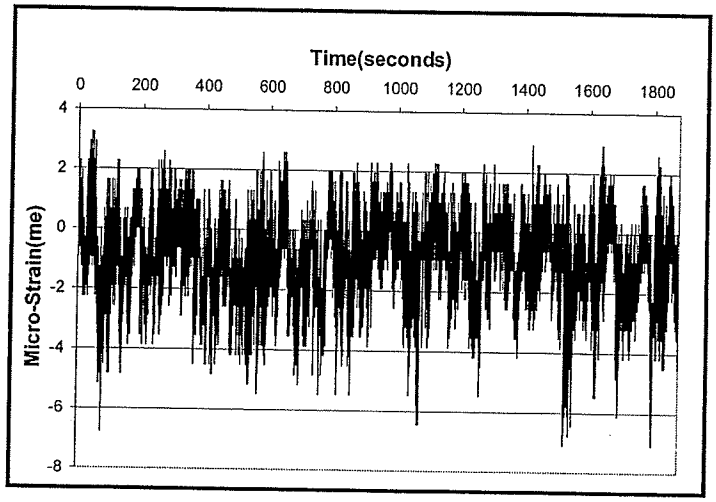

Figure 5-14: Strain vs. time of actual strain gauge south (S.G.S.6) on March 28, 2004

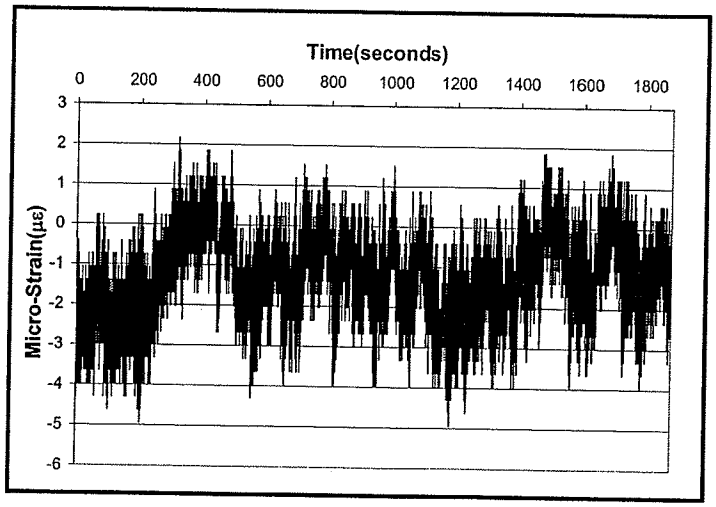

Figure 5-15: Strain vs. time of actual strain gauge south (S.G.S.6) on December 10, 2003

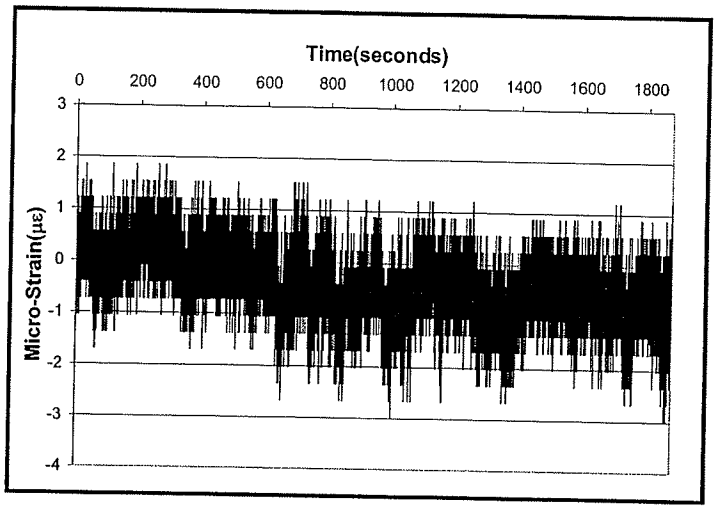

Figure 5-16: Strain vs. time of actual strain gauge south (S.G.S.6) on February 22, 2004

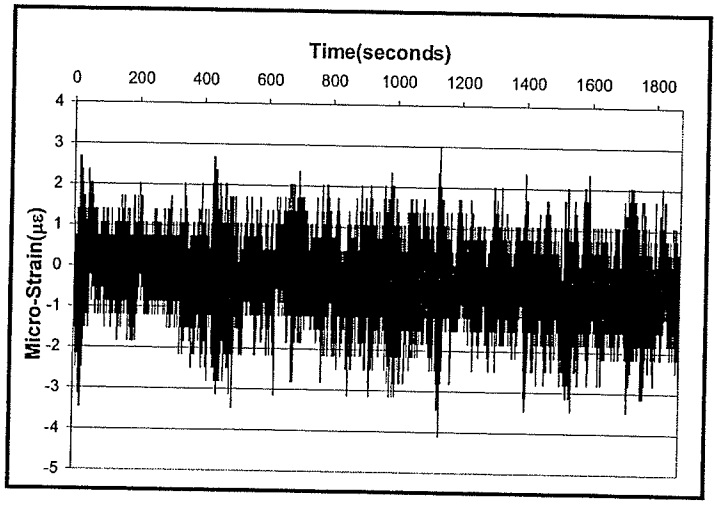

Figure 5-17: Strain vs. time of actual strain gauge south (S.G.S.6) on November 3, 2003

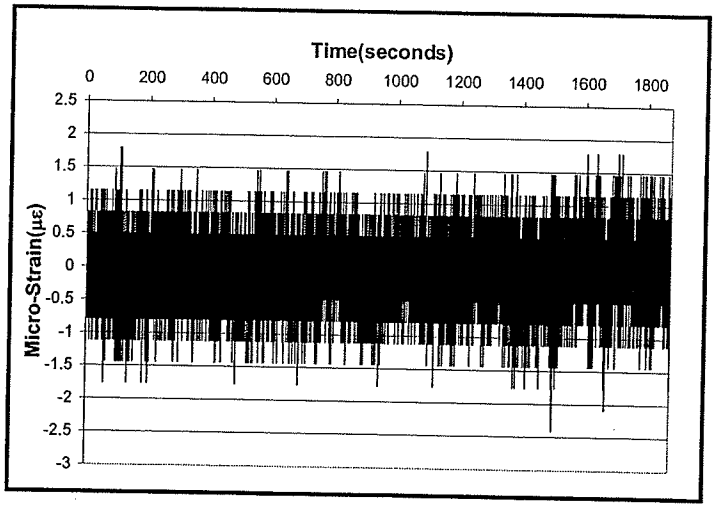

Figure 5-18: Strain vs. time of actual strain gauge south (S.G.S.6) on December 14, 2003

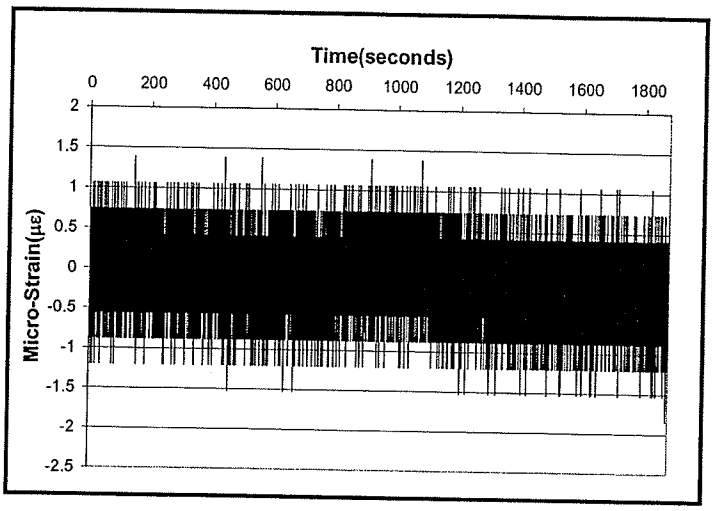

Figure 5-19: Strain vs. time of actual strain gauge south (S.G.S.6) on October 26, 2003

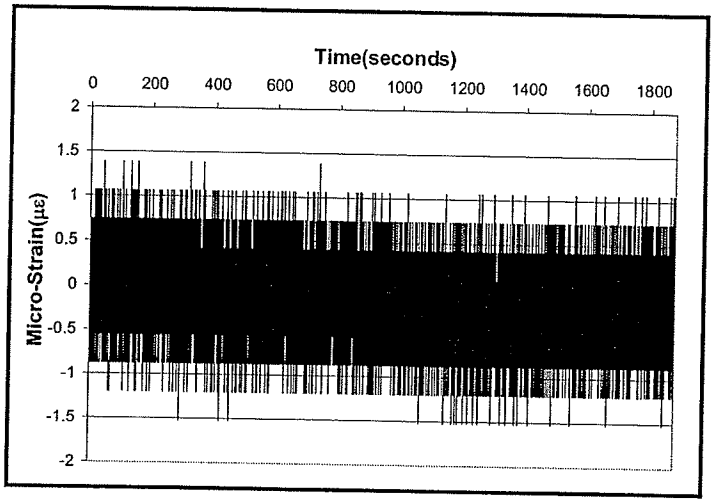

Figure 5-20: Strain vs. time of actual strain gauge south (S.G.S.6) on December 22, 2003

Appendix B

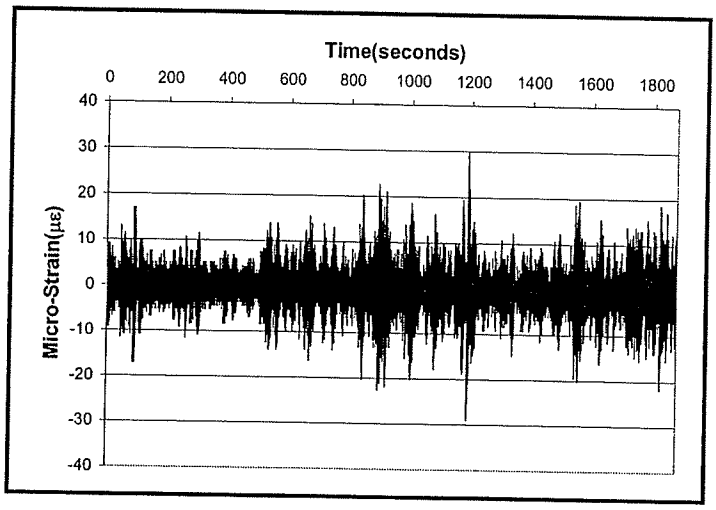

Figure 5-23: Strain vs. Time of Y-Accelerometer Analysis on January 21,2004

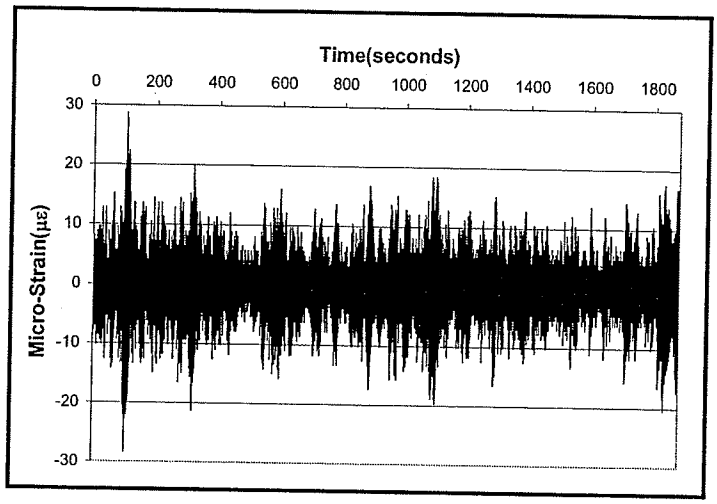

Figure 5-24: Strain vs. Time of Y-Accelerometer Analysis on January 2,2004

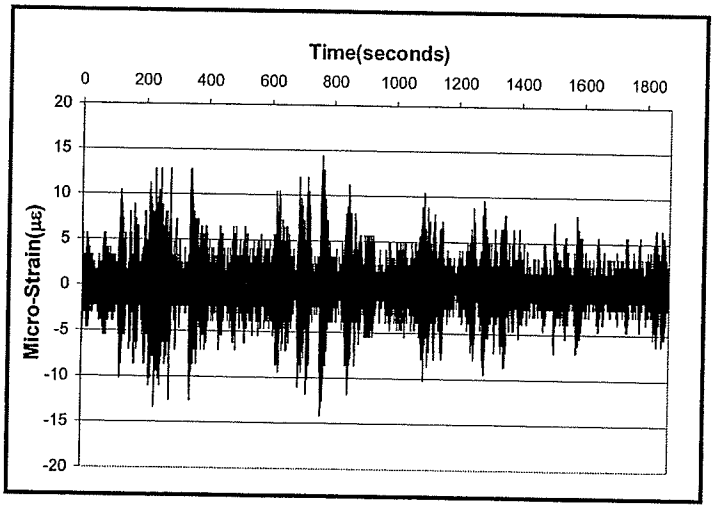

Figure 5-25: Strain vs. time of Y-Accelerometer analysis on October 27,2003

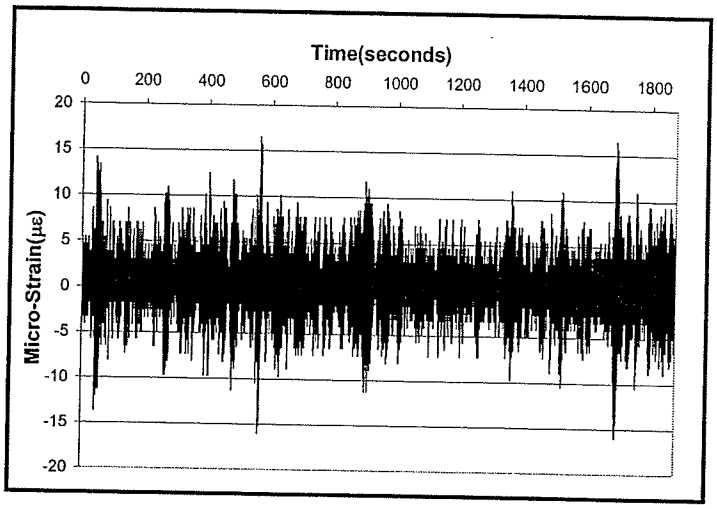

Figure 5-26: Strain vs. time of Y-Accelerometer analysis on October 22,2003

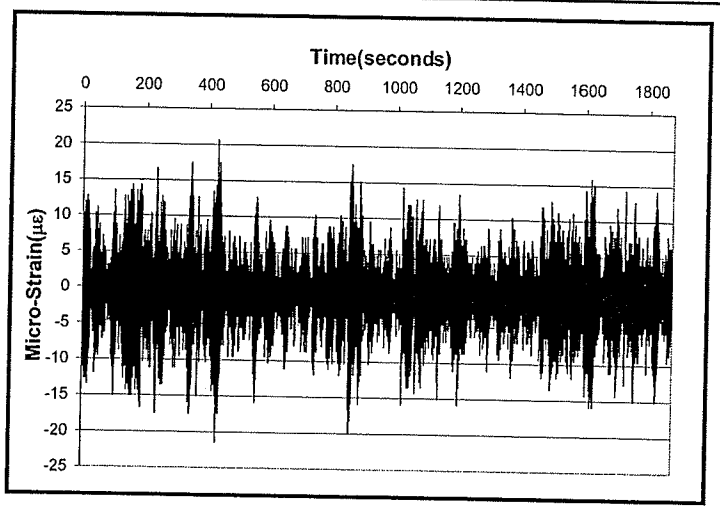

Figure 5-27: Strain vs. time of Y-Accelerometer analysis on November 20,2003

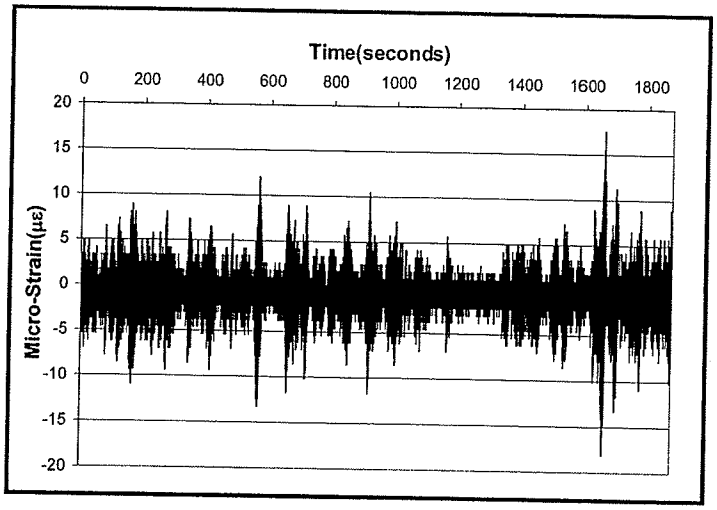

Figure 5-28: Strain vs. time of Y-Accelerometer analysis on March 1,2004

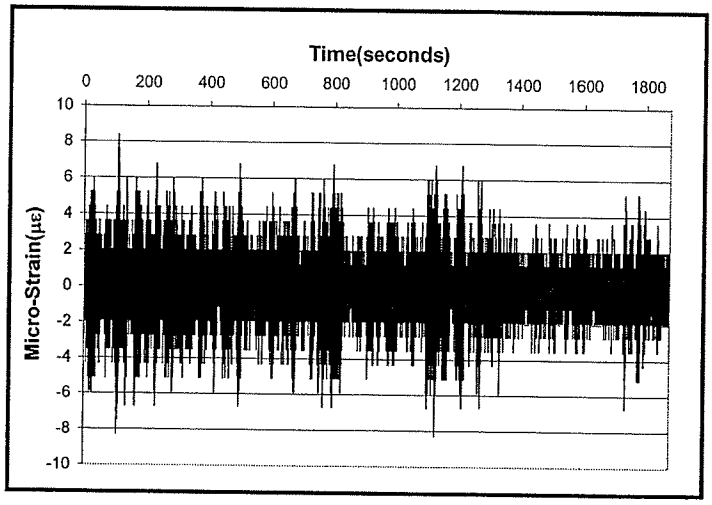

Figure 5-29: Strain vs. time of Y-Accelerometer analysis on February 26,2004

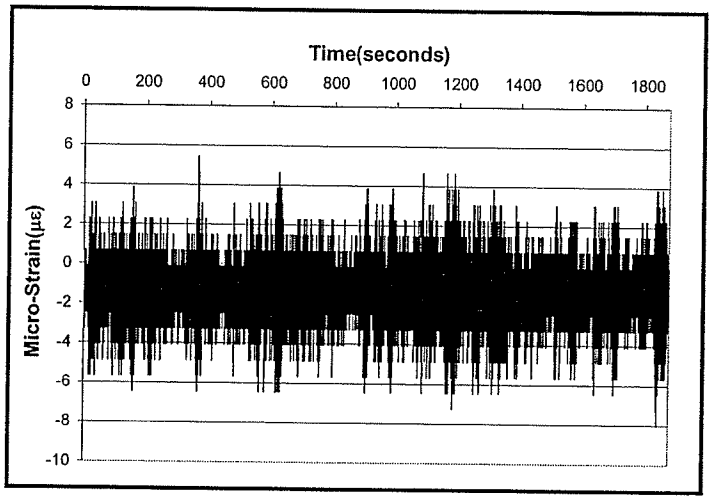

Figure 5-30: Strain vs. time of Y-Accelerometer analysis on March 20,2004

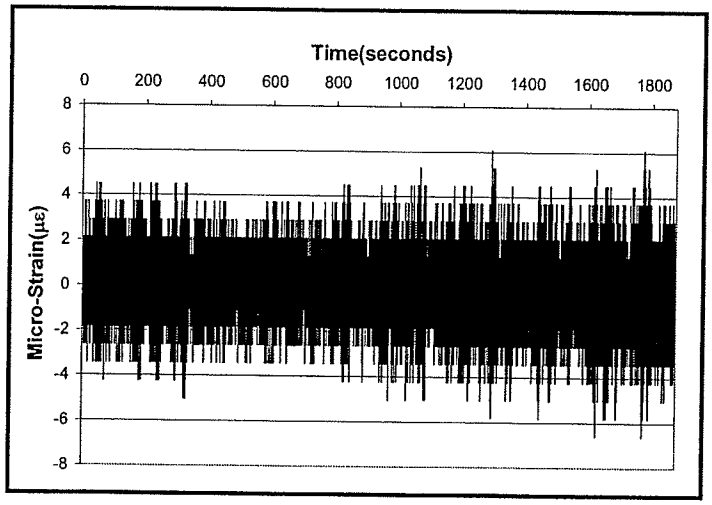

Figure 5-31: Strain vs. time of Y-Accelerometer analysis on February 11,2004

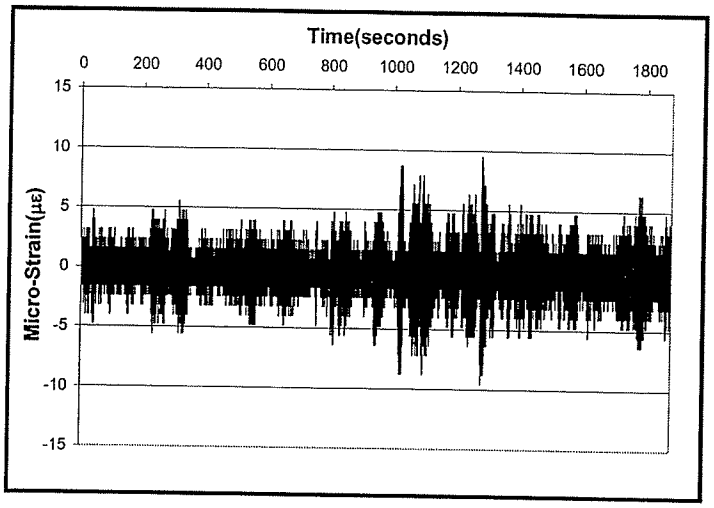

Figure 5-32: Strain vs. time of Y-Accelerometer analysis on December 22,2003

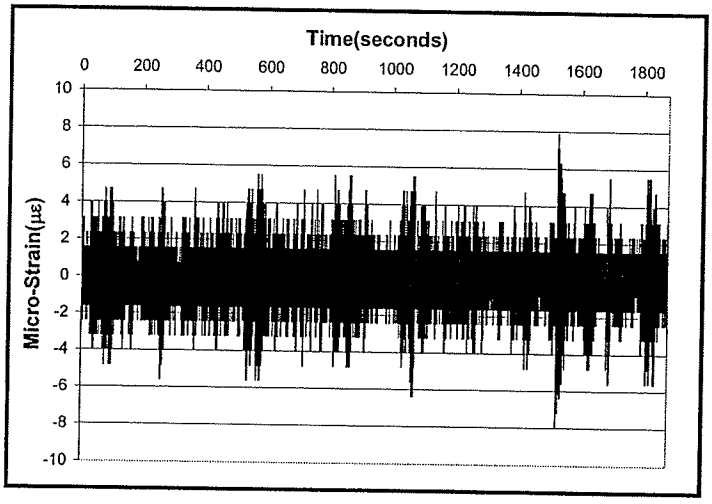

Figure 5-33: Strain vs. time of Y-Accelerometer analysis on March 28,2004

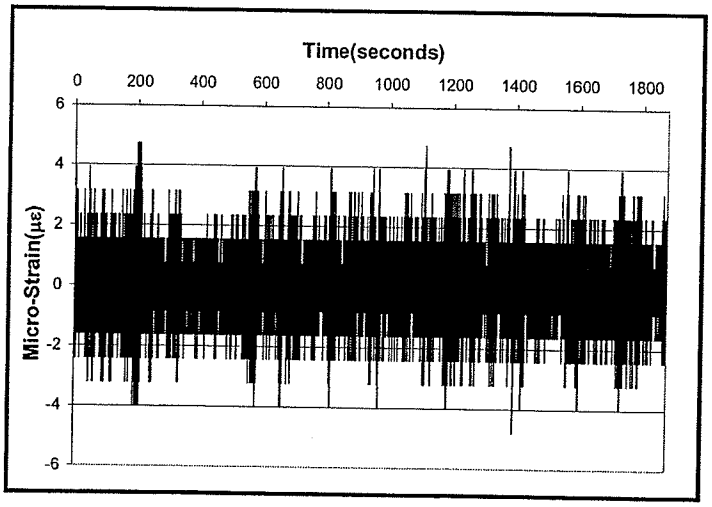

Figure 5-34: Strain vs. time of Y-Accelerometer analysis on December 10,2003

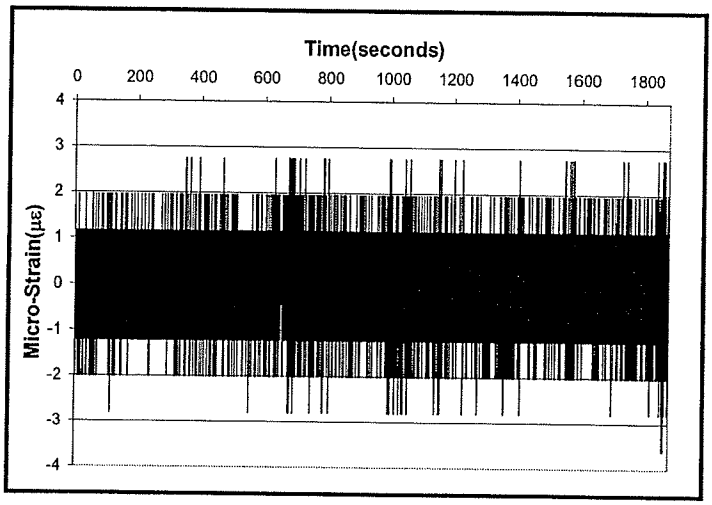

Figure 5-35: Strain vs. time of Y-Accelerometer analysis on February 22,2004

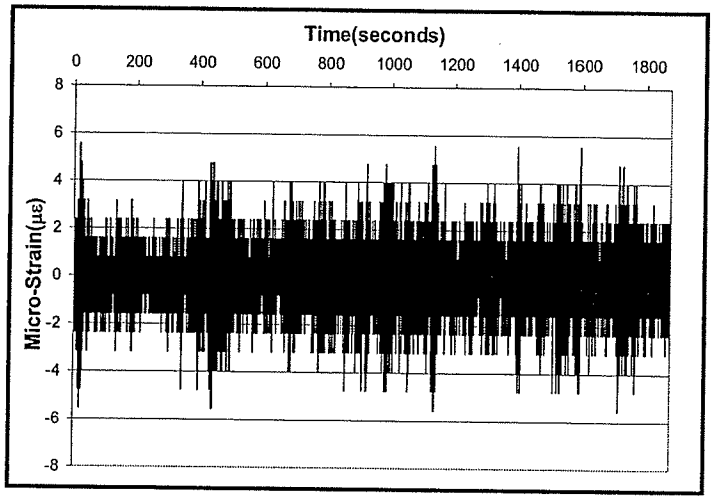

Figure 5-36: Strain vs. time of Y-Accelerometer analysis on November 3,2003

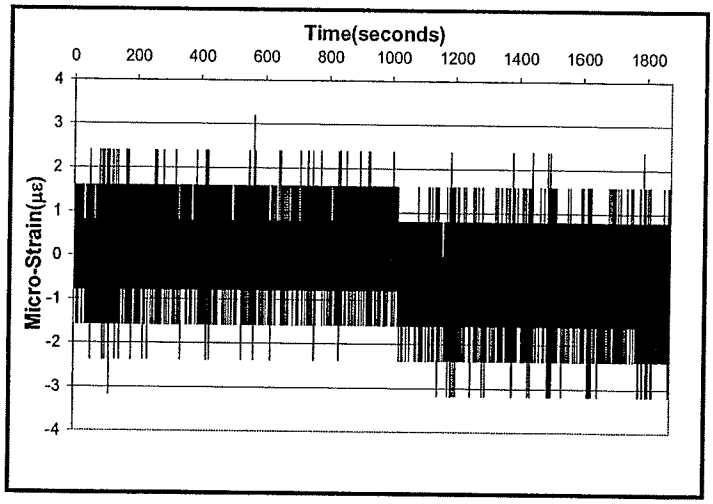

Figure 5-37: Strain vs. time of Y-Accelerometer analysis on December 14,2003

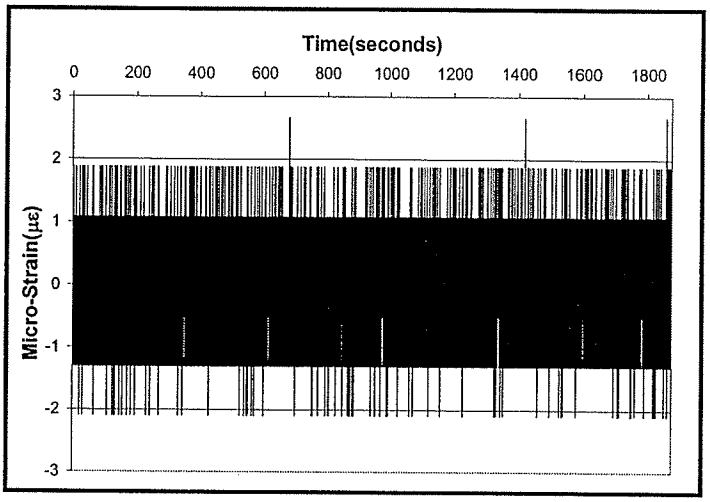

Figure 5-38: Strain vs. time of Y-Accelerometer analysis on October 26,2003

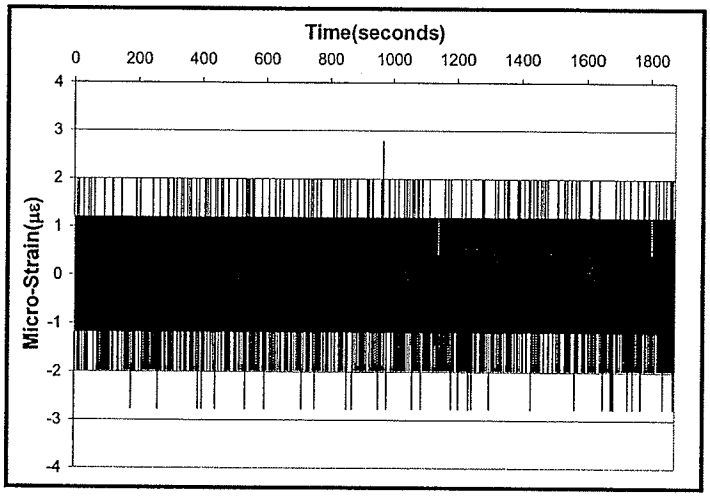

Figure 5-39: Strain vs. time of Y-Accelerometer analysis on December 22,2003

Appendix C

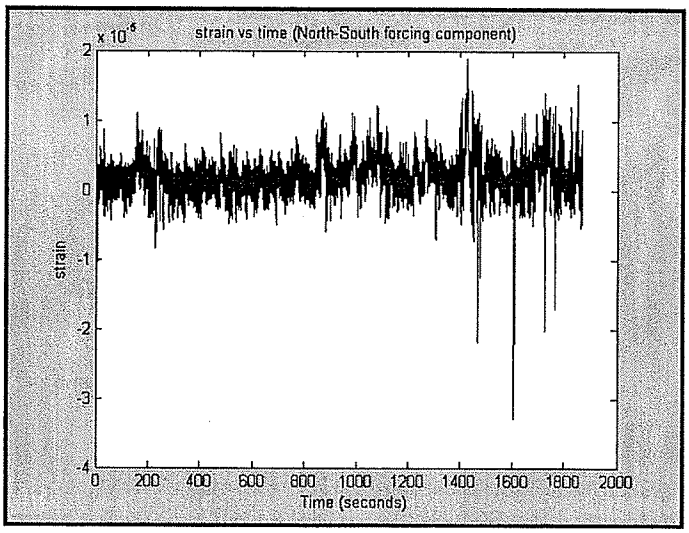

Figure 5-53: Strain vs Time (Dynamic Analysis on January 21,2004)

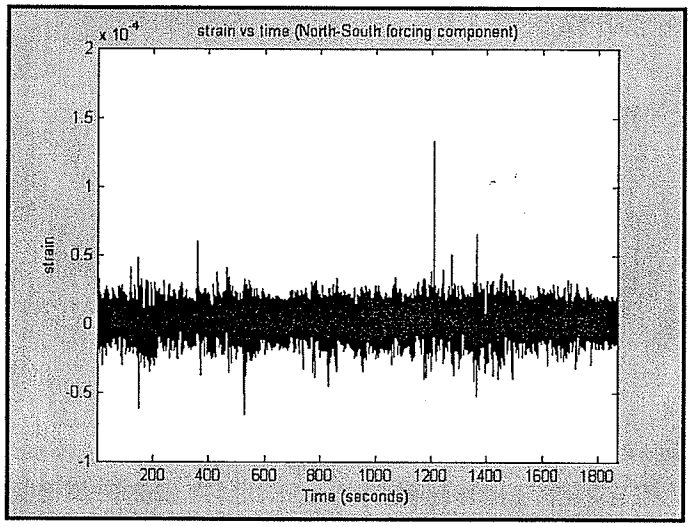

Figure 5-54: Strain vs Time (Dynamic Analysis on January 2,2004)

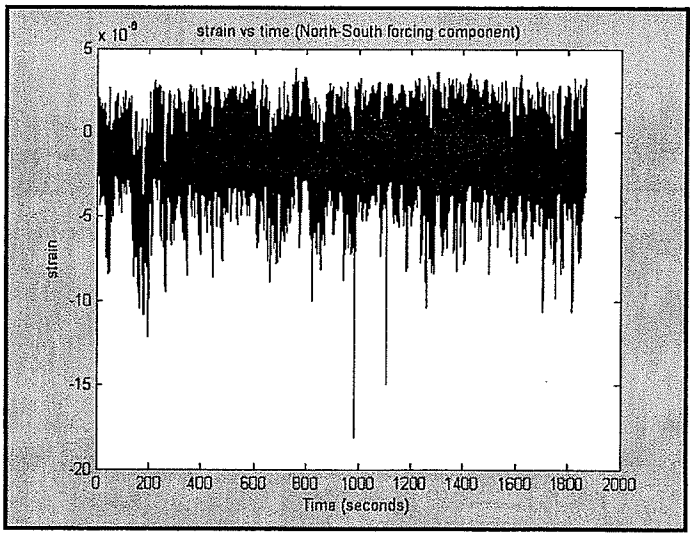

Figure 5-55: Strain vs time of dynamic analysis on October 27,2003

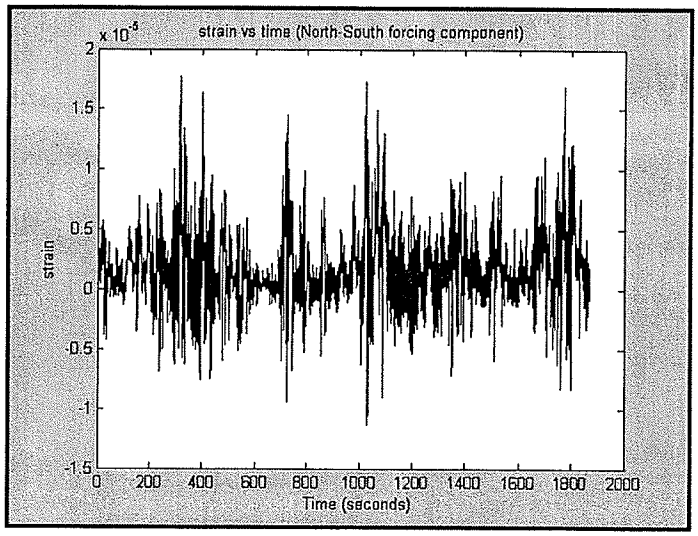

Figure 5-56: Strain vs time of dynamic analysis on October 22,2003

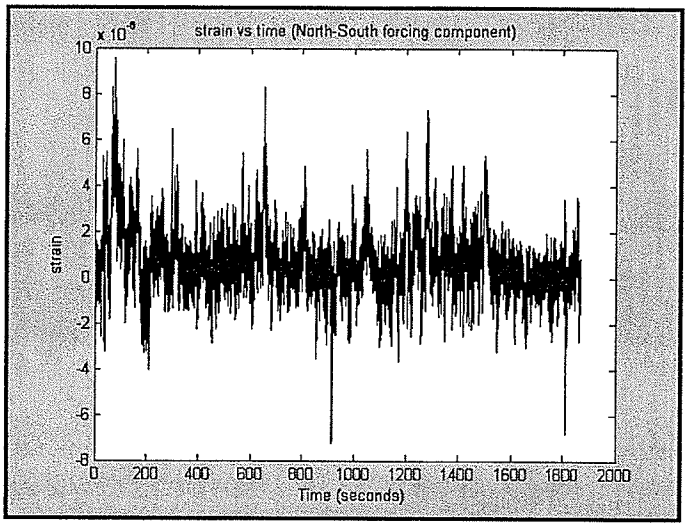

Figure 5-57: Strain vs time of dynamic analysis on November 20,2003

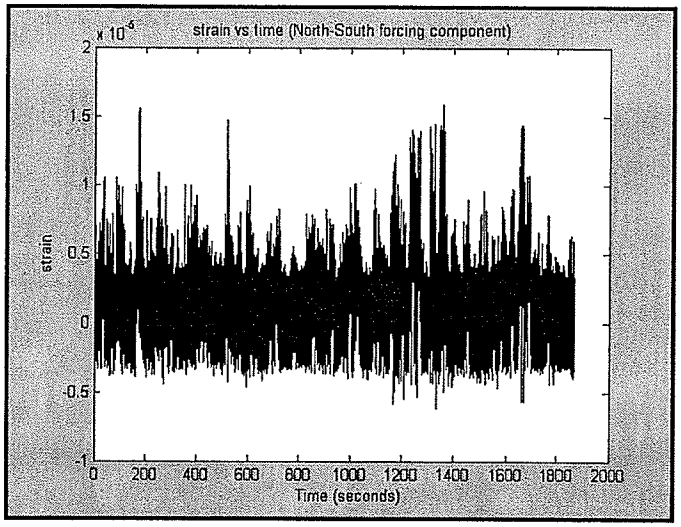

Figure 5-58: Strain vs time of dynamic analysis on March 1,2004

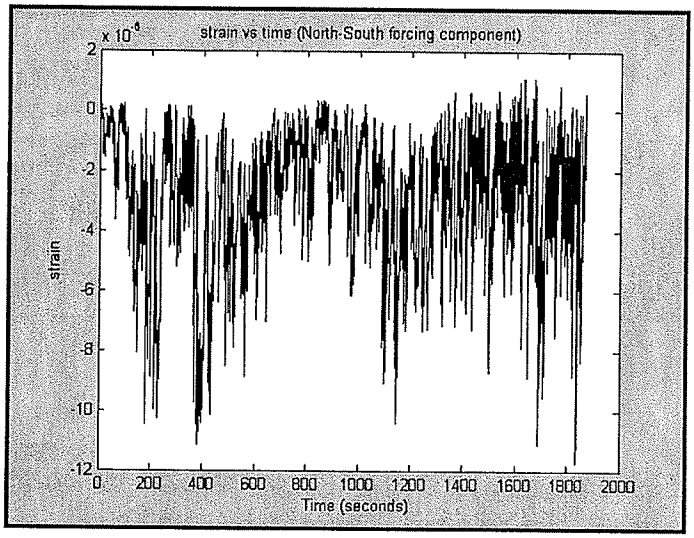

Figure 5-59: Strain vs time of dynamic analysis on February 26,2004

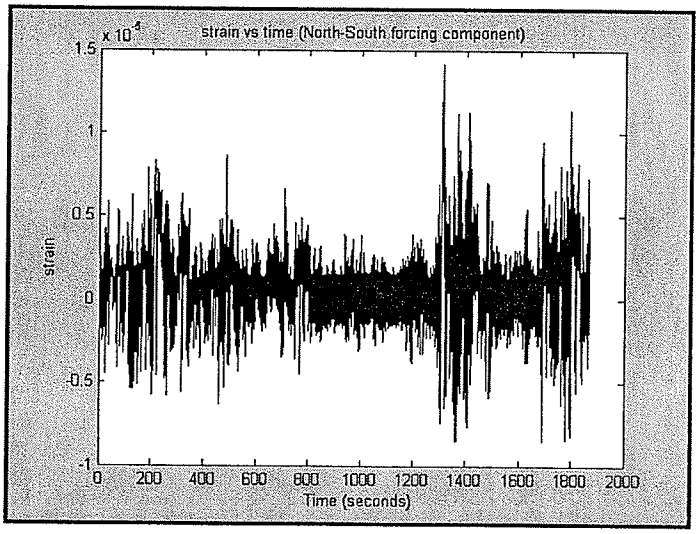

Figure 5-60: Strain vs time of dynamic analysis on March 20,2004

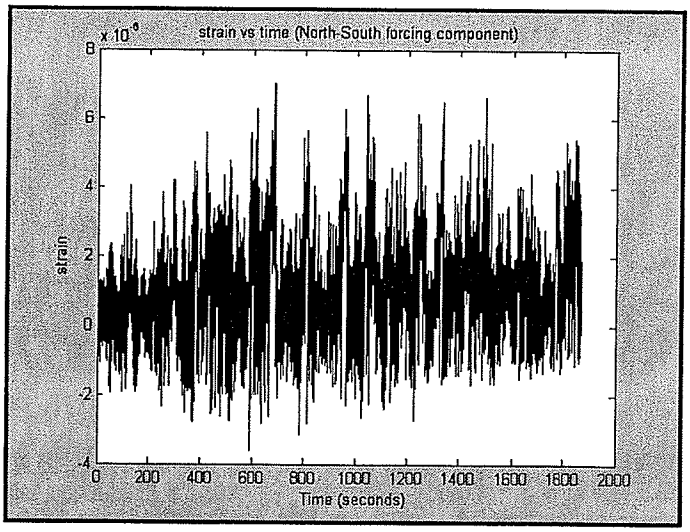

Figure 5-61: Strain vs time of dynamic analysis on February 11,2004

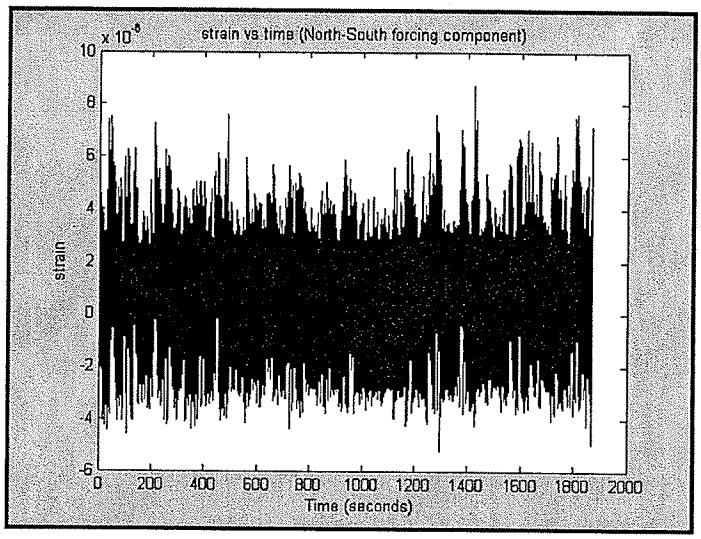

Figure 5-62: Strain vs time of dynamic analysis on March 28,2004

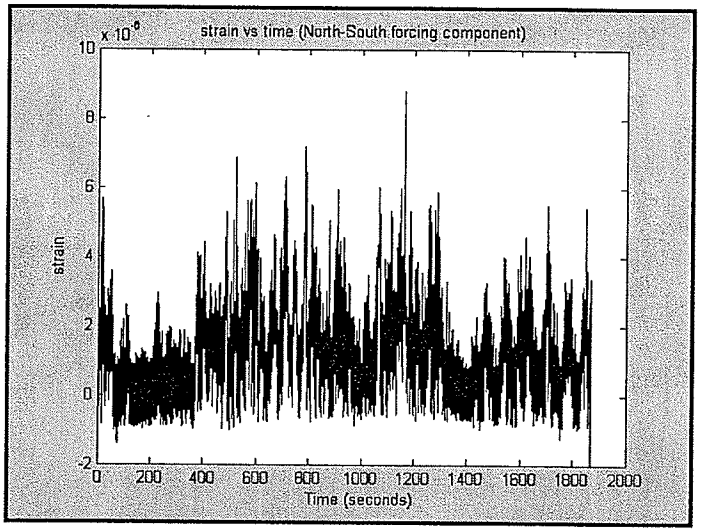

Figure 5-63: Strain vs time of dynamic analysis on December 10,2003

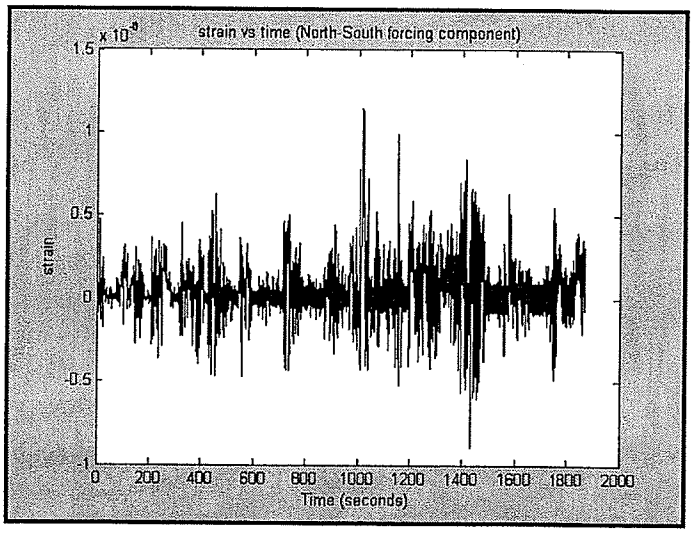

Figure 5-64: Strain vs time of dynamic analysis on February 22,2004

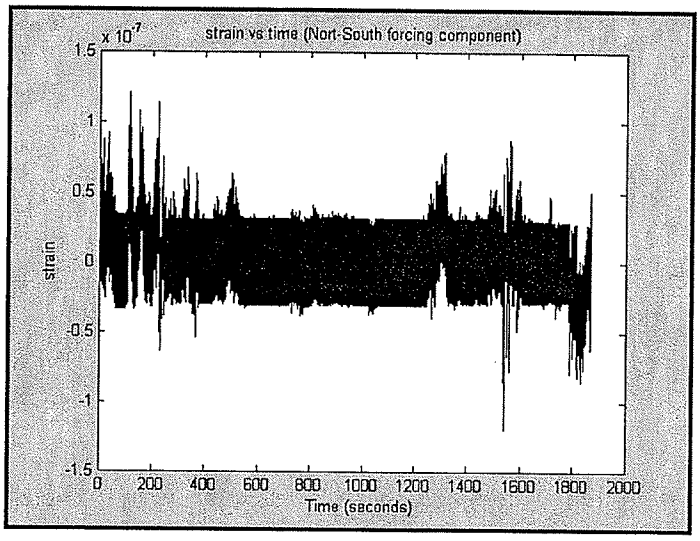

Figure 5-65: Strain vs time of dynamic analysis on October 26,2003

Appendix D

****

Golden Boy Strain, Accelometer, Temperature, Wind Meter Data File:d:\GoldenBoyData\ Jan 02 - 2004(8_13_46 PM).dat

****

		Strain1	Strain3	Strain4	Strain6	Strain8	Accelometer1-x	Accelometer1-y	Accelometer1-z	Accelometr	Accelometr	Accelometr
Fri, Jan 02, 2004	9:16:17 PM	-30.684	-29.297	-26.488	-31.837	-28.331	-0.002	0.022	0.049	0.002	0.012	0.005
Fri, Jan 02, 2004	9:16:17 PM	-29.714	-28.975	-29.067	-28.929	-27.362	-0.001	0.018	0.042	0	0.01	0.005
Fri, Jan 02, 2004	9:16:17 PM	-30.36	-28.653	-30.356	-29.575	-25.102	-0.002	0.015	0.042	-0.003	0.005	0.005
Fri, Jan 02, 2004	9:16:17 PM	-31.33	-28.009	-31.646	-31.837	-23.811	-0.001	0.004	0.038	-0.007	-0.004	0.004
Fri, Jan 02, 2004	9:16:17 PM	-31.976	-28.009	-33.903	-35.392	-21.873	-0.001	-0.001	0.036	-0.009	-0.011	0.004
Fri, Jan 02, 2004	9:16:17 PM	-32.299	-27.044	-33.903	-37.978	-20.582	-0.003	-0.001	0.039	-0.005	-0.012	0.004
Fri, Jan 02, 2004	9:16:17 PM	-33.268	-28.331	-33.58	-38.947	-22.196	-0.002	-0.002	0.044	0	-0.009	0.005
Fri, Jan 02, 2004	9:16:17 PM	-32.945	-28.975	-31.646	-38.624	-23.488	-0.002	0.006	0.047	0.004	-0.005	0.004
Fri, Jan 02, 2004	9:16:17 PM	-33.268	-28.331	-29.711	-37.008	-24.779	-0.001	0.009	0.048	0.004	0.003	0.004
Fri, Jan 02, 2004	9:16:17 PM	-31.653	-29.297	-29.067	-33.453	-26.394	-0.001	0.016	0.051	0.006	0.008	0.005
Fri, Jan 02, 2004	9:16:17 PM	-30.36	-29.297	-28.1	-31.514	-27.039	0.001	0.022	0.047	0.005	0.01	0.005
Fri, Jan 02, 2004	9:16:17 PM	-30.36	-28.975	-27.455	-29.898	-27.685	0	0.017	0.045	0.001	0.011	0.004
Fri, Jan 02, 2004	9:16:17 PM	-30.684	-29.94	-29.389	-29.898	-26.716	-0.001	0.014	0.042	-0.002	0.005	0.003
Fri, Jan 02, 2004	9:16:17 PM	-31.007	-27.366	-30.034	-32.161	-24.779	-0.002	0.007	0.041	-0.002	-0.004	0.003
Fri, Jan 02, 2004	9:16:17 PM	-31.976	-28.653	-31.968	-34.423	-23.488	-0.003	-0.002	0.041	-0.005	-0.008	0.004
Fri, Jan 02, 2004	9:16:17 PM	-32.299	-28.975	-32.291	-37.008	-23.165	-0.003	0.001	0.041	-0.003	-0.01	0.004
Fri, Jan 02, 2004	9:16:17 PM	-32.622	-28.009	-31.968	-38.947	-22.519	-0.003	-0.003	0.041	-0.003	-0.01	0.004
Fri, Jan 02, 2004	9:16:17 PM	-32.945	-28.975	-31.646	-37.655	-23.488	-0.002	0.008	0.042	-0.001	-0.003	0.004
Fri, Jan 02, 2004	9:16:17 PM	-32.622	-28.009	-30.034	-36.685	-24.456	-0.002	0.009	0.047	0.002	0.003	0.004
Fri, Jan 02, 2004	9:16:17 PM	-31.976	-28.975	-28.1	-33.453	-26.394	-0.001	0.019	0.048	0.004	0.007	0.005
Fri, Jan 02, 2004	9:16:17 PM	-30.36	-29.618	-27.777	-30.545	-27.362	-0.001	0.016	0.048	0.004	0.009	0.004
Fri, Jan 02, 2004	9:16:17 PM	-30.037	-29.297	-27.132	-30.545	-28.331	-0.001	0.017	0.048	0.002	0.008	0.003
Fri, Jan 02, 2004	9:16:17 PM	-30.037	-29.618	-27.777	-30.545	-28.008	-0.002	0.016	0.048	0.003	0.002	0.004
Fri, Jan 02, 2004	9:16:17 PM	-30.684	-28.975	-27.455	-31.514	-27.039	-0.001	0.009	0.046	0.001	-0.004	0.004
Fri, Jan 02, 2004	9:16:17 PM	-31.976	-28.653	-27.777	-34.423	-26.394	-0.003	-0.001	0.039	-0.005	-0.009	0.004
Fri, Jan 02, 2004	9:16:17 PM	-31.976	-29.297	-30.034	-35.716	-24.779	-0.002	-0.001	0.041	-0.005	-0.011	0.004
Fri, Jan 02, 2004	9:16:17 PM	-32.945	-28.331	-30.679	-37.332	-24.456	-0.002	0	0.042	-0.003	-0.007	0.005
Fri, Jan 02, 2004	9:16:17 PM	-32.622	-28.653	-30.356	-37.332	-24.779	0	0.004	0.043	-0.002	-0.002	0.005
Fri, Jan 02, 2004	9:16:17 PM	-32.299	-29.297	-30.679	-35.392	-25.425	-0.001	0.008	0.044	-0.001	0.002	0.003
Fri, Jan 02, 2004	9:16:17 PM	-31.33	-28.975	-28.744	-33.13	-26.071	0	0.016	0.047	0.003	0.008	0.006
Fri, Jan 02, 2004	9:16:17 PM	-30.36	-29.297	-28.744	-31.191	-27.039	0	0.018	0.048	0.004	0.009	0.004
Fri, Jan 02, 2004	9:16:17 PM	-30.037	-29.618	-28.422	-29.898	-28.654	-0.002	0.019	0.045	0.002	0.008	0.004
Fri, Jan 02, 2004	9:16:17 PM	-30.36	-28.975	-27.132	-30.222	-28.008	-0.002	0.014	0.043	0.001	0.003	0.004
Fri, Jan 02, 2004	9:16:17 PM	-30.684	-28.975	-28.422	-31.514	-26.716	-0.003	0.011	0.044	0.001	-0.003	0.004
Fri, Jan 02, 2004	9:16:17 PM	-31.007	-28.653	-28.744	-34.423	-25.748	-0.003	0.004	0.042	-0.005	-0.007	0.005
Fri, Jan 02, 2004	9:16:17 PM	-31.976	-28.975	-29.389	-36.039	-25.425	-0.002	0	0.04	-0.004	-0.009	0.005
Fri, Jan 02, 2004	9:16:17 PM	-32.622	-28.653	-30.679	-36.685	-25.102	-0.003	0	0.04	-0.003	-0.008	0.004
Fri, Jan 02, 2004	9:16:17 PM	-32.299	-27.687	-28.422	-36.685	-24.779	-0.001	0.006	0.043	0	-0.003	0.004
Fri, Jan 02, 2004	9:16:17 PM	-31.976	-28.653	-29.389	-34.423	-26.071	-0.001	0.013	0.047	0.002	0.002	0.004
Fri, Jan 02, 2004	9:16:17 PM	-31.33	-29.94	-27.777	-32.807	-27.362	-0.001	0.016	0.048	0.004	0.007	0.004
Fri, Jan 02, 2004	9:16:17 PM	-30.684	-29.618	-26.165	-30.868	-28.331	-0.001	0.016	0.049	0.003	0.008	0.004
Fri, Jan 02, 2004	9:16:17 PM	-29.714	-29.618	-27.777	-28.606	-28.331	-0.001	0.019	0.047	0.004	0.009	0.005
Fri, Jan 02, 2004	9:16:17 PM	-30.037	-29.297	-26.81	-28.929	-27.685	-0.001	0.013	0.047	0.002	0.004	0.004
Fri, Jan 02, 2004	9:16:17 PM	-30.36	-28.653	-28.422	-30.222	-27.039	-0.001	0.008	0.042	-0.002	-0.001	0.005
Fri, Jan 02, 2004	9:16:17 PM	-31.007	-29.618	-30.356	-31.514	-25.102	-0.002	0	0.039	-0.006	-0.007	0.004
Fri, Jan 02, 2004	9:16:17 PM	-31.976	-27.366	-31.001	-34.746	-23.488	-0.001	0.003	0.038	-0.006	-0.01	0.004
Fri, Jan 02, 2004	9:16:17 PM	-31.33	-28.653	-32.935	-35.392	-22.842	-0.001	0.003	0.04	-0.005	-0.007	0.004
Fri, Jan 02, 2004	9:16:17 PM	-32.299	-28.653	-31.323	-35.392	-23.165	-0.002	0.007	0.04	-0.002	-0.004	0.003
Fri, Jan 02, 2004	9:16:17 PM	-31.653	-28.009	-29.067	-33.453	-24.134	-0.001	0.009	0.044	0.002	0.002	0.005
Fri, Jan 02, 2004	9:16:17 PM	-30.684	-28.975	-28.744	-31.514	-26.716	-0.001	0.012	0.05	0.005	0.006	0.005
Fri, Jan 02, 2004	9:16:17 PM	-30.037	-29.94	-26.165	-30.222	-28.331	-0.001	0.016	0.052	0.009	0.008	0.004
Fri, Jan 02, 2004	9:16:17 PM	-29.391	-29.94	-24.876	-28.282	-29.945	-0.001	0.014	0.052	0.008	0.006	0.006
Fri, Jan 02, 2004	9:16:17 PM	-30.037	-30.262	-25.52	-28.929	-30.591	-0.002	0.011	0.047	0.005	0.001	0.004
Fri, Jan 02, 2004	9:16:17 PM	-30.36	-28.975	-25.843	-30.868	-28.654	-0.001	0.004	0.047	0.001	-0.003	0.005
Fri, Jan 02, 2004	9:16:17 PM	-30.684	-28.331	-28.744	-31.514	-26.394	-0.002	0.003	0.04	-0.005	-0.005	0.003
Fri, Jan 02, 2004	9:16:17 PM	-31.33	-29.297	-31.646	-33.453	-23.811	-0.002	0.001	0.034	-0.008	-0.007	0.004
Fri, Jan 02, 2004	9:16:17 PM	-31.976	-27.366	-32.935	-34.1	-22.196	-0.002	0.006	0.031	-0.012	-0.007	0.004
Fri, Jan 02, 2004	9:16:17 PM	-31.33	-27.687	-34.225	-33.453	-21.551	-0.002	0.009	0.039	-0.005	-0.002	0.004
Fri, Jan 02, 2004	9:16:17 PM	-31.33	-27.366	-31.646	-33.453	-22.842	-0.002	0.009	0.042	-0.001	0.002	0.005
Fri, Jan 02, 2004	9:16:17 PM	-31.007	-28.975	-29.711	-31.191	-25.102	0	0.013	0.048	0.005	0.005	0.005
Fri, Jan 02, 2004	9:16:17 PM	-30.037	-29.618	-28.1	-29.898	-28.331	-0.001	0.016	0.052	0.008	0.005	0.005
Fri, Jan 02, 2004	9:16:17 PM	-29.714	-29.297	-24.876	-29.252	-30.268	-0.001	0.015	0.055	0.011	0.004	0.005
Fri, Jan 02, 2004	9:16:17 PM	-29.714	-30.262	-24.876	-29.252	-30.914	-0.003	0.01	0.052	0.008	0.003	0.005
Fri, Jan 02, 2004	9:16:17 PM	-30.684	-29.94	-24.553	-30.545	-30.591	-0.002	0.006	0.048	0.003	-0.002	0.004
Fri, Jan 02, 2004	9:16:17 PM	-30.684	-29.618	-26.165	-31.837	-28.654	-0.001	0.008	0.041	-0.001	-0.005	0.004
Fri, Jan 02, 2004	9:16:17 PM	-31.007	-29.297	-29.711	-32.807	-26.071	-0.001	0.004	0.035	-0.008	-0.005	0.004
Fri, Jan 02, 2004	9:16:17 PM	-31.007	-28.009	-31.646	-33.13	-23.488	-0.002	0.006	0.034	-0.01	-0.004	0.005
Fri, Jan 02, 2004	9:16:17 PM	-31.653	-27.687	-33.258	-32.807	-22.196	-0.002	0.005	0.034	-0.009	-0.003	0.004
Fri, Jan 02, 2004	9:16:17 PM	-31.653	-28.653	-32.935	-32.807	-22.842	0	0.008	0.039	-0.005	0.001	0.004
Fri, Jan 02, 2004	9:16:17 PM	-30.36	-28.009	-30.679	-31.837	-23.488	0	0.012	0.047	0.004	0.002	0.004
Fri, Jan 02, 2004	9:16:17 PM	-30.684	-29.297	-29.389	-30.868	-26.716	-0.001	0.017	0.052	0.009	0.004	0.005
Fri, Jan 02, 2004	9:16:17 PM	-30.037	-29.618	-26.488	-30.545	-28.654	-0.001	0.012	0.055	0.011	0.002	0.004
Fri, Jan 02, 2004	9:16:17 PM	-30.684	-29.94	-24.876	-30.868	-30.591	-0.001	0.009	0.051	0.008	0.002	0.005
Fri, Jan 02, 2004	9:16:17 PM	-30.684	-30.262	-25.198	-31.514	-29.622	-0.001	0.009	0.049	0.004	-0.002	0.006
Fri, Jan 02, 2004	9:16:17 PM	-30.684	-28.653	-26.81	-31.837	-28.331	-0.003	0.004	0.042	-0.003	-0.001	0.005
Fri, Jan 02, 2004	9:16:17 PM	-30.684	-28.975	-29.389	-32.484	-26.716	-0.002	0.01	0.035	-0.008	-0.003	0.004
Fri, Jan 02, 2004	9:16:17 PM	-31.007	-28.331	-31.968	-33.13	-23.811	0	0.003	0.031	-0.011	-0.003	0.005

Fri, Jan 02, 2004	9:16:17 PM	-31.976	-27.687	-32.613	-33.453	-21.873	-0.002	0.009	0.034	-0.011	-0.003	0.005
Fri, Jan 02, 2004	9:16:17 PM	-31.33	-27.687	-32.613	-32.807	-22.196	-0.002	0.007	0.041	-0.003	0.001	0.003
Fri, Jan 02, 2004	9:16:17 PM	-31.653	-28.331	-30.679	-33.13	-24.134	-0.001	0.013	0.045	0.002	0.002	0.005
Fri, Jan 02, 2004	9:16:17 PM	-30.36	-28.653	-27.455	-32.161	-27.039	-0.002	0.012	0.055	0.01	0.002	0.005
Fri, Jan 02, 2004	9:16:17 PM	-31.007	-29.94	-25.52	-32.484	-29.299	-0.002	0.012	0.057	0.013	0.001	0.005
Fri, Jan 02, 2004	9:16:17 PM	-31.007	-30.906	-23.586	-32.484	-31.237	-0.002	0.01	0.056	0.012	0.002	0.004
Fri, Jan 02, 2004	9:16:17 PM	-31.007	-30.584	-24.553	-31.514	-30.591	-0.001	0.007	0.049	0.005	0.002	0.004
Fri, Jan 02, 2004	9:16:17 PM	-30.037	-30.262	-27.132	-32.161	-28.654	-0.002	0.012	0.042	-0.002	-0.001	0.004
Fri, Jan 02, 2004	9:16:17 PM	-31.33	-28.975	-30.356	-33.13	-25.102	-0.001	0.008	0.032	-0.012	-0.002	0.005
Fri, Jan 02, 2004	9:16:17 PM	-31.33	-28.009	-33.58	-33.777	-22.196	-0.001	0.003	0.03	-0.015	-0.003	0.004
Fri, Jan 02, 2004	9:16:17 PM	-31.653	-27.366	-34.225	-34.746	-19.613	-0.003	0.004	0.032	-0.014	-0.005	0.004
Fri, Jan 02, 2004	9:16:17 PM	-32.299	-27.044	-34.87	-34.746	-20.259	0	0.01	0.038	-0.006	-0.001	0.005
Fri, Jan 02, 2004	9:16:17 PM	-31.653	-28.331	-33.258	-34.423	-22.842	-0.001	0.008	0.048	0.004	0.001	0.004
Fri, Jan 02, 2004	9:16:17 PM	-31.007	-28.975	-27.777	-33.453	-26.071	-0.002	0.008	0.054	0.011	0.001	0.005
Fri, Jan 02, 2004	9:16:17 PM	-31.007	-30.584	-25.52	-31.837	-30.268	-0.001	0.01	0.058	0.015	0.003	0.006
Fri, Jan 02, 2004	9:16:17 PM	-30.684	-30.262	-22.941	-31.837	-32.205	-0.001	0.01	0.058	0.011	0.003	0.005
Fri, Jan 02, 2004	9:16:17 PM	-30.684	-30.262	-23.264	-30.868	-32.205	-0.001	0.009	0.051	0.008	0.001	0.004
Fri, Jan 02, 2004	9:16:17 PM	-31.007	-30.262	-25.843	-31.514	-30.268	0	0.012	0.041	-0.003	0	0.004
Fri, Jan 02, 2004	9:16:17 PM	-31.33	-28.331	-28.422	-32.161	-26.071	-0.002	0.006	0.035	-0.01	-0.003	0.005
Fri, Jan 02, 2004	9:16:17 PM	-30.684	-28.331	-32.291	-32.161	-22.519	-0.001	0.007	0.029	-0.014	-0.004	0.004
Fri, Jan 02, 2004	9:16:17 PM	-31.976	-27.044	-33.903	-33.13	-21.551	-0.001	0.008	0.029	-0.014	-0.004	0.004
Fri, Jan 02, 2004	9:16:17 PM	-31.653	-27.044	-32.935	-33.453	-21.551	-0.002	0.008	0.037	-0.006	-0.003	0.004
Fri, Jan 02, 2004	9:16:17 PM	-31.653	-28.331	-31.968	-32.807	-24.134	-0.002	0.013	0.044	0.001	-0.001	0.004
Fri, Jan 02, 2004	9:16:17 PM	-30.684	-28.331	-28.422	-31.837	-27.039	-0.002	0.008	0.055	0.012	0.002	0.005
Fri, Jan 02, 2004	9:16:17 PM	-31.007	-30.262	-25.198	-31.514	-30.591	0	0.011	0.056	0.013	0.005	0.005
Fri, Jan 02, 2004	9:16:17 PM	-30.36	-31.228	-22.941	-31.191	-32.851	-0.002	0.01	0.059	0.014	0.004	0.006
Fri, Jan 02, 2004	9:16:17 PM	-30.36	-30.262	-22.619	-31.191	-32.851	-0.001	0.009	0.051	0.007	0.002	0.005
Fri, Jan 02, 2004	9:16:17 PM	-30.037	-29.94	-25.198	-30.545	-29.945	0	0.006	0.043	-0.002	-0.002	0.005
Fri, Jan 02, 2004	9:16:17 PM	-30.684	-29.297	-28.1	-32.484	-27.685	-0.001	0.004	0.036	-0.008	-0.002	0.003
Fri, Jan 02, 2004	9:16:17 PM	-31.653	-27.366	-31.001	-33.453	-23.488	-0.002	0.006	0.031	-0.014	-0.004	0.004
Fri, Jan 02, 2004	9:16:17 PM	-31.976	-27.687	-33.903	-33.453	-21.228	-0.002	0.009	0.028	-0.016	-0.003	0.005
Fri, Jan 02, 2004	9:16:17 PM	-31.976	-26.722	-33.903	-34.423	-20.582	-0.001	0.005	0.034	-0.009	-0.004	0.005
Fri, Jan 02, 2004	9:16:17 PM	-31.976	-27.687	-32.613	-33.777	-22.519	-0.001	0.007	0.048	0.003	0	0.005
Fri, Jan 02, 2004	9:16:17 PM	-31.007	-29.618	-29.711	-33.453	-26.071	-0.003	0.012	0.051	0.008	0.001	0.004
Fri, Jan 02, 2004	9:16:17 PM	-31.007	-28.975	-24.231	-32.807	-29.622	-0.002	0.014	0.059	0.015	0.003	0.005
Fri, Jan 02, 2004	9:16:17 PM	-30.684	-31.228	-23.586	-30.545	-31.882	0	0.012	0.059	0.015	0.002	0.005
Fri, Jan 02, 2004	9:16:17 PM	-30.684	-30.906	-22.296	-31.514	-33.82	-0.002	0.015	0.054	0.01	0.006	0.006
Fri, Jan 02, 2004	9:16:17 PM	-30.684	-29.94	-23.586	-30.868	-30.914	-0.002	0.009	0.042	-0.001	0	0.004
Fri, Jan 02, 2004	9:16:17 PM	-31.33	-30.262	-28.422	-31.191	-28.008	-0.002	0.01	0.034	-0.011	0	0.004
Fri, Jan 02, 2004	9:16:17 PM	-31.653	-27.366	-31.323	-32.807	-24.134	0	0.009	0.029	-0.014	-0.003	0.004
Fri, Jan 02, 2004	9:16:17 PM	-31.976	-27.044	-33.903	-32.484	-21.551	-0.004	0.001	0.028	-0.015	-0.003	0.003
Fri, Jan 02, 2004	9:16:17 PM	-31.33	-28.009	-34.225	-33.453	-20.905	-0.001	0.003	0.037	-0.008	-0.004	0.004
Fri, Jan 02, 2004	9:16:17 PM	-31.653	-27.687	-31.323	-34.1	-22.519	-0.001	0.009	0.043	-0.001	0.001	0.005
Fri, Jan 02, 2004	9:16:17 PM	-31.007	-28.975	-29.711	-32.161	-25.748	-0.003	0.008	0.056	0.012	0.001	0.005
Fri, Jan 02, 2004	9:16:17 PM	-30.684	-29.618	-25.843	-32.484	-29.299	-0.002	0.013	0.058	0.012	0.004	0.006
Fri, Jan 02, 2004	9:16:17 PM	-31.007	-30.262	-22.296	-31.514	-32.205	-0.002	0.015	0.059	0.014	0.005	0.005
Fri, Jan 02, 2004	9:16:17 PM	-30.684	-31.549	-22.941	-31.191	-32.851	-0.001	0.009	0.053	0.008	0.005	0.005
Fri, Jan 02, 2004	9:16:17 PM	-30.36	-29.94	-24.876	-31.514	-30.591	-0.003	0.013	0.045	0.001	0.001	0.003
Fri, Jan 02, 2004	9:16:17 PM	-31.007	-30.262	-28.422	-32.161	-28.331	-0.001	0.01	0.038	-0.006	-0.002	0.003
Fri, Jan 02, 2004	9:16:17 PM	-31.653	-28.331	-31.001	-33.777	-24.779	-0.002	0.007	0.031	-0.013	-0.006	0.004
Fri, Jan 02, 2004	9:16:17 PM	-32.622	-27.044	-32.935	-35.392	-21.873	-0.001	0.004	0.031	-0.012	-0.005	0.004
Fri, Jan 02, 2004	9:16:17 PM	-31.976	-27.687	-34.87	-34.423	-20.259	-0.002	0.008	0.034	-0.011	-0.004	0.005
Fri, Jan 02, 2004	9:16:17 PM	-31.976	-27.687	-32.935	-35.069	-21.551	-0.001	0.004	0.045	0	-0.003	0.005
Fri, Jan 02, 2004	9:16:17 PM	-31.653	-28.331	-30.034	-34.1	-25.102	-0.003	0.011	0.051	0.007	0.002	0.004
Fri, Jan 02, 2004	9:16:17 PM	-31.007	-30.262	-28.1	-32.484	-28.331	-0.002	0.016	0.056	0.012	0.003	0.005
Fri, Jan 02, 2004	9:16:17 PM	-31.007	-29.618	-23.908	-32.161	-30.914	-0.002	0.015	0.057	0.012	0.006	0.006
Fri, Jan 02, 2004	9:16:17 PM	-30.684	-30.584	-24.553	-31.191	-31.237	-0.002	0.012	0.054	0.01	0.003	0.004
Fri, Jan 02, 2004	9:16:17 PM	-31.007	-30.262	-25.52	-32.161	-30.268	-0.001	0.014	0.045	0.002	0.003	0.005
Fri, Jan 02, 2004	9:16:17 PM	-31.653	-28.975	-26.81	-33.13	-27.685	-0.002	0.011	0.036	-0.007	-0.004	0.006
Fri, Jan 02, 2004	9:16:17 PM	-31.33	-28.653	-31.001	-34.1	-25.102	-0.002	0.005	0.033	-0.009	-0.005	0.004
Fri, Jan 02, 2004	9:16:17 PM	-32.299	-27.366	-32.291	-36.039	-21.551	-0.003	-0.001	0.03	-0.014	-0.009	0.004
Fri, Jan 02, 2004	9:16:17 PM	-32.945	-27.366	-33.903	-36.685	-21.228	-0.001	0.001	0.036	-0.005	-0.007	0.005
Fri, Jan 02, 2004	9:16:17 PM	-32.622	-28.009	-32.291	-36.362	-21.551	-0.002	0.003	0.044	-0.002	-0.004	0.004
Fri, Jan 02, 2004	9:16:17 PM	-31.653	-28.653	-29.711	-35.716	-25.102	-0.002	0.012	0.053	0.01	0.002	0.004
Fri, Jan 02, 2004	9:16:17 PM	-31.33	-30.262	-26.81	-33.777	-28.331	-0.002	0.01	0.055	0.011	0.004	0.005
Fri, Jan 02, 2004	9:16:17 PM	-31.33	-30.906	-24.231	-32.807	-30.914	-0.002	0.019	0.054	0.011	0.008	0.005
Fri, Jan 02, 2004	9:16:17 PM	-30.36	-29.618	-23.908	-31.514	-29.299	-0.001	0.016	0.052	0.008	0.006	0.005
Fri, Jan 02, 2004	9:16:17 PM	-30.36	-30.262	-26.165	-30.868	-29.299	-0.002	0.014	0.041	-0.002	0.005	0.003
Fri, Jan 02, 2004	9:16:17 PM	-31.33	-29.297	-28.1	-32.484	-26.394	-0.001	0.011	0.038	-0.007	0	0.004
Fri, Jan 02, 2004	9:16:17 PM	-32.299	-28.331	-30.679	-33.453	-23.811	-0.002	0.007	0.033	-0.011	-0.004	0.004
Fri, Jan 02, 2004	9:16:17 PM	-32.622	-28.009	-32.291	-36.362	-22.196	-0.002	0	0.035	-0.008	-0.009	0.004
Fri, Jan 02, 2004	9:16:17 PM	-32.945	-27.366	-32.291	-37.655	-21.551	-0.001	0.003	0.038	-0.007	-0.006	0.004
Fri, Jan 02, 2004	9:16:17 PM	-32.945	-28.331	-31.968	-37.332	-23.488	-0.002	0.005	0.045	0.001	-0.006	0.003
Fri, Jan 02, 2004	9:16:17 PM	-33.268	-28.653	-29.389	-37.978	-25.748	-0.001	0.007	0.052	0.009	0	0.005
Fri, Jan 02, 2004	9:16:17 PM	-32.299	-28.653	-26.165	-35.716	-28.008	-0.001	0.012	0.051	0.008	0.003	0.005
Fri, Jan 02, 2004	9:16:17 PM	-31.653	-30.906	-26.165	-34.1	-30.268	-0.001	0.018	0.054	0.01	0.007	0.006
Fri, Jan 02, 2004	9:16:17 PM	-31.653	-30.584	-24.553	-33.777	-30.591	-0.001	0.016	0.047	0.003	0.005	0.004
Fri, Jan 02, 2004	9:16:17 PM	-31.33	-29.618	-26.488	-32.161	-28.977	-0.001	0.012	0.045	0	0.003	0.005
Fri, Jan 02, 2004	9:16:17 PM	-30.684	-29.618	-28.1	-32.484	-26.071	-0.002	0.007	0.035	-0.009	-0.001	0.005
Fri, Jan 02, 2004	9:16:17 PM	-31.976	-27.044	-29.711	-34.746	-24.779	0	0.005	0.038	-0.007	-0.003	0.004
Fri, Jan 02, 2004	9:16:17 PM	-31.976	-28.331	-31.646	-36.039	-22.842	-0.002	0.003	0.035	-0.008	-0.007	0.005

****

Golden Boy Strain, Accelometer, Temperature, Wind Meter Data File:e:\GoldenBoyData\ Sep 23 - 2003(1_01_32 PM).dat

****

		Strain1	Strain3	Strain4	Strain6	Strain8	Accelometer1-x	Accelometer1-y	Accelometer1-z	Accelomet	Accelomet	Accelomet
Wed, Sep 24, 2003	10:44:11 AM	8.734	19.301	9.944	9.855	20.748	-0.008	0.008	0.038	-0.018	-0.003	0.017
Wed, Sep 24, 2003	10:44:11 AM	7.442	19.623	6.398	6.623	24.945	-0.007	0.002	0.04	-0.014	-0.004	0.015
Wed, Sep 24, 2003	10:44:11 AM	6.795	19.623	5.43	4.683	25.591	-0.007	0.014	0.044	-0.011	0.002	0.016
Wed, Sep 24, 2003	10:44:11 AM	6.795	19.623	7.365	5.33	24.622	-0.007	0.012	0.048	-0.007	0.009	0.015
Wed, Sep 24, 2003	10:44:11 AM	8.088	18.98	8.655	8.239	21.716	-0.006	0.022	0.057	0.002	0.015	0.016
Wed, Sep 24, 2003	10:44:11 AM	8.734	17.692	12.524	11.471	18.164	-0.006	0.033	0.065	0.01	0.023	0.017
Wed, Sep 24, 2003	10:44:11 AM	9.38	17.37	16.393	14.056	14.29	-0.007	0.034	0.067	0.011	0.026	0.015
Wed, Sep 24, 2003	10:44:11 AM	10.35	16.083	17.682	15.026	12.998	-0.006	0.032	0.066	0.012	0.021	0.017
Wed, Sep 24, 2003	10:44:11 AM	10.35	16.727	16.715	15.026	12.675	-0.006	0.023	0.061	0.006	0.016	0.015
Wed, Sep 24, 2003	10:44:11 AM	9.703	17.37	14.781	13.41	15.581	-0.007	0.018	0.047	-0.007	0.007	0.015
Wed, Sep 24, 2003	10:44:11 AM	8.411	18.336	11.879	9.855	19.456	-0.007	0.014	0.042	-0.013	0.007	0.016
Wed, Sep 24, 2003	10:44:11 AM	7.442	19.301	8.332	7.592	23.331	-0.008	0.008	0.036	-0.018	0.001	0.014
Wed, Sep 24, 2003	10:44:11 AM	7.442	20.267	5.753	4.683	25.591	-0.008	0.008	0.039	-0.016	0.002	0.016
Wed, Sep 24, 2003	10:44:11 AM	6.795	20.267	6.075	4.037	24.945	-0.008	0.006	0.043	-0.01	-0.001	0.016
Wed, Sep 24, 2003	10:44:11 AM	7.442	19.623	8.655	5.007	23.331	-0.006	0.029	0.053	0	0.013	0.016
Wed, Sep 24, 2003	10:44:11 AM	7.118	17.37	12.201	6.946	18.81	-0.007	0.027	0.061	0.006	0.014	0.017
Wed, Sep 24, 2003	10:44:11 AM	8.734	16.727	16.715	9.208	13.967	-0.007	0.027	0.071	0.017	0.021	0.017
Wed, Sep 24, 2003	10:44:11 AM	9.38	15.761	19.295	10.824	11.061	-0.007	0.02	0.067	0.012	0.012	0.015
Wed, Sep 24, 2003	10:44:11 AM	9.38	15.439	20.262	11.471	10.415	-0.005	0.028	0.064	0.009	0.02	0.016
Wed, Sep 24, 2003	10:44:11 AM	9.703	15.761	19.295	11.148	11.384	-0.006	0.023	0.054	-0.001	0.012	0.015
Wed, Sep 24, 2003	10:44:11 AM	9.38	17.048	15.425	11.148	15.581	-0.007	0.022	0.044	-0.013	0.014	0.017
Wed, Sep 24, 2003	10:44:11 AM	8.088	18.336	11.234	8.562	19.456	-0.007	0.011	0.039	-0.015	-0.003	0.015
Wed, Sep 24, 2003	10:44:11 AM	6.795	19.301	8.01	7.269	23.008	-0.006	0.013	0.036	-0.019	0.007	0.016
Wed, Sep 24, 2003	10:44:11 AM	7.442	18.658	7.687	5.976	24.299	-0.006	0.011	0.049	-0.005	0.003	0.016
Wed, Sep 24, 2003	10:44:11 AM	7.118	19.301	8.01	5.653	23.008	-0.007	0.025	0.044	-0.011	0.012	0.015
Wed, Sep 24, 2003	10:44:11 AM	7.442	18.336	11.234	7.915	20.102	-0.006	0.016	0.062	0.007	0.01	0.016
Wed, Sep 24, 2003	10:44:11 AM	8.734	17.692	14.136	9.532	16.55	-0.005	0.034	0.061	0.006	0.02	0.016
Wed, Sep 24, 2003	10:44:11 AM	9.703	17.37	17.36	11.148	13.967	-0.007	0.031	0.071	0.015	0.018	0.016
Wed, Sep 24, 2003	10:44:11 AM	10.026	16.405	17.682	12.117	12.675	-0.006	0.031	0.06	0.005	0.02	0.017
Wed, Sep 24, 2003	10:44:11 AM	9.38	16.727	17.682	12.764	13.321	-0.007	0.015	0.056	0	0.01	0.014
Wed, Sep 24, 2003	10:44:11 AM	9.057	17.692	14.781	11.148	16.55	-0.007	0.015	0.047	-0.005	0.008	0.015
Wed, Sep 24, 2003	10:44:11 AM	8.411	18.658	11.234	9.855	19.456	-0.006	0.017	0.039	-0.017	0.005	0.015
Wed, Sep 24, 2003	10:44:11 AM	8.088	19.623	9.622	7.592	23.008	-0.007	0.013	0.042	-0.012	0.007	0.016
Wed, Sep 24, 2003	10:44:11 AM	8.088	18.98	8.332	7.269	23.008	-0.006	0.014	0.039	-0.016	0.004	0.015
Wed, Sep 24, 2003	10:44:11 AM	8.411	18.658	8.655	8.239	22.362	-0.007	0.016	0.054	-0.003	0.008	0.016
Wed, Sep 24, 2003	10:44:11 AM	8.411	18.658	12.201	9.208	19.456	-0.006	0.023	0.055	-0.001	0.013	0.015
Wed, Sep 24, 2003	10:44:11 AM	8.734	17.048	15.425	10.824	15.904	-0.006	0.028	0.067	0.014	0.017	0.016
Wed, Sep 24, 2003	10:44:11 AM	9.38	16.083	18.005	12.764	12.029	-0.006	0.024	0.062	0.008	0.019	0.016
Wed, Sep 24, 2003	10:44:11 AM	10.35	16.083	19.617	14.056	10.738	-0.006	0.027	0.061	0.007	0.017	0.015
Wed, Sep 24, 2003	10:44:11 AM	10.026	15.761	18.972	14.056	11.384	-0.006	0.02	0.055	0	0.015	0.015
Wed, Sep 24, 2003	10:44:11 AM	8.734	16.727	17.682	13.087	12.998	-0.006	0.022	0.053	-0.004	0.009	0.015
Wed, Sep 24, 2003	10:44:11 AM	9.703	17.048	15.425	12.117	15.581	-0.007	0.015	0.052	-0.002	0.007	0.015
Wed, Sep 24, 2003	10:44:11 AM	8.734	17.37	13.169	11.148	17.519	-0.007	0.012	0.042	-0.014	0.003	0.016
Wed, Sep 24, 2003	10:44:11 AM	8.734	18.98	11.556	9.855	19.133	-0.007	0.014	0.049	-0.006	0.005	0.016
Wed, Sep 24, 2003	10:44:11 AM	8.734	18.336	11.234	10.501	20.425	-0.008	0.021	0.047	-0.01	0.01	0.016
Wed, Sep 24, 2003	10:44:11 AM	9.057	18.336	12.201	11.471	19.456	-0.006	0.022	0.053	-0.002	0.015	0.017
Wed, Sep 24, 2003	10:44:11 AM	10.026	17.692	12.524	14.056	17.841	-0.006	0.026	0.052	-0.003	0.014	0.014
Wed, Sep 24, 2003	10:44:11 AM	10.026	17.692	13.491	15.026	17.196	-0.005	0.027	0.062	0.007	0.018	0.017
Wed, Sep 24, 2003	10:44:11 AM	10.673	17.37	15.425	15.673	14.29	-0.007	0.024	0.061	0.003	0.017	0.015
Wed, Sep 24, 2003	10:44:11 AM	10.673	16.727	16.715	17.289	14.29	-0.007	0.026	0.054	-0.001	0.019	0.016
Wed, Sep 24, 2003	10:44:11 AM	10.996	16.727	16.07	15.996	15.581	-0.006	0.021	0.052	-0.002	0.01	0.016
Wed, Sep 24, 2003	10:44:11 AM	9.38	17.37	14.136	13.733	16.55	-0.005	0.021	0.048	-0.006	0.01	0.015
Wed, Sep 24, 2003	10:44:11 AM	9.703	18.014	12.846	12.44	17.841	-0.008	0.017	0.05	-0.004	0.003	0.017
Wed, Sep 24, 2003	10:44:11 AM	8.734	18.336	12.524	10.501	18.164	-0.007	0.013	0.047	-0.009	0.006	0.016
Wed, Sep 24, 2003	10:44:11 AM	8.734	18.336	12.524	10.178	18.487	-0.007	0.019	0.056	0.002	0.003	0.015
Wed, Sep 24, 2003	10:44:11 AM	8.411	18.336	11.879	11.148	19.133	-0.008	0.022	0.05	-0.005	0.013	0.016
Wed, Sep 24, 2003	10:44:11 AM	9.38	17.692	13.169	11.471	18.81	-0.007	0.025	0.058	0.002	0.013	0.015
Wed, Sep 24, 2003	10:44:11 AM	10.026	17.692	12.846	14.38	17.841	-0.006	0.025	0.053	-0.001	0.021	0.015
Wed, Sep 24, 2003	10:44:11 AM	10.673	17.692	13.491	15.026	16.55	-0.006	0.024	0.056	0.002	0.017	0.015
Wed, Sep 24, 2003	10:44:11 AM	11.319	18.336	13.169	16.319	17.841	-0.006	0.028	0.053	0	0.019	0.015
Wed, Sep 24, 2003	10:44:11 AM	10.673	18.014	11.879	15.673	18.81	-0.006	0.019	0.052	-0.005	0.009	0.015
Wed, Sep 24, 2003	10:44:11 AM	10.35	18.014	11.879	14.056	18.487	-0.007	0.018	0.053	-0.002	0.012	0.016
Wed, Sep 24, 2003	10:44:11 AM	9.057	18.336	11.879	12.117	18.81	-0.006	0.01	0.046	-0.01	0.003	0.015
Wed, Sep 24, 2003	10:44:11 AM	9.057	18.658	11.556	10.178	19.779	-0.006	0.02	0.051	-0.002	0.008	0.016
Wed, Sep 24, 2003	10:44:11 AM	8.088	18.98	11.556	9.855	20.102	-0.008	0.015	0.049	-0.006	0.003	0.015
Wed, Sep 24, 2003	10:44:11 AM	8.734	17.37	12.201	9.208	18.164	-0.006	0.022	0.055	0.003	0.01	0.017
Wed, Sep 24, 2003	10:44:11 AM	8.411	18.336	13.813	10.178	17.519	-0.007	0.025	0.052	-0.002	0.012	0.015
Wed, Sep 24, 2003	10:44:11 AM	9.057	17.692	14.781	12.117	16.55	-0.007	0.026	0.057	0.004	0.019	0.015
Wed, Sep 24, 2003	10:44:11 AM	9.703	17.048	14.136	13.733	16.227	-0.006	0.024	0.058	0.002	0.016	0.016
Wed, Sep 24, 2003	10:44:11 AM	10.026	18.336	14.458	14.056	16.227	-0.007	0.028	0.054	-0.001	0.016	0.016
Wed, Sep 24, 2003	10:44:11 AM	10.35	17.37	13.813	14.056	16.55	-0.008	0.024	0.052	-0.004	0.011	0.016
Wed, Sep 24, 2003	10:44:11 AM	9.703	17.692	11.879	13.41	18.164	-0.006	0.024	0.046	-0.006	0.012	0.015
Wed, Sep 24, 2003	10:44:11 AM	9.703	18.98	11.234	12.117	19.133	-0.007	0.017	0.05	-0.004	0.009	0.015
Wed, Sep 24, 2003	10:44:11 AM	9.057	18.658	10.267	11.148	20.425	-0.008	0.018	0.047	-0.009	0.006	0.016
Wed, Sep 24, 2003	10:44:11 AM	9.057	18.336	11.879	10.501	19.779	-0.006	0.014	0.052	-0.002	0.009	0.015
Wed, Sep 24, 2003	10:44:11 AM	9.38	18.98	11.234	10.824	19.456	-0.007	0.023	0.055	0	0.009	0.015
Wed, Sep 24, 2003	10:44:11 AM	9.703	18.336	12.524	12.117	18.164	-0.007	0.028	0.056	0.002	0.014	0.016
Wed, Sep 24, 2003	10:44:11 AM	9.38	18.336	13.813	12.117	17.196	-0.008	0.027	0.056	0	0.017	0.015
Wed, Sep 24, 2003	10:44:11 AM	10.026	17.37	14.781	14.703	16.55	-0.007	0.029	0.056	0.002	0.017	0.016
Wed, Sep 24, 2003	10:44:11 AM	9.703	17.048	14.136	14.056	16.55	-0.006	0.025	0.053	0	0.015	0.016

Wed, Sep 24, 2003	10:44:11 AM	9.703	18.014	13.491	13.41	18.164	-0.006	0.021	0.051	-0.004	0.011	0.015
Wed, Sep 24, 2003	10:44:11 AM	9.703	18.336	12.524	12.44	18.164	-0.007	0.017	0.052	-0.002	0.01	0.015
Wed, Sep 24, 2003	10:44:11 AM	9.38	18.336	12.201	11.148	18.487	-0.007	0.015	0.047	-0.006	0.005	0.015
Wed, Sep 24, 2003	10:44:11 AM	8.734	18.336	10.912	9.208	19.133	-0.006	0.019	0.053	-0.003	0.008	0.016
Wed, Sep 24, 2003	10:44:11 AM	8.411	18.658	10.912	9.532	20.425	-0.008	0.016	0.051	-0.004	0.005	0.016
Wed, Sep 24, 2003	10:44:11 AM	8.411	18.336	11.556	9.532	19.133	-0.007	0.019	0.055	0	0.012	0.015
Wed, Sep 24, 2003	10:44:11 AM	9.38	18.658	12.201	11.471	18.81	-0.008	0.025	0.054	-0.003	0.012	0.015
Wed, Sep 24, 2003	10:44:11 AM	10.026	18.014	11.879	13.087	18.81	-0.006	0.033	0.055	-0.001	0.023	0.016
Wed, Sep 24, 2003	10:44:11 AM	10.35	18.336	12.524	14.703	18.487	-0.007	0.025	0.054	-0.001	0.015	0.016
Wed, Sep 24, 2003	10:44:11 AM	10.35	17.37	11.879	15.026	19.133	-0.007	0.035	0.053	-0.003	0.022	0.018
Wed, Sep 24, 2003	10:44:11 AM	9.057	17.37	11.556	14.703	19.456	-0.006	0.017	0.052	-0.002	0.006	0.014
Wed, Sep 24, 2003	10:44:11 AM	10.026	18.336	10.912	12.764	19.779	-0.005	0.022	0.048	-0.006	0.014	0.016
Wed, Sep 24, 2003	10:44:11 AM	9.057	18.98	11.234	11.471	20.102	-0.007	0.007	0.053	-0.001	-0.001	0.015
Wed, Sep 24, 2003	10:44:11 AM	8.088	18.658	11.556	9.208	19.779	-0.007	0.018	0.05	-0.005	0.01	0.016
Wed, Sep 24, 2003	10:44:11 AM	8.088	18.336	10.912	9.208	18.81	-0.008	0.009	0.054	-0.001	-0.002	0.016
Wed, Sep 24, 2003	10:44:11 AM	8.411	18.014	11.879	9.532	18.487	-0.005	0.027	0.051	-0.003	0.018	0.016
Wed, Sep 24, 2003	10:44:11 AM	8.734	17.692	12.524	10.824	18.487	-0.006	0.018	0.056	0	0.01	0.015
Wed, Sep 24, 2003	10:44:11 AM	9.703	17.692	11.879	13.733	18.164	-0.005	0.038	0.052	-0.003	0.026	0.016
Wed, Sep 24, 2003	10:44:11 AM	10.35	17.37	13.491	15.026	17.196	-0.006	0.025	0.055	-0.002	0.015	0.014
Wed, Sep 24, 2003	10:44:11 AM	10.35	18.014	12.846	15.673	17.841	-0.006	0.034	0.053	0	0.024	0.016
Wed, Sep 24, 2003	10:44:11 AM	10.026	18.336	12.201	14.38	18.164	-0.006	0.018	0.053	-0.001	0.008	0.015
Wed, Sep 24, 2003	10:44:11 AM	9.703	18.658	12.524	12.764	18.487	-0.007	0.014	0.056	-0.001	0.007	0.015
Wed, Sep 24, 2003	10:44:11 AM	8.088	18.014	12.201	9.208	18.164	-0.01	0.005	0.051	-0.004	-0.004	0.016
Wed, Sep 24, 2003	10:44:11 AM	7.765	18.336	12.846	6.946	18.487	-0.007	0.017	0.053	-0.001	0.004	0.015
Wed, Sep 24, 2003	10:44:11 AM	7.442	18.658	11.879	7.915	18.81	-0.006	0.012	0.05	-0.003	0.002	0.015
Wed, Sep 24, 2003	10:44:11 AM	9.057	18.658	10.912	9.208	20.102	-0.006	0.023	0.053	-0.001	0.017	0.015
Wed, Sep 24, 2003	10:44:11 AM	8.734	18.658	11.879	11.148	19.456	-0.007	0.02	0.05	-0.003	0.015	0.016
Wed, Sep 24, 2003	10:44:11 AM	10.35	18.336	11.234	14.703	19.133	-0.007	0.037	0.051	-0.003	0.026	0.015
Wed, Sep 24, 2003	10:44:11 AM	10.35	17.692	11.879	16.319	18.487	-0.006	0.029	0.055	0	0.02	0.015
Wed, Sep 24, 2003	10:44:11 AM	10.026	18.658	12.201	16.319	18.487	-0.005	0.031	0.05	-0.006	0.019	0.016
Wed, Sep 24, 2003	10:44:11 AM	9.703	18.336	11.556	15.349	18.81	-0.006	0.017	0.055	0	0.009	0.016
Wed, Sep 24, 2003	10:44:11 AM	9.703	18.336	12.524	12.764	17.841	-0.008	0.015	0.049	-0.006	0.004	0.018
Wed, Sep 24, 2003	10:44:11 AM	8.411	18.658	11.879	9.532	18.81	-0.007	0.009	0.052	-0.002	0	0.015
Wed, Sep 24, 2003	10:44:11 AM	8.411	17.692	11.556	8.239	18.81	-0.007	0.017	0.045	-0.008	0.004	0.015
Wed, Sep 24, 2003	10:44:11 AM	7.765	18.658	12.524	7.269	18.81	-0.006	0.015	0.056	-0.001	0.006	0.017
Wed, Sep 24, 2003	10:44:11 AM	7.765	17.37	12.846	8.239	16.873	-0.007	0.02	0.048	-0.007	0.012	0.016
Wed, Sep 24, 2003	10:44:11 AM	9.057	17.37	14.136	9.855	17.196	-0.008	0.03	0.054	-0.001	0.018	0.015
Wed, Sep 24, 2003	10:44:11 AM	9.703	17.37	15.103	11.471	15.904	-0.006	0.028	0.057	0.001	0.02	0.016
Wed, Sep 24, 2003	10:44:11 AM	9.38	16.405	16.07	12.764	13.967	-0.007	0.03	0.061	0.005	0.019	0.017
Wed, Sep 24, 2003	10:44:11 AM	9.057	16.405	17.36	11.148	12.675	-0.008	0.018	0.06	0.005	0.01	0.016
Wed, Sep 24, 2003	10:44:11 AM	8.734	16.405	17.682	10.178	13.644	-0.006	0.013	0.051	-0.002	0.009	0.016
Wed, Sep 24, 2003	10:44:11 AM	8.411	17.692	15.103	7.915	15.581	-0.007	0.012	0.05	-0.003	0.004	0.016
Wed, Sep 24, 2003	10:44:11 AM	7.765	18.014	14.136	5.976	16.873	-0.007	0.014	0.045	-0.01	0.005	0.017
Wed, Sep 24, 2003	10:44:11 AM	7.118	17.048	11.879	5.33	19.456	-0.007	0.014	0.052	-0.004	0.002	0.015
Wed, Sep 24, 2003	10:44:11 AM	8.088	18.336	11.234	5.976	20.425	-0.007	0.011	0.04	-0.014	0.006	0.015
Wed, Sep 24, 2003	10:44:11 AM	7.765	19.301	11.234	7.269	20.425	-0.006	0.023	0.054	0.002	0.009	0.016
Wed, Sep 24, 2003	10:44:11 AM	9.057	18.014	11.879	10.501	19.456	-0.007	0.032	0.051	-0.003	0.018	0.014
Wed, Sep 24, 2003	10:44:11 AM	9.38	17.692	13.491	12.764	17.519	-0.007	0.032	0.061	0.007	0.021	0.017
Wed, Sep 24, 2003	10:44:11 AM	10.026	17.048	14.458	15.026	15.581	-0.008	0.027	0.057	0.002	0.022	0.015
Wed, Sep 24, 2003	10:44:11 AM	10.673	17.37	14.458	15.996	15.258	-0.005	0.031	0.057	0.001	0.018	0.015
Wed, Sep 24, 2003	10:44:11 AM	9.703	17.692	14.458	14.703	16.873	-0.007	0.016	0.053	-0.001	0.01	0.015
Wed, Sep 24, 2003	10:44:11 AM	9.703	17.692	12.524	13.41	17.519	-0.006	0.02	0.047	-0.007	0.007	0.016
Wed, Sep 24, 2003	10:44:11 AM	9.38	18.014	11.556	11.148	19.133	-0.007	0.013	0.049	-0.005	-0.001	0.015
Wed, Sep 24, 2003	10:44:11 AM	8.411	19.301	10.589	8.885	20.425	-0.007	0.012	0.042	-0.012	0.004	0.016
Wed, Sep 24, 2003	10:44:11 AM	8.411	18.658	9.299	9.532	21.07	-0.008	0.015	0.05	-0.004	0.005	0.015
Wed, Sep 24, 2003	10:44:11 AM	9.057	18.336	11.556	10.824	19.779	-0.007	0.026	0.047	-0.008	0.013	0.015
Wed, Sep 24, 2003	10:44:11 AM	9.38	18.014	12.846	13.087	18.164	-0.006	0.028	0.056	0.001	0.014	0.017
Wed, Sep 24, 2003	10:44:11 AM	10.35	16.727	14.781	15.026	15.258	-0.007	0.031	0.058	0.004	0.022	0.016
Wed, Sep 24, 2003	10:44:11 AM	11.319	17.048	17.36	16.965	13.321	-0.006	0.028	0.063	0.008	0.021	0.016
Wed, Sep 24, 2003	10:44:11 AM	11.642	15.761	18.327	17.289	12.029	-0.006	0.033	0.063	0.008	0.02	0.017
Wed, Sep 24, 2003	10:44:11 AM	10.673	16.405	19.295	15.673	11.384	-0.008	0.017	0.055	0	0.01	0.014
Wed, Sep 24, 2003	10:44:11 AM	9.703	16.727	17.36	12.764	13.321	-0.007	0.012	0.053	0.001	0.005	0.016
Wed, Sep 24, 2003	10:44:11 AM	9.057	17.692	14.458	11.148	16.55	-0.007	0.009	0.046	-0.01	-0.002	0.014
Wed, Sep 24, 2003	10:44:11 AM	8.411	18.014	12.524	8.562	18.164	-0.007	0.015	0.049	-0.006	0.002	0.016
Wed, Sep 24, 2003	10:44:11 AM	8.088	18.98	10.589	8.239	20.748	-0.009	0.015	0.042	-0.015	0.002	0.015
Wed, Sep 24, 2003	10:44:11 AM	9.057	19.301	9.622	10.178	21.716	-0.006	0.029	0.047	-0.008	0.014	0.015
Wed, Sep 24, 2003	10:44:11 AM	9.703	18.658	10.267	13.087	21.07	-0.007	0.027	0.047	-0.009	0.016	0.015
Wed, Sep 24, 2003	10:44:11 AM	10.673	18.014	11.879	15.349	18.81	-0.005	0.034	0.055	0.001	0.025	0.017
Wed, Sep 24, 2003	10:44:11 AM	10.996	17.37	15.425	17.289	15.904	-0.006	0.034	0.059	0.004	0.02	0.015
Wed, Sep 24, 2003	10:44:11 AM	11.642	17.048	17.36	18.258	13.644	-0.008	0.032	0.059	0.007	0.02	0.016
Wed, Sep 24, 2003	10:44:11 AM	11.319	16.083	18.005	16.965	12.352	-0.008	0.02	0.064	0.007	0.01	0.015
Wed, Sep 24, 2003	10:44:11 AM	9.703	15.761	18.65	13.733	11.384	-0.006	0.018	0.058	0.002	0.007	0.015
Wed, Sep 24, 2003	10:44:11 AM	8.734	16.405	17.038	10.178	12.352	-0.007	0.006	0.054	0.001	0	0.016
Wed, Sep 24, 2003	10:44:11 AM	8.734	16.405	16.393	8.562	14.29	-0.007	0.01	0.046	-0.008	0.001	0.016
Wed, Sep 24, 2003	10:44:11 AM	7.765	17.692	13.813	7.592	17.196	-0.007	0.014	0.047	-0.007	0.002	0.016
Wed, Sep 24, 2003	10:44:11 AM	9.057	17.692	12.524	9.208	18.164	-0.008	0.025	0.047	-0.01	0.011	0.016
Wed, Sep 24, 2003	10:44:11 AM	9.057	17.692	12.846	11.148	18.81	-0.007	0.026	0.048	-0.007	0.015	0.016
Wed, Sep 24, 2003	10:44:11 AM	10.026	17.692	12.846	15.026	17.841	-0.007	0.027	0.05	-0.005	0.022	0.016
Wed, Sep 24, 2003	10:44:11 AM	10.996	17.37	13.813	17.289	16.873	-0.006	0.032	0.055	0.001	0.022	0.017
Wed, Sep 24, 2003	10:44:11 AM	10.996	17.692	16.07	17.612	15.258	-0.006	0.034	0.061	0.005	0.021	0.017
Wed, Sep 24, 2003	10:44:18 AM	10.35	16.727	17.36	16.965	12.998	-0.007	0.024	0.06	0.004	0.016	0.017
Wed, Sep 24, 2003	10:44:18 AM	10.35	16.727	18.005	14.38	12.675	-0.007	0.016	0.059	0.006	0.006	0.016
Wed, Sep 24, 2003	10:44:18 AM	9.057	16.727	17.36	10.824	13.967	-0.007	0.015	0.053	-0.002	0.002	0.016
Wed, Sep 24, 2003	10:44:18 AM	9.057	17.048	15.748	8.239	15.904	-0.008	0.012	0.051	-0.001	-0.001	0.015

****

Golden Boy Strain, Accelometer, Temperature, Wind Meter Data File:d:\GoldenBoyData\ Mar 19 - 2004(11_13_36 PM).dat

****

		Strain1	Strain3	Strain4	Strain6	Strain8	Accelometer1-x	Accelometer1-y	Accelometer1-z	Accelomet	Accelomet	Accelomet
Sat, Mar 20, 2004	1:48:51 PM	-10.329	-24.469	-21.007	-24.081	-24.134	-0.001	0.018	0.048	-0.004	0.005	0.009
Sat, Mar 20, 2004	1:48:51 PM	-10.329	-23.826	-20.684	-24.727	-23.488	-0.002	0.019	0.049	-0.001	0.007	0.011
Sat, Mar 20, 2004	1:48:51 PM	-10.329	-23.826	-19.717	-24.081	-24.134	-0.001	0.016	0.051	0	0.006	0.009
Sat, Mar 20, 2004	1:48:51 PM	-10.006	-24.791	-20.684	-24.404	-24.779	-0.002	0.015	0.051	0	0.004	0.01
Sat, Mar 20, 2004	1:48:51 PM	-10.652	-24.147	-19.395	-25.051	-25.102	-0.001	0.015	0.051	0	0.002	0.008
Sat, Mar 20, 2004	1:48:51 PM	-10.006	-24.469	-20.362	-24.727	-24.779	-0.002	0.014	0.052	0.001	-0.001	0.009
Sat, Mar 20, 2004	1:48:51 PM	-11.621	-24.791	-20.04	-26.99	-24.779	-0.001	0.012	0.05	-0.002	0	0.01
Sat, Mar 20, 2004	1:48:51 PM	-11.621	-23.826	-19.395	-26.343	-25.102	-0.003	0.012	0.049	-0.004	-0.001	0.01
Sat, Mar 20, 2004	1:48:51 PM	-10.975	-24.147	-20.362	-26.343	-24.134	-0.001	0.014	0.047	-0.003	0.002	0.009
Sat, Mar 20, 2004	1:48:51 PM	-10.975	-23.826	-21.007	-26.343	-23.811	-0.002	0.017	0.049	-0.003	0.004	0.01
Sat, Mar 20, 2004	1:48:51 PM	-10.652	-23.826	-20.684	-25.697	-23.165	-0.001	0.018	0.047	-0.005	0.006	0.009
Sat, Mar 20, 2004	1:48:51 PM	-9.683	-24.791	-21.329	-23.758	-23.488	-0.001	0.017	0.047	-0.005	0.005	0.01
Sat, Mar 20, 2004	1:48:51 PM	-10.329	-23.182	-20.04	-24.727	-23.488	0	0.017	0.049	0	0.004	0.009
Sat, Mar 20, 2004	1:48:51 PM	-10.652	-24.147	-21.007	-24.404	-24.779	-0.001	0.018	0.051	0.001	0.004	0.009
Sat, Mar 20, 2004	1:48:51 PM	-10.652	-24.469	-20.04	-25.374	-24.134	-0.001	0.013	0.052	-0.003	0.002	0.01
Sat, Mar 20, 2004	1:48:51 PM	-10.975	-24.147	-19.395	-26.02	-24.779	-0.003	0.014	0.05	-0.002	0.002	0.01
Sat, Mar 20, 2004	1:48:51 PM	-10.006	-24.791	-20.684	-25.697	-24.779	-0.002	0.012	0.051	0	0.001	0.011
Sat, Mar 20, 2004	1:48:51 PM	-10.975	-24.791	-20.04	-27.313	-24.456	-0.001	0.015	0.049	-0.001	0.002	0.008
Sat, Mar 20, 2004	1:48:51 PM	-10.652	-23.826	-19.717	-26.02	-23.811	-0.001	0.014	0.048	-0.001	0.003	0.01
Sat, Mar 20, 2004	1:48:51 PM	-10.006	-23.504	-21.007	-25.374	-24.134	-0.002	0.017	0.047	-0.006	0.006	0.009
Sat, Mar 20, 2004	1:48:51 PM	-10.652	-24.147	-21.329	-25.697	-23.488	-0.001	0.017	0.045	-0.005	0.005	0.009
Sat, Mar 20, 2004	1:48:51 PM	-10.006	-23.504	-21.652	-23.758	-23.488	-0.001	0.018	0.047	-0.001	0.006	0.01
Sat, Mar 20, 2004	1:48:51 PM	-9.683	-24.469	-21.329	-24.404	-23.165	0	0.017	0.049	0	0.004	0.01
Sat, Mar 20, 2004	1:48:51 PM	-10.006	-24.147	-20.362	-25.051	-24.134	-0.001	0.017	0.048	0	0.004	0.01
Sat, Mar 20, 2004	1:48:51 PM	-10.975	-23.504	-20.362	-24.404	-24.779	0	0.013	0.05	-0.001	0.001	0.009
Sat, Mar 20, 2004	1:48:51 PM	-10.329	-24.147	-20.362	-26.343	-24.456	-0.002	0.012	0.052	0.002	0.001	0.01
Sat, Mar 20, 2004	1:48:51 PM	-10.975	-24.147	-19.072	-26.99	-25.102	-0.001	0.013	0.052	-0.002	0.002	0.009
Sat, Mar 20, 2004	1:48:51 PM	-11.298	-25.113	-20.684	-26.667	-25.102	-0.001	0.014	0.049	0	0.001	0.009
Sat, Mar 20, 2004	1:48:51 PM	-10.329	-24.147	-20.684	-26.343	-24.456	-0.001	0.016	0.048	-0.004	0.002	0.009
Sat, Mar 20, 2004	1:48:51 PM	-10.329	-24.469	-21.007	-26.02	-23.488	-0.002	0.016	0.048	-0.004	0.005	0.008
Sat, Mar 20, 2004	1:48:51 PM	-10.652	-23.826	-21.652	-24.727	-23.811	-0.001	0.017	0.045	-0.003	0.006	0.011
Sat, Mar 20, 2004	1:48:51 PM	-10.329	-23.826	-21.007	-25.374	-23.488	-0.001	0.019	0.047	-0.002	0.006	0.01
Sat, Mar 20, 2004	1:48:51 PM	-10.329	-23.182	-20.684	-24.404	-23.488	-0.001	0.016	0.048	-0.004	0.004	0.009
Sat, Mar 20, 2004	1:48:51 PM	-10.329	-24.147	-21.007	-24.404	-24.134	-0.001	0.016	0.051	0.001	0.002	0.009
Sat, Mar 20, 2004	1:48:51 PM	-10.652	-24.147	-19.717	-25.697	-24.779	0	0.014	0.052	0.002	0.001	0.011
Sat, Mar 20, 2004	1:48:51 PM	-10.975	-24.469	-19.717	-25.697	-25.425	-0.002	0.011	0.051	-0.001	0.001	0.009
Sat, Mar 20, 2004	1:48:51 PM	-10.975	-24.469	-20.04	-26.667	-25.425	0	0.014	0.051	-0.001	0.001	0.01
Sat, Mar 20, 2004	1:48:51 PM	-10.975	-23.826	-19.072	-26.343	-24.456	-0.001	0.014	0.049	-0.002	0.002	0.01
Sat, Mar 20, 2004	1:48:51 PM	-10.975	-24.469	-20.684	-26.02	-24.779	-0.002	0.015	0.048	-0.001	0.003	0.009
Sat, Mar 20, 2004	1:48:51 PM	-10.975	-24.469	-21.007	-26.343	-24.134	0	0.017	0.047	-0.003	0.006	0.01
Sat, Mar 20, 2004	1:48:51 PM	-10.329	-23.826	-21.652	-25.374	-23.165	-0.002	0.018	0.047	-0.003	0.007	0.01
Sat, Mar 20, 2004	1:48:51 PM	-10.006	-23.826	-22.619	-23.758	-22.196	0	0.019	0.048	-0.004	0.006	0.009
Sat, Mar 20, 2004	1:48:51 PM	-10.652	-23.826	-22.296	-24.727	-23.165	-0.002	0.016	0.048	-0.001	0.008	0.009
Sat, Mar 20, 2004	1:48:51 PM	-10.329	-23.504	-20.362	-24.081	-23.488	-0.002	0.016	0.049	-0.003	0.004	0.009
Sat, Mar 20, 2004	1:48:51 PM	-10.975	-24.147	-21.007	-25.051	-24.134	-0.002	0.014	0.05	-0.001	0.001	0.01
Sat, Mar 20, 2004	1:48:51 PM	-10.006	-23.826	-20.362	-25.697	-24.779	-0.002	0.013	0.053	0	0.001	0.01
Sat, Mar 20, 2004	1:48:51 PM	-10.975	-25.113	-19.395	-26.02	-25.748	-0.001	0.011	0.052	0.001	0	0.009
Sat, Mar 20, 2004	1:48:51 PM	-10.975	-24.791	-20.04	-26.343	-24.779	-0.002	0.014	0.05	-0.001	0	0.009
Sat, Mar 20, 2004	1:48:51 PM	-10.652	-23.826	-20.04	-26.02	-24.134	0	0.013	0.046	-0.003	0.003	0.009
Sat, Mar 20, 2004	1:48:51 PM	-10.975	-24.147	-21.007	-25.374	-23.488	-0.002	0.018	0.047	-0.004	0.005	0.01
Sat, Mar 20, 2004	1:48:51 PM	-10.652	-24.147	-21.329	-25.374	-23.488	0	0.017	0.045	-0.006	0.006	0.01
Sat, Mar 20, 2004	1:48:51 PM	-10.652	-23.504	-20.684	-24.081	-23.488	-0.001	0.018	0.047	-0.003	0.006	0.01
Sat, Mar 20, 2004	1:48:51 PM	-10.329	-24.147	-21.974	-23.758	-23.488	-0.001	0.017	0.048	-0.004	0.005	0.009
Sat, Mar 20, 2004	1:48:51 PM	-10.006	-23.826	-21.652	-24.081	-23.811	-0.002	0.017	0.05	0	0.004	0.01
Sat, Mar 20, 2004	1:48:51 PM	-10.329	-23.504	-20.362	-24.727	-24.134	-0.001	0.015	0.05	-0.002	0.002	0.01
Sat, Mar 20, 2004	1:48:51 PM	-10.329	-24.791	-20.362	-25.374	-24.779	-0.002	0.013	0.051	0	0.001	0.009
Sat, Mar 20, 2004	1:48:51 PM	-10.975	-23.826	-19.717	-26.02	-24.779	0	0.013	0.051	0.002	0.002	0.01
Sat, Mar 20, 2004	1:48:51 PM	-10.652	-23.826	-20.04	-26.343	-25.102	0	0.014	0.05	-0.003	0.002	0.011
Sat, Mar 20, 2004	1:48:51 PM	-10.652	-24.791	-20.684	-26.02	-24.456	-0.001	0.015	0.05	-0.002	0.003	0.009
Sat, Mar 20, 2004	1:48:51 PM	-10.329	-23.826	-20.04	-25.374	-24.134	-0.001	0.016	0.047	-0.004	0.003	0.009
Sat, Mar 20, 2004	1:48:51 PM	-10.329	-23.504	-21.652	-24.727	-23.811	-0.001	0.018	0.047	-0.003	0.005	0.009
Sat, Mar 20, 2004	1:48:51 PM	-9.683	-24.147	-21.974	-24.404	-23.488	-0.001	0.019	0.046	-0.003	0.007	0.01
Sat, Mar 20, 2004	1:48:51 PM	-10.329	-23.182	-21.007	-24.404	-23.488	0	0.017	0.048	-0.002	0.006	0.009
Sat, Mar 20, 2004	1:48:51 PM	-9.683	-23.826	-21.329	-23.758	-22.842	-0.001	0.018	0.049	0	0.004	0.009
Sat, Mar 20, 2004	1:48:51 PM	-10.329	-24.147	-20.684	-25.051	-24.779	-0.002	0.014	0.049	-0.002	0.002	0.01
Sat, Mar 20, 2004	1:48:51 PM	-10.006	-24.469	-20.04	-24.727	-24.134	-0.001	0.013	0.052	0.002	0	0.009
Sat, Mar 20, 2004	1:48:51 PM	-10.652	-24.147	-20.04	-25.697	-24.779	-0.002	0.014	0.052	0.001	0.001	0.009
Sat, Mar 20, 2004	1:48:51 PM	-10.329	-24.469	-19.395	-26.02	-25.102	-0.001	0.012	0.052	0	0	0.009
Sat, Mar 20, 2004	1:48:51 PM	-10.975	-24.147	-19.072	-25.697	-25.102	-0.002	0.015	0.048	-0.004	0.002	0.008
Sat, Mar 20, 2004	1:48:51 PM	-10.329	-24.791	-20.04	-25.697	-24.779	-0.002	0.016	0.049	-0.004	0.004	0.01
Sat, Mar 20, 2004	1:48:51 PM	-10.006	-24.147	-20.362	-25.374	-23.488	-0.001	0.019	0.046	-0.004	0.006	0.011
Sat, Mar 20, 2004	1:48:51 PM	-10.329	-24.147	-21.329	-23.758	-23.811	-0.001	0.017	0.046	-0.002	0.005	0.008
Sat, Mar 20, 2004	1:48:51 PM	-9.683	-24.147	-21.974	-24.081	-22.842	-0.001	0.019	0.047	-0.007	0.005	0.011
Sat, Mar 20, 2004	1:48:51 PM	-10.006	-23.182	-20.684	-23.758	-23.165	-0.002	0.018	0.048	0	0.004	0.009
Sat, Mar 20, 2004	1:48:51 PM	-10.006	-23.826	-20.684	-24.404	-23.488	-0.001	0.017	0.05	-0.001	0.002	0.009
Sat, Mar 20, 2004	1:48:51 PM	-10.329	-24.469	-19.717	-25.697	-24.456	-0.001	0.012	0.05	-0.001	0	0.008
Sat, Mar 20, 2004	1:48:51 PM	-10.652	-24.147	-19.072	-26.02	-25.102	-0.001	0.013	0.052	0.004	0	0.009
Sat, Mar 20, 2004	1:48:51 PM	-10.329	-25.113	-20.04	-25.697	-25.748	-0.001	0.014	0.051	0.001	0.001	0.008
Sat, Mar 20, 2004	1:48:51 PM	-10.652	-24.147	-19.717	-25.697	-24.779	-0.001	0.015	0.051	-0.001	0.002	0.009
Sat, Mar 20, 2004	1:48:51 PM	-9.683	-24.147	-19.395	-24.727	-25.102	-0.001	0.017	0.047	-0.003	0.004	0.009
Sat, Mar 20, 2004	1:48:51 PM	-10.006	-24.469	-21.007	-24.081	-24.456	-0.001	0.018	0.045	-0.003	0.005	0.01
Sat, Mar 20, 2004	1:48:51 PM	-10.652	-23.504	-20.362	-24.081	-24.134	-0.002	0.019	0.046	-0.005	0.006	0.01

Sat, Mar 20, 2004	1:48:51 PM	-10.006	-24.147	-21.652	-23.758	-23.488	-0.001	0.017	0.047	-0.003	0.006	0.01
Sat, Mar 20, 2004	1:48:51 PM	-10.006	-24.147	-21.329	-23.435	-23.165	-0.002	0.017	0.048	-0.002	0.004	0.009
Sat, Mar 20, 2004	1:48:51 PM	-10.006	-23.504	-20.04	-24.404	-24.134	-0.001	0.015	0.05	0	0.003	0.01
Sat, Mar 20, 2004	1:48:51 PM	-10.329	-23.826	-21.329	-24.404	-24.779	-0.002	0.014	0.052	0	0.002	0.009
Sat, Mar 20, 2004	1:48:51 PM	-10.006	-23.826	-18.75	-26.02	-25.425	-0.001	0.013	0.053	0.002	-0.001	0.009
Sat, Mar 20, 2004	1:48:51 PM	-10.329	-23.826	-18.428	-26.02	-25.425	-0.002	0.013	0.052	0.002	0	0.01
Sat, Mar 20, 2004	1:48:51 PM	-10.652	-24.469	-19.717	-24.404	-25.102	-0.002	0.015	0.049	-0.003	0	0.009
Sat, Mar 20, 2004	1:48:51 PM	-10.652	-23.826	-20.362	-25.697	-24.134	0	0.016	0.048	-0.003	0.002	0.009
Sat, Mar 20, 2004	1:48:51 PM	-10.329	-23.826	-21.329	-24.404	-23.165	-0.001	0.018	0.046	-0.005	0.005	0.011
Sat, Mar 20, 2004	1:48:51 PM	-10.006	-24.147	-22.619	-24.081	-23.165	-0.001	0.018	0.046	-0.004	0.005	0.009
Sat, Mar 20, 2004	1:48:51 PM	-10.006	-22.86	-21.007	-23.435	-22.842	0	0.018	0.046	-0.004	0.005	0.009
Sat, Mar 20, 2004	1:48:51 PM	-10.329	-23.182	-21.329	-24.404	-22.842	-0.001	0.016	0.047	-0.003	0.004	0.009
Sat, Mar 20, 2004	1:48:51 PM	-10.006	-24.469	-21.974	-24.081	-22.842	-0.001	0.017	0.05	0	0.002	0.01
Sat, Mar 20, 2004	1:48:51 PM	-10.975	-23.826	-20.684	-24.404	-23.811	-0.002	0.013	0.05	0	0	0.008
Sat, Mar 20, 2004	1:48:51 PM	-10.006	-24.147	-20.684	-25.051	-23.811	-0.001	0.012	0.052	0.003	0.001	0.009
Sat, Mar 20, 2004	1:48:51 PM	-10.652	-24.147	-20.362	-26.343	-25.102	-0.002	0.013	0.05	-0.001	0	0.01
Sat, Mar 20, 2004	1:48:51 PM	-10.652	-23.504	-19.395	-26.343	-24.456	-0.001	0.015	0.051	0	0.004	0.009
Sat, Mar 20, 2004	1:48:51 PM	-10.975	-24.791	-20.684	-25.051	-24.456	-0.001	0.017	0.046	0	0.003	0.01
Sat, Mar 20, 2004	1:48:51 PM	-10.975	-23.504	-20.684	-25.697	-24.134	-0.001	0.017	0.046	-0.001	0.005	0.01
Sat, Mar 20, 2004	1:48:51 PM	-10.975	-23.504	-21.007	-24.404	-22.519	-0.001	0.018	0.047	-0.003	0.004	0.008
Sat, Mar 20, 2004	1:48:51 PM	-10.006	-24.147	-23.586	-23.435	-22.519	-0.001	0.019	0.047	-0.006	0.004	0.009
Sat, Mar 20, 2004	1:48:51 PM	-10.006	-22.86	-21.329	-24.081	-22.519	-0.001	0.016	0.047	-0.002	0.005	0.011
Sat, Mar 20, 2004	1:48:51 PM	-10.006	-23.826	-21.329	-24.404	-22.519	-0.002	0.016	0.048	-0.005	0.003	0.009
Sat, Mar 20, 2004	1:48:51 PM	-10.652	-23.504	-21.974	-25.051	-23.488	-0.002	0.014	0.053	0.002	0.002	0.009
Sat, Mar 20, 2004	1:48:51 PM	-11.298	-23.182	-19.717	-26.02	-24.456	-0.001	0.013	0.051	-0.001	0.001	0.01
Sat, Mar 20, 2004	1:48:51 PM	-10.329	-24.791	-20.362	-25.697	-24.456	-0.002	0.014	0.052	-0.001	0.001	0.01
Sat, Mar 20, 2004	1:48:51 PM	-10.329	-24.791	-20.362	-26.02	-25.425	-0.001	0.014	0.049	-0.001	0.002	0.011
Sat, Mar 20, 2004	1:48:51 PM	-10.652	-23.826	-20.04	-26.02	-24.456	-0.003	0.014	0.049	-0.001	0.002	0.01
Sat, Mar 20, 2004	1:48:51 PM	-10.329	-24.791	-21.329	-25.374	-23.811	-0.001	0.017	0.046	-0.005	0.005	0.009
Sat, Mar 20, 2004	1:48:51 PM	-10.329	-23.826	-20.684	-24.727	-23.488	-0.002	0.018	0.045	-0.006	0.005	0.01
Sat, Mar 20, 2004	1:48:51 PM	-10.329	-23.826	-21.652	-24.404	-22.519	-0.001	0.018	0.045	-0.006	0.004	0.009
Sat, Mar 20, 2004	1:48:51 PM	-9.683	-24.469	-22.619	-23.435	-22.519	-0.001	0.018	0.046	-0.007	0.005	0.01
Sat, Mar 20, 2004	1:48:51 PM	-9.683	-23.182	-21.652	-24.727	-22.519	-0.001	0.016	0.05	-0.001	0.004	0.009
Sat, Mar 20, 2004	1:48:51 PM	-10.006	-23.504	-21.007	-24.081	-23.488	-0.001	0.014	0.049	-0.004	0.001	0.011
Sat, Mar 20, 2004	1:48:51 PM	-10.329	-23.826	-20.362	-25.051	-24.134	-0.002	0.012	0.052	0	0	0.009
Sat, Mar 20, 2004	1:48:51 PM	-10.975	-23.182	-18.428	-26.02	-24.779	-0.001	0.013	0.052	0.001	0.001	0.009
Sat, Mar 20, 2004	1:48:51 PM	-10.975	-24.469	-20.362	-25.374	-25.425	-0.001	0.015	0.051	0.002	0.003	0.009
Sat, Mar 20, 2004	1:48:51 PM	-10.329	-24.791	-20.04	-25.374	-24.779	-0.001	0.014	0.05	-0.002	0.002	0.01
Sat, Mar 20, 2004	1:48:51 PM	-10.329	-23.504	-20.684	-24.727	-24.456	0	0.017	0.047	-0.002	0.003	0.009
Sat, Mar 20, 2004	1:48:51 PM	-9.683	-23.826	-22.296	-23.435	-22.842	0	0.018	0.047	-0.006	0.006	0.009
Sat, Mar 20, 2004	1:48:51 PM	-10.329	-24.147	-22.296	-24.081	-22.842	0	0.017	0.046	-0.004	0.005	0.009
Sat, Mar 20, 2004	1:48:51 PM	-10.652	-23.182	-21.652	-24.404	-23.488	-0.002	0.016	0.046	-0.003	0.004	0.009
Sat, Mar 20, 2004	1:48:51 PM	-10.006	-23.504	-23.264	-24.404	-22.842	-0.001	0.016	0.047	-0.002	0.004	0.01
Sat, Mar 20, 2004	1:48:51 PM	-10.329	-23.504	-21.007	-25.697	-23.165	-0.002	0.014	0.051	0.001	0	0.01
Sat, Mar 20, 2004	1:48:51 PM	-10.329	-24.147	-21.007	-25.051	-23.165	-0.001	0.015	0.051	0.001	0.001	0.009
Sat, Mar 20, 2004	1:48:51 PM	-10.652	-25.435	-21.007	-25.697	-24.134	-0.002	0.014	0.052	0	0	0.01
Sat, Mar 20, 2004	1:48:51 PM	-10.329	-23.826	-18.75	-26.667	-25.425	0	0.014	0.051	-0.002	0.002	0.01
Sat, Mar 20, 2004	1:48:51 PM	-10.652	-24.147	-20.684	-25.374	-24.779	-0.003	0.017	0.05	-0.002	0.003	0.01
Sat, Mar 20, 2004	1:48:51 PM	-10.329	-24.469	-19.717	-25.374	-24.456	-0.002	0.017	0.05	-0.001	0.004	0.009
Sat, Mar 20, 2004	1:48:51 PM	-10.975	-23.504	-20.04	-25.051	-24.134	-0.001	0.019	0.045	-0.004	0.004	0.009
Sat, Mar 20, 2004	1:48:51 PM	-9.683	-23.826	-22.296	-24.081	-22.842	0	0.018	0.046	-0.002	0.004	0.01
Sat, Mar 20, 2004	1:48:51 PM	-10.006	-23.826	-22.296	-24.081	-22.842	-0.001	0.015	0.046	-0.004	0.003	0.008
Sat, Mar 20, 2004	1:48:51 PM	-9.683	-23.182	-22.296	-24.404	-22.196	-0.001	0.015	0.047	-0.004	0.003	0.01
Sat, Mar 20, 2004	1:48:51 PM	-10.652	-23.504	-22.619	-24.404	-22.196	0	0.013	0.049	-0.003	0.001	0.01
Sat, Mar 20, 2004	1:48:51 PM	-10.975	-24.147	-21.007	-26.343	-23.488	-0.001	0.012	0.051	0	0.001	0.01
Sat, Mar 20, 2004	1:48:51 PM	-11.298	-23.826	-20.684	-25.697	-23.811	-0.001	0.013	0.051	0.002	0.002	0.009
Sat, Mar 20, 2004	1:48:51 PM	-10.652	-24.469	-20.362	-25.697	-24.456	-0.001	0.014	0.052	-0.001	0.003	0.009
Sat, Mar 20, 2004	1:48:51 PM	-10.329	-23.504	-20.04	-25.374	-24.134	-0.001	0.016	0.05	-0.001	0.005	0.01
Sat, Mar 20, 2004	1:48:51 PM	-10.006	-24.469	-21.007	-24.081	-24.456	-0.003	0.017	0.047	-0.002	0.005	0.01
Sat, Mar 20, 2004	1:48:51 PM	-10.652	-23.182	-21.007	-24.727	-23.811	-0.001	0.017	0.048	-0.002	0.005	0.01
Sat, Mar 20, 2004	1:48:51 PM	-10.006	-23.504	-20.684	-25.374	-24.134	-0.002	0.018	0.047	-0.006	0.004	0.009
Sat, Mar 20, 2004	1:48:51 PM	-10.652	-24.147	-21.974	-23.435	-23.488	-0.001	0.017	0.048	-0.004	0.004	0.008
Sat, Mar 20, 2004	1:48:51 PM	-10.329	-23.826	-22.296	-24.727	-23.165	-0.002	0.014	0.047	-0.001	0.001	0.009
Sat, Mar 20, 2004	1:48:51 PM	-10.329	-22.86	-22.296	-25.697	-22.196	-0.002	0.013	0.049	-0.001	0	0.008
Sat, Mar 20, 2004	1:48:51 PM	-10.329	-24.791	-21.652	-25.697	-23.165	0	0.013	0.05	0	0.001	0.009
Sat, Mar 20, 2004	1:48:51 PM	-10.652	-23.826	-20.04	-26.343	-23.811	-0.001	0.014	0.05	0.001	0.001	0.01
Sat, Mar 20, 2004	1:48:51 PM	-10.975	-24.147	-20.362	-25.374	-24.456	-0.002	0.016	0.051	0.001	0.004	0.011
Sat, Mar 20, 2004	1:48:51 PM	-10.329	-23.826	-20.684	-24.727	-24.456	-0.002	0.017	0.051	0.001	0.005	0.009
Sat, Mar 20, 2004	1:48:51 PM	-10.006	-23.826	-19.717	-24.404	-24.134	-0.002	0.018	0.051	0	0.007	0.008
Sat, Mar 20, 2004	1:48:51 PM	-10.006	-24.147	-21.007	-23.111	-24.456	-0.002	0.017	0.047	-0.003	0.007	0.009
Sat, Mar 20, 2004	1:48:51 PM	-10.006	-24.147	-21.329	-23.435	-23.165	-0.001	0.017	0.047	-0.003	0.006	0.01
Sat, Mar 20, 2004	1:48:51 PM	-10.329	-22.86	-21.974	-23.758	-23.165	-0.001	0.014	0.047	-0.006	0.002	0.009
Sat, Mar 20, 2004	1:48:51 PM	-10.329	-23.182	-21.652	-24.404	-23.811	0	0.013	0.049	-0.003	0.001	0.009
Sat, Mar 20, 2004	1:48:51 PM	-10.652	-23.826	-21.007	-25.051	-23.165	-0.002	0.012	0.049	-0.002	0	0.01
Sat, Mar 20, 2004	1:48:51 PM	-10.652	-23.826	-20.684	-25.374	-24.456	-0.002	0.014	0.05	-0.003	0	0.008
Sat, Mar 20, 2004	1:48:51 PM	-10.975	-25.113	-21.329	-26.02	-24.779	-0.002	0.014	0.052	0.003	0.002	0.01
Sat, Mar 20, 2004	1:48:51 PM	-10.652	-24.147	-19.395	-25.697	-25.425	-0.003	0.016	0.052	-0.002	0.004	0.009
Sat, Mar 20, 2004	1:48:51 PM	-10.006	-24.469	-19.717	-24.404	-25.748	-0.001	0.018	0.051	0	0.005	0.01
Sat, Mar 20, 2004	1:48:56 PM	-10.006	-24.469	-19.395	-23.758	-25.102	-0.001	0.02	0.049	-0.003	0.006	0.009
Sat, Mar 20, 2004	1:48:56 PM	-9.683	-23.826	-19.395	-24.081	-24.456	-0.001	0.019	0.047	-0.006	0.005	0.011
Sat, Mar 20, 2004	1:48:56 PM	-9.683	-24.147	-20.684	-22.788	-24.134	-0.002	0.018	0.047	-0.004	0.006	0.01
Sat, Mar 20, 2004	1:48:56 PM	-9.683	-23.826	-21.652	-23.435	-22.842	-0.002	0.014	0.047	-0.003	0.002	0.01
Sat, Mar 20, 2004	1:48:56 PM	-10.006	-23.504	-21.329	-24.081	-23.488	-0.001	0.013	0.046	-0.004	0	0.009
Sat, Mar 20, 2004	1:48:56 PM	-10.652	-23.826	-22.296	-25.051	-23.165	-0.002	0.012	0.047	0	0	0.009
Sat, Mar 20, 2004	1:48:56 PM	-10.329	-23.826	-21.007	-26.667	-23.488	-0.002	0.013	0.05	-0.003	0	0.01
Sat, Mar 20, 2004	1:48:56 PM	-10.975	-23.504	-19.395	-25.697	-24.134	-0.002	0.013	0.051	-0.003	0.002	0.011

Appendix E

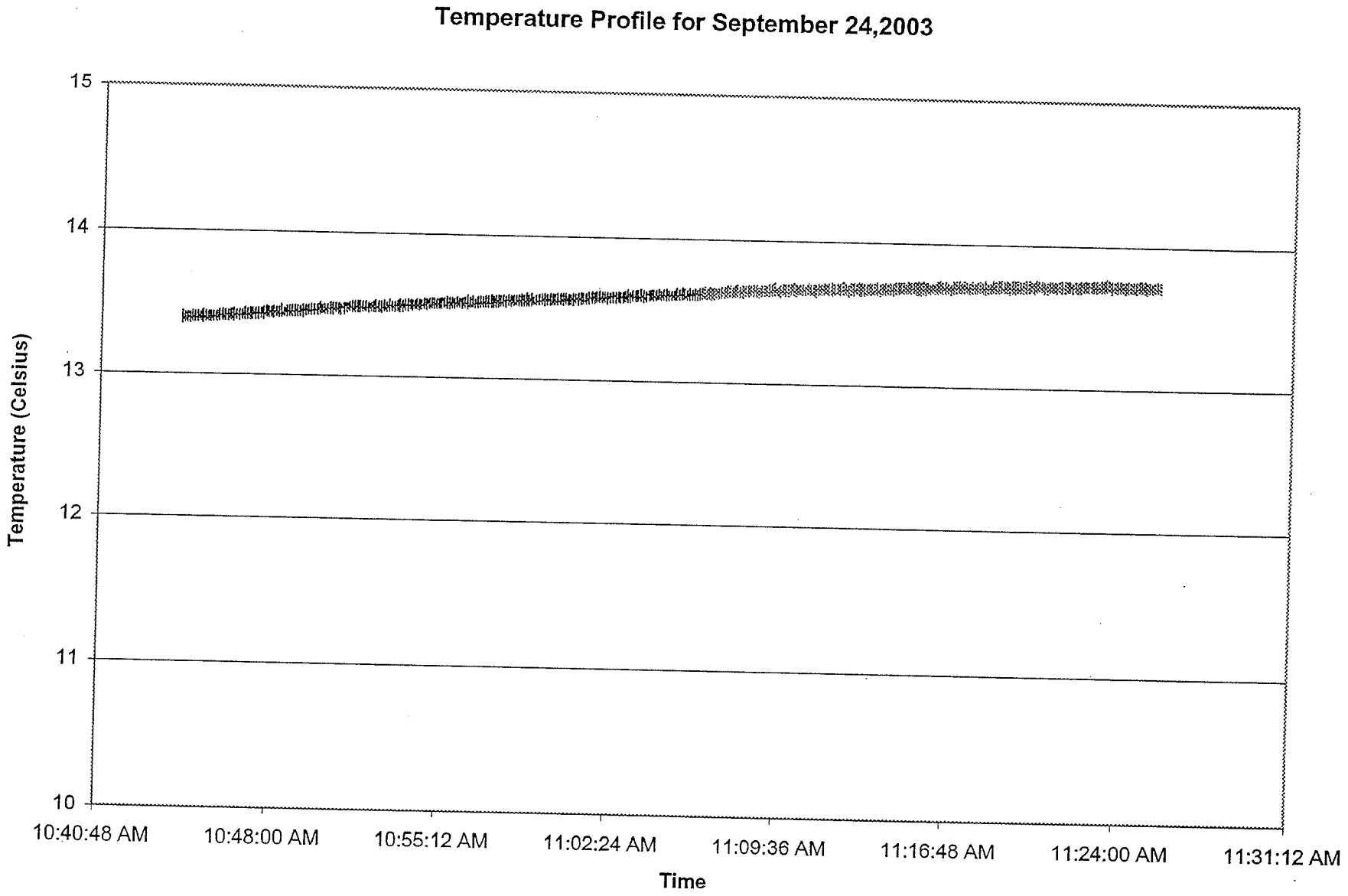
Temperature Profile for September 24,2003
15
14
13
12
11
10
Temperature (Celsius)
10:40:48 AM
10:48:00 AM
10:55:12 AM
11:02:24 AM
11:09:36 AM
11:16:48 AM
11:24:00 AM
11:31:12 AM
Time

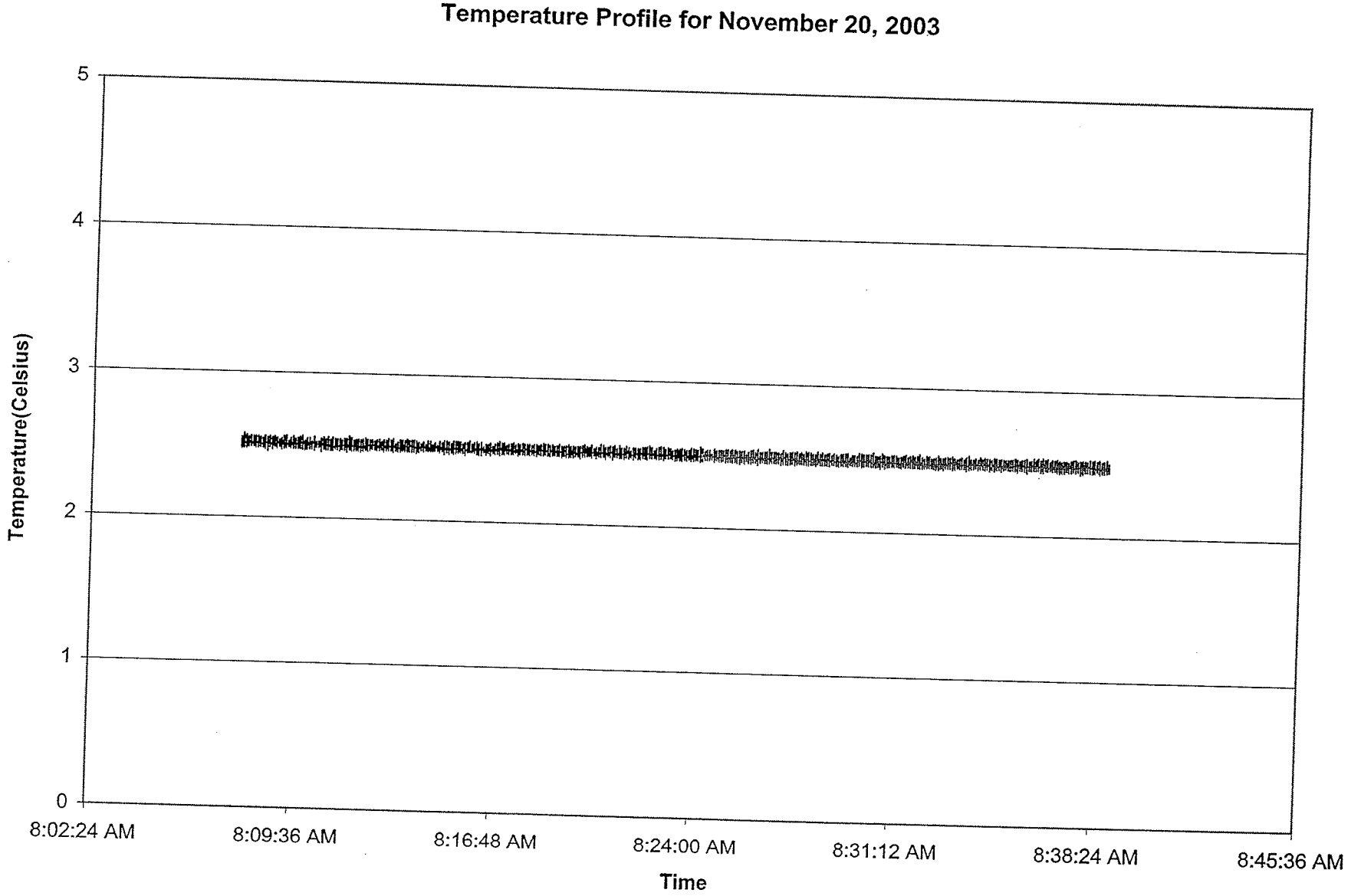
Temperature Profile for November 20, 2003
Temperature(Celsius)
5
4
3
2
1
0
8:02:24 AM
8:09:36 AM
8:16:48 AM
8:24:00 AM
8:31:12 AM
8:38:24 AM
8:45:36 AM
Time

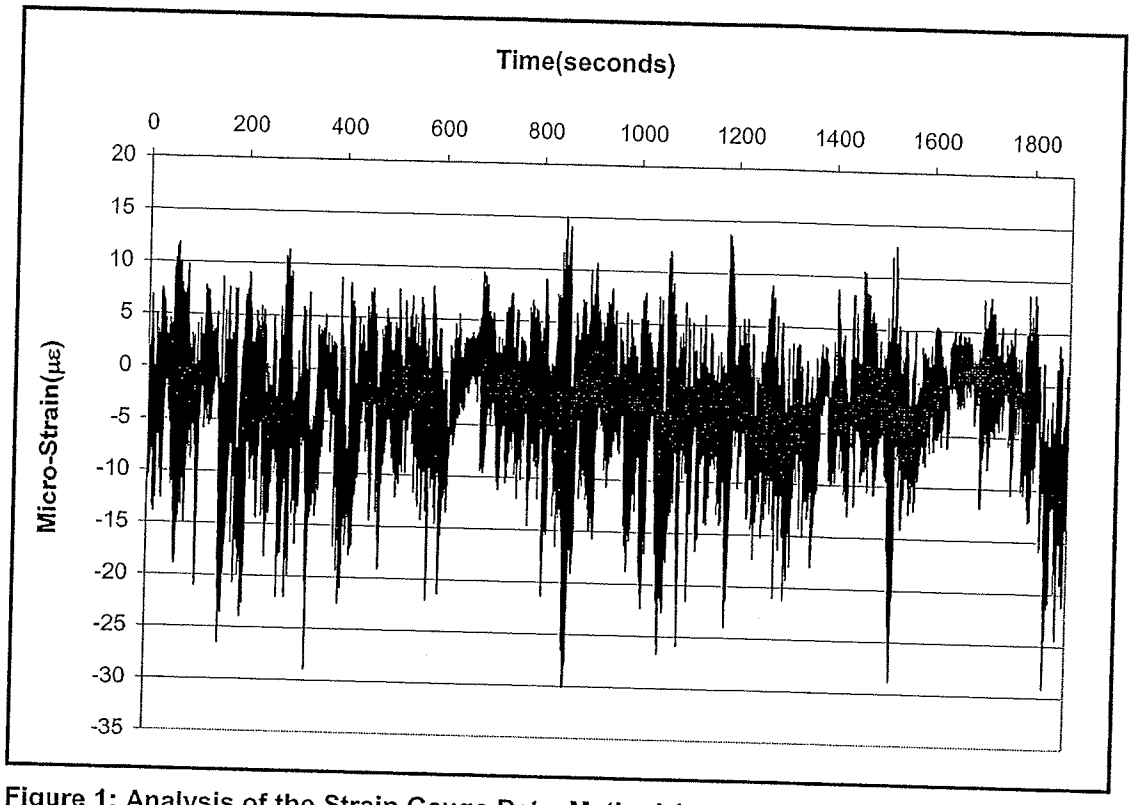

Figure 1: Analysis of the Strain Gauge Data, Method 1

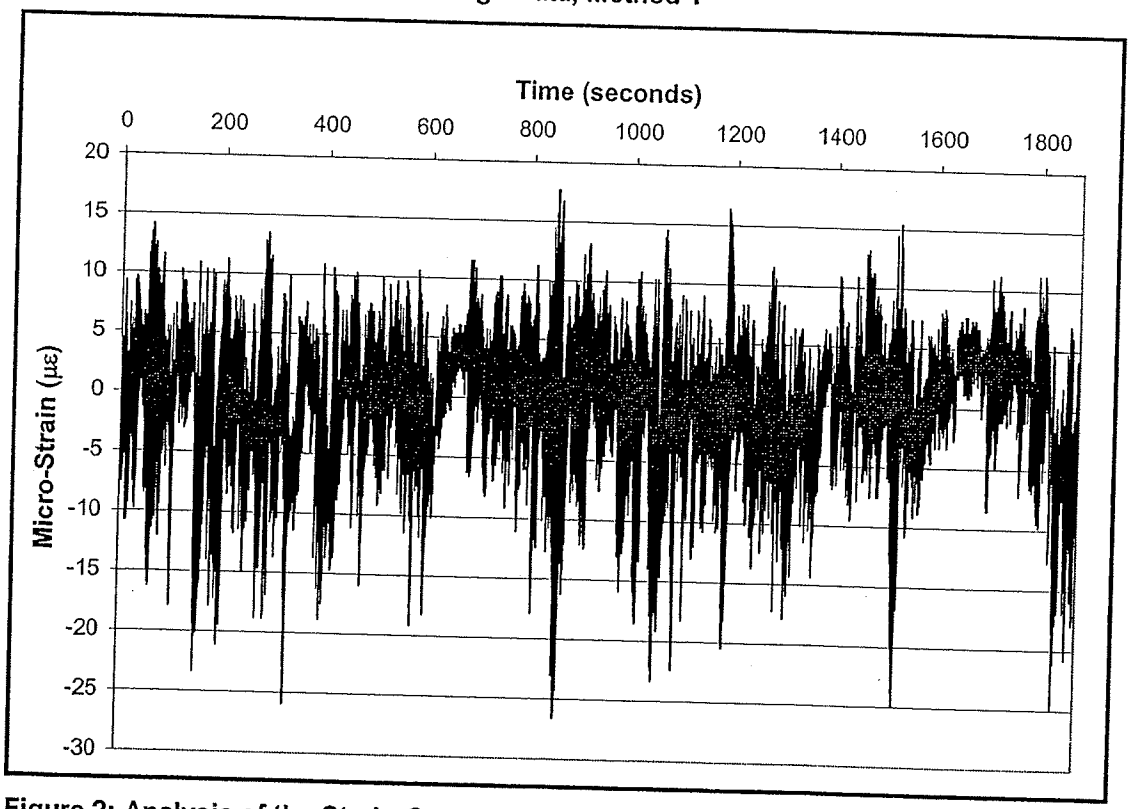

Figure 2: Analysis of the Strain Gauge Data, Method 2

Appendix F

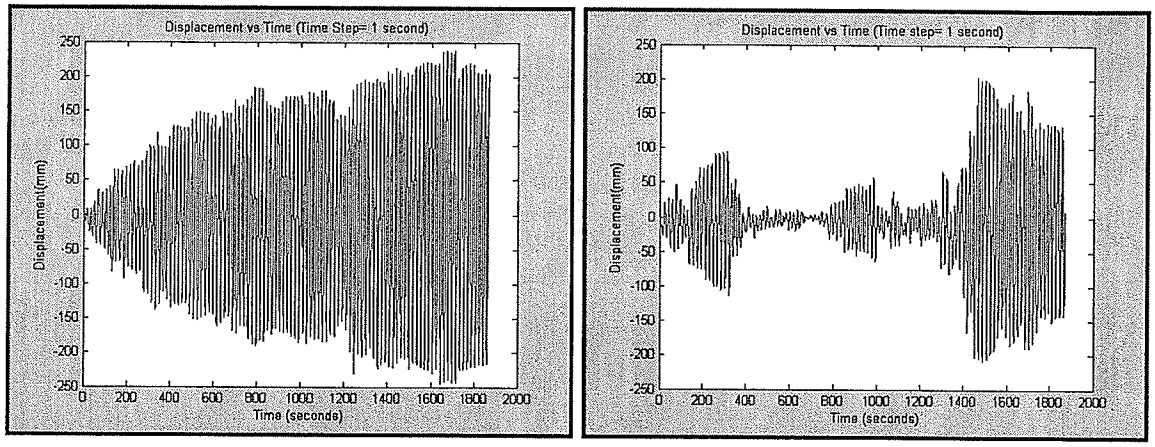

Figure 5-45: Dynamic Displacement Analysis Using a Time Step (Δt=1second)

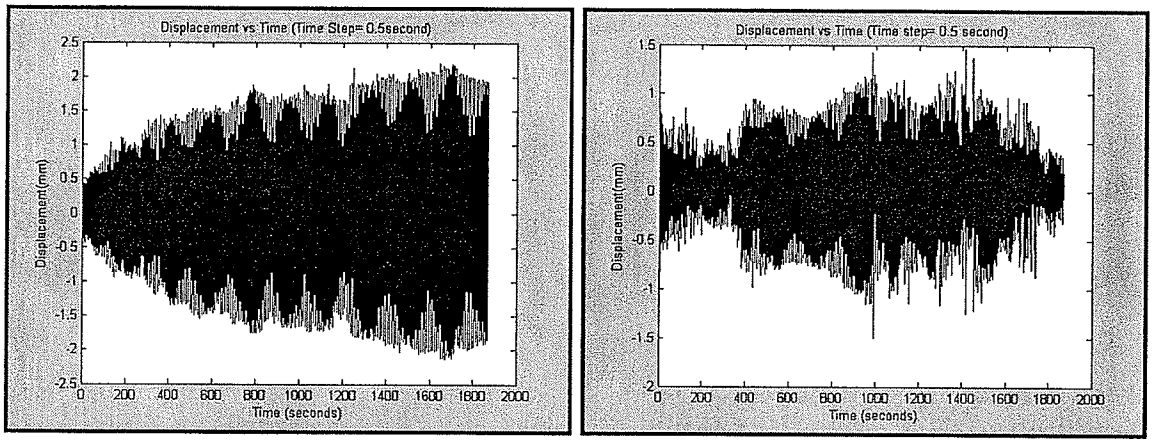

Figure 5-46: Dynamic Displacement Analysis Using a Time Step (Δt=0.5second)

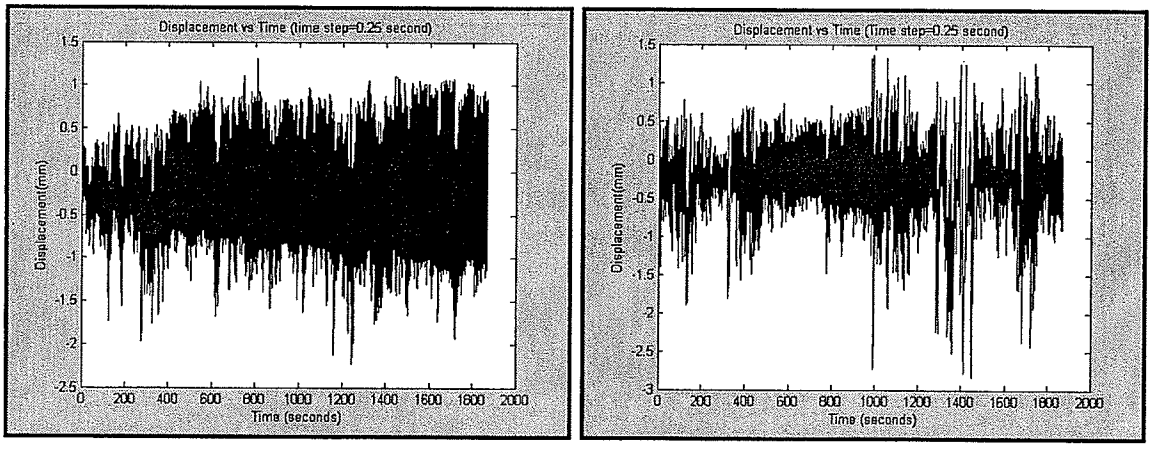

Figure 5-47: Dynamic Displacement Analysis Using a Time Step (Δt=0.25second)

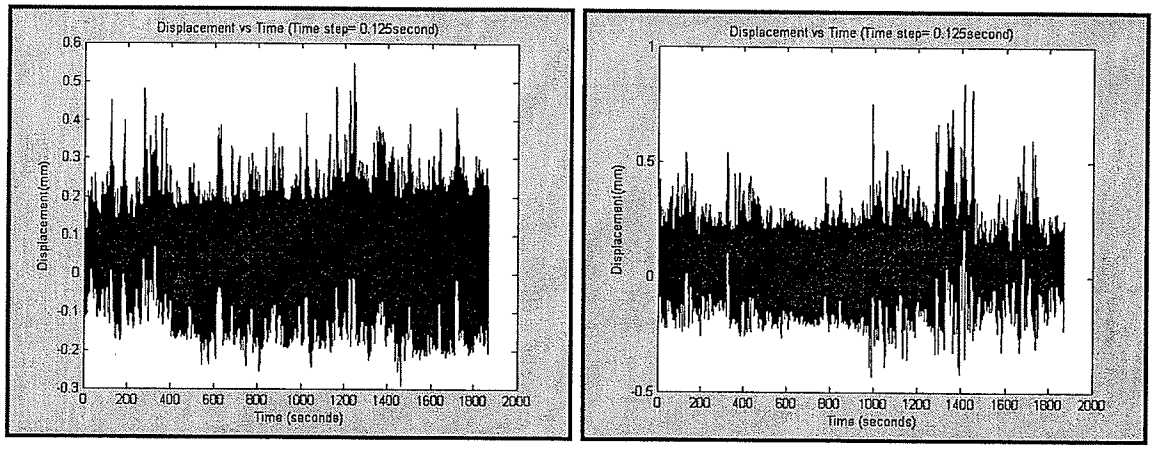

Figure 5-48: Dynamic Displacement Analysis Using a Time Step (Δt=0.125second)

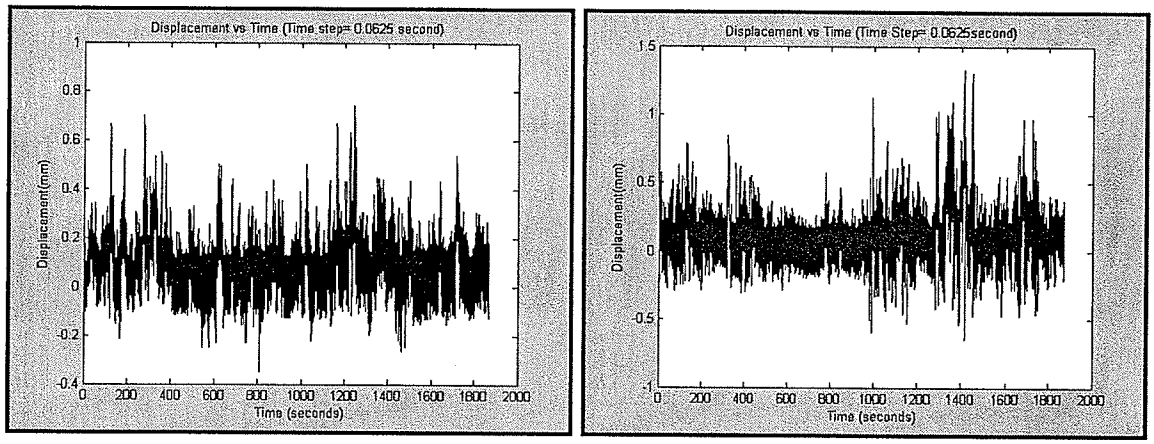

Figure 5-49; Dynamic Displacement Analysis Using a Time Step (Δt=0.0625second)

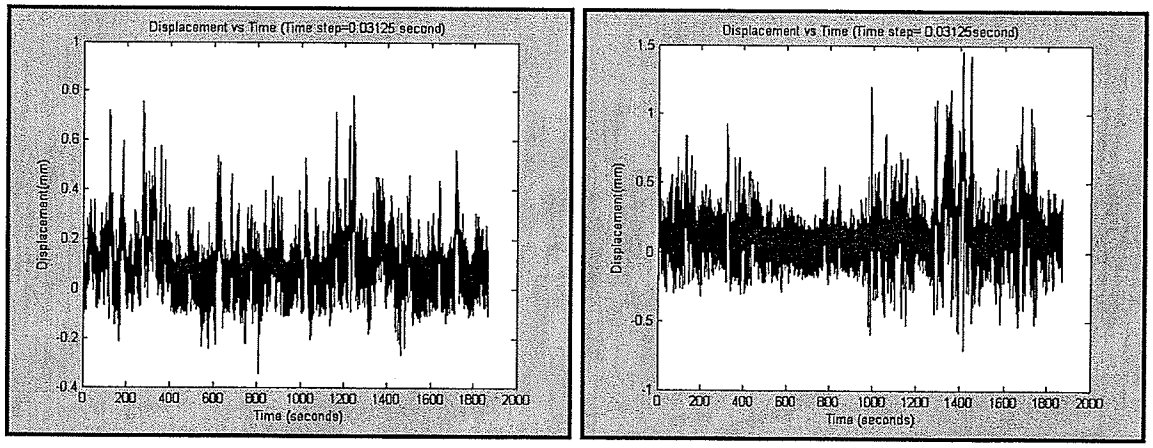

Figure 5-50: Dynamic Displacement Analysis Using a Time Step (Δt=0.03125second)

APPENDIX G

```
clear all;
a=xlsread('F:\GB Analysis\Folder1\B1sept24.xls');
time=a(:,1);
forceNS=a(:,2);


new_time(1)=0.5;
for i=2:3750
    new_time(i)=new_time(i-1)+0.5;
end;

new_time=new_time(1:3740)';

new_forceNS=ones(3740,1);
new_forceNS(1)=forceNS(1);
x=1;
for i=2:length(forceNS)
    new_forceNS(x+2)=forceNS(i);
    x=x+2;
end;
new_forceNS(2)=(new_forceNS(1)+new_forceNS(3))/2;
y=4;
for i=1:length(forceNS)-2
    new_forceNS(y)=(new_forceNS(y-1)+new_forceNS(y+1))/2;
    y=y+2;
end;


new_time=new_time(1:3739);
new_forceNS=new_forceNS(1:3739);

time=new_time;
forceNS=new_forceNS;



new_time(1)=0.25;
for i=2:7490
    new_time(i)=new_time(i-1)+0.25;
end;

new_time=new_time(1:7480)';

new_forceNS=ones(7480,1);
new_forceNS(1)=forceNS(1);
x=1;
for i=2:length(forceNS)
    new_forceNS(x+2)=forceNS(i);
    x=x+2;
end;
new_forceNS(2)=(new_forceNS(1)+new_forceNS(3))/2;
y=4;
for i=1:length(forceNS)-2
    new_forceNS(y)=(new_forceNS(y-1)+new_forceNS(y+1))/2;
    y=y+2;
end;
new_time=new_time';


time1=new_time(1:7479);
forceNS1=new_forceNS(1:7479);

new_time(1)=0.125;
```

```
for i=2:14970
    new_time(i)=new_time(i-1)+0.125;
end;

new_time=new_time(1:14960)';

new_forceNS=ones(14960,1);
new_forceNS(1)=forceNS1(1);
x=1;
for i=2:length(forceNS1)
    new_forceNS(x+2)=forceNS1(i);
    x=x+2;
end;
new_forceNS(2)=(new_forceNS(1)+new_forceNS(3))/2;
y=4;
for i=1:length(forceNS1)-2
    new_forceNS(y)=(new_forceNS(y-1)+new_forceNS(y+1))/2;
    y=y+2;
end;
new_time=new_time';


time2=new_time(1:14959);
forceNS2=new_forceNS(1:14959);

new_time(1)=0.0625;
for i=2:29930
    new_time(i)=new_time(i-1)+0.0625;
end;

new_time=new_time(1:29920)';

new_forceNS=ones(29920,1);
new_forceNS(1)=forceNS2(1);
x=1;
for i=2:length(forceNS2)
    new_forceNS(x+2)=forceNS2(i);
    x=x+2;
end;
new_forceNS(2)=(new_forceNS(1)+new_forceNS(3))/2;
y=4;
for i=1:length(forceNS2)-2
    new_forceNS(y)=(new_forceNS(y-1)+new_forceNS(y+1))/2;
    y=y+2;
end;
new_time=new_time';


time3=new_time(1:29919);
forceNS3=new_forceNS(1:29919);

m=1.575;
p=18.5;
delt=0.0625;

for i=1:length(time3)
    const=(delt)/(m*p);
    variable1=0;
    for j=1:i
        variable1=variable1 + (forceNS3(j)*cos(p*time3(j)));
    end;
    var_1=sin(p*time3(i))*variable1;
    variable2=0;
```

```
    for k=1:i
        variable2=variable2 + (forceNS3(k)*sin(p*time3(k)));
    end;
    var_2=cos(p*time3(i))*variable2;
    Xns(i)=const*(var_1-var_2);
    ens(i)= Xns(i)*3*69.85/(2750*2750);
end;

figure(1)
plot(time3,Xns);
xlabel('Time (seconds)');
ylabel('Displacement');
title('Displacement vs Time (North Forcing Components)  ');

figure(2)
plot(time3,ens);
xlabel('Time (seconds)');
ylabel ('strain');
title ('strain vs time (North forcing component)');

data(:,1)=time3;
data(:,2)=ens';


save T5windNSstrainsept24.out data -ASCII -double -tabs
```

```
clear all;
a=xlsread('F:\GB Analysis\Folder1\B1march10.xls');
time=a(:,1);
forceNS=a(:,2);


new_time(1)=0.5;
for i=2:3750
    new_time(i)=new_time(i-1)+0.5;
end;

new_time=new_time(1:3740)';

new_forceNS=ones(3740,1);
new_forceNS(1)=forceNS(1);
x=1;
for i=2:length(forceNS)
    new_forceNS(x+2)=forceNS(i);
    x=x+2;
end;
new_forceNS(2)=(new_forceNS(1)+new_forceNS(3))/2;
y=4;
for i=1:length(forceNS)-2
    new_forceNS(y)=(new_forceNS(y-1)+new_forceNS(y+1))/2;
    y=y+2;
end;


new_time=new_time(1:3739);
new_forceNS=new_forceNS(1:3739);

time=new_time;
forceNS=new_forceNS;



new_time(1)=0.25;
for i=2:7490
    new_time(i)=new_time(i-1)+0.25;
end;

new_time=new_time(1:7480)';

new_forceNS=ones(7480,1);
new_forceNS(1)=forceNS(1);
x=1;
for i=2:length(forceNS)
    new_forceNS(x+2)=forceNS(i);
    x=x+2;
end;
new_forceNS(2)=(new_forceNS(1)+new_forceNS(3))/2;
y=4;
for i=1:length(forceNS)-2
    new_forceNS(y)=(new_forceNS(y-1)+new_forceNS(y+1))/2;
    y=y+2;
end;
new_time=new_time';


time1=new_time(1:7479);
forceNS1=new_forceNS(1:7479);

new_time(1)=0.125;
```

```
for i=2:14970
    new_time(i)=new_time(i-1)+0.125;
end;

new_time=new_time(1:14960)';

new_forceNS=ones(14960,1);
new_forceNS(1)=forceNS1(1);
x=1;
for i=2:length(forceNS1)
    new_forceNS(x+2)=forceNS1(i);
    x=x+2;
end;
new_forceNS(2)=(new_forceNS(1)+new_forceNS(3))/2;
y=4;
for i=1:length(forceNS1)-2
    new_forceNS(y)=(new_forceNS(y-1)+new_forceNS(y+1))/2;
    y=y+2;
end;
new_time=new_time';


time2=new_time(1:14959);
forceNS2=new_forceNS(1:14959);

new_time(1)=0.0625;
for i=2:29930
    new_time(i)=new_time(i-1)+0.0625;
end;

new_time=new_time(1:29920)';

new_forceNS=ones(29920,1);
new_forceNS(1)=forceNS2(1);
x=1;
for i=2:length(forceNS2)
    new_forceNS(x+2)=forceNS2(i);
    x=x+2;
end;
new_forceNS(2)=(new_forceNS(1)+new_forceNS(3))/2;
y=4;
for i=1:length(forceNS2)-2
    new_forceNS(y)=(new_forceNS(y-1)+new_forceNS(y+1))/2;
    y=y+2;
end;
new_time=new_time';


time3=new_time(1:29919);
forceNS3=new_forceNS(1:29919);




new_time(1)=0.03125;
for i=2:59850
    new_time(i)=new_time(i-1)+0.03125;
end;

new_time=new_time(1:59840)';
```

```
new_forceNS=ones(59840,1);
new_forceNS(1)=forceNS2(1);
x=1;
for i=2:length(forceNS2)
    new_forceNS(x+2)=forceNS2(i);
    x=x+2;
end;
new_forceNS(2)=(new_forceNS(1)+new_forceNS(3))/2;
y=4;
for i=1:length(forceNS2)-2
    new_forceNS(y)=(new_forceNS(y-1)+new_forceNS(y+1))/2;
    y=y+2;
end;
new_time=new_time';


time4=new_time(1:59839);
forceNS4=new_forceNS(1:59839);




m=1.575;
p=18.5;
delt=0.03125;

for i=1:length(time4)
    const=(delt)/(m*p);
    variable1=0;
    for j=1:i
        variable1=variable1 + (forceNS4(j)*cos(p*time4(j)));
    end;
    var_1=sin(p*time4(i))*variable1;
    variable2=0;
    for k=1:i
        variable2=variable2 + (forceNS4(k)*sin(p*time4(k)));
    end;
    var_2=cos(p*time4(i))*variable2;
    Xns(i)=const*(var_1-var_2);
    ens(i)= Xns(i)*3*69.85/(2750*2750);
end;

figure(1)
plot(time4,Xns);
xlabel('Time (seconds)');
ylabel('Displacement');
title('Displacement vs Time (North Forcing Components)  ');

figure(2)
plot(time4,ens);
xlabel('Time (seconds)');
ylabel ('strain');
title ('strain vs time (North forcing component)');

data(:,1)=time3;
data(:,2)=ens';


save T6windNSstrainmarch10.out data -ASCII -double -tabs
```